

CARBOTHERMIC PRODUCTION OF HEXAGONAL BORON NITRIDE

A THESIS SUBMITTED TO
THE GRADUATE SCHOOL OF NATURAL AND APPLIED SCIENCES
OF
MIDDLE EAST TECHNICAL UNIVERSITY

BY

HASAN ERDEM ÇAMURLU

IN PARTIAL FULFILLMENT OF THE REQUIREMENTS
FOR
THE DEGREE OF DOCTOR OF PHILOSOPHY
IN
METALLURGICAL AND MATERIALS ENGINEERING

NOVEMBER 2006

Approval of the Graduate School of Natural and Applied Sciences

Prof. Dr. Canan Özgen
Director

I certify that this thesis satisfies all the requirements as a thesis for the degree of Doctor of Philosophy.

Prof. Dr. Tayfur Öztürk
Head of Department

This is to certify that we have read this thesis and that in our opinion it is fully adequate, in scope and quality, as a thesis and for the degree of Doctor of Philosophy.

Prof. Dr. Yavuz A. Topkaya
Co-Supervisor

Prof. Dr. Naci Sevinç
Supervisor

Examining Committee Members

Prof. Dr Ahmet Geveci (METU, METE)

Prof. Dr. Naci Sevinç (METU, METE)

Prof. Dr. Yavuz A. Topkaya (METU, METE)

Prof. Dr. Önder Özbelge (METU, CHE)

Assoc. Prof. Dr. Nuri Durlu (ETÜ, ME)

I hereby declare that all information in this document has been obtained and presented in accordance with academic rules and ethical conduct. I also declare that, as required by these rules and conduct, I have fully cited and referenced all material and results that are not original to this work.

Name, Last name: Hasan Erdem Çamurlu

Signature :

ABSTRACT

CARBOTHERMIC PRODUCTION OF HEXAGONAL BORON NITRIDE

Çamurlu, Hasan Erdem

Ph.D., Department of Metallurgical and Materials Engineering

Supervisor : Prof. Dr. Naci Sevinç

Co-Supervisor: Prof. Dr. Yavuz A. Topkaya

October 2006, 124 pages

Formation of hexagonal boron nitride (h-BN) by carbothermic reduction of B_2O_3 under nitrogen atmosphere at $1500^\circ C$ was investigated. Reaction products were subjected to powder X-ray diffraction analysis, chemical analysis and were examined by SEM. B_4C was found to exist in the reaction products of the experiments in which h-BN formation was not complete. One of the aims of this study was to investigate the role of B_4C in the carbothermic production of h-BN. For this purpose, conversion reaction of B_4C into h-BN was studied. B_4C used in these experiments was produced in the same conditions that h-BN was formed, but under argon atmosphere. It was found that formation of h-BN from $B_4C-B_2O_3$ mixtures was slower than activated $C-B_2O_3$ mixtures. It was concluded that B_4C is not a necessary intermediate product in the carbothermic production of h-BN.

Some additives are known to catalytically affect the h-BN formation. The second aim of this study was to examine the catalytic effect of some alkaline earth metal oxides and carbonates, some transition metal oxides and cupric nitrate. It was

found that addition of 10wt% CaCO_3 into the $\text{B}_2\text{O}_3+\text{C}$ mixture was optimum for increasing the rate and yield of h-BN formation and decreasing the B_4C amount in the products and that the reaction was complete in 2 hours. CaCO_3 was observed to be effective in increasing the rate and grain size of the formed h-BN. Addition of cupric nitrate together with CaCO_3 provided a further increase in the size of the h-BN grains.

Keywords: Hexagonal boron nitride, boron carbide, carbothermic formation, calcium carbonate, cupric nitrate, catalyst

ÖZ

KARBOTERMİK YÖNTEMLE HEKZAGONAL BOR NİTRÜR ÜRETİMİ

Çamurlu, Hasan Erdem

Doktora, Metalurji ve Malzeme Mühendisliği Bölümü

Tez Yöneticisi: Prof. Dr. Naci Sevinç

Ortak Tez Yöneticisi: Prof. Dr. Yavuz A. Topkaya

Ekim 2006, 124 sayfa

Bor oksitin nitrojen atmosferinde 1500°C’de karbotermik indirgenmesi ile heksagonal bor nitrür oluşumu incelenmiştir. Reaksiyon ürünleri X-ışını kırınımı ve kimyasal analize tabi tutulmuş ve tarama elektron mikroskobu ile incelenmiştir. Hekzagonal bor nitrür oluşumunun tamamlanmadığı durumlarda reaksiyon ürünlerinde bor karbürün de bulunduğu görülmüştür. Bu çalışmanın amaçlarından birisi karbotermik yöntemle heksagonal bor nitrür üretiminde bor karbürün rolünün incelenmesidir. Bu maksatla bor karbürün heksagonal bor nitrüre dönüşüm reaksiyonu incelenmiştir. Bu deneylerde kullanılan bor karbür, bor nitrürle aynı şartlarda fakat argon atmosferinde üretilmiştir. Bor nitrürün bor karbür-bor oksit karışımlarından oluşumunun aktif karbon-bor oksit karışımlarından oluşumundan daha yavaş olduğu bulunmuştur. Bor karbürün, bor nitrürün karbotermik yöntemle üretimi sırasında gerekli bir ara ürün olmadığına karar verilmiştir.

Bazı katkı malzemelerinin bor nitrür oluşumunu katalitik olarak etkilediği bilinmektedir. Bu çalışmanın ikinci amacı bazı toprak alkali metal oksitlerinin ve karbonatlarının, bazı geçiş metali oksitlerinin ve bakır nitratın katalitik etkisinin incelenmesidir. B_2O_3+C karışımına ağırlıkça %10 $CaCO_3$ eklemenin bor nitrürü artırmada ve bor karbür miktarını azaltmada optimum değer olduğu ve reaksiyonun 2 saatte tamamlandığı bulunmuştur. Kalsiyum karbonatın bor nitrürün oluşum hızını ve tane boyunu arttırıcı etkisinin olduğu görülmüştür. Kalsiyum karbonatla birlikte bakır nitrat eklenmesi tane boyunu daha fazla arttırmıştır.

Anahtar Kelimeler: Hekzagonal bor nitrür, bor karbür, karbotermik oluşum, kalsiyum karbonat, bakır nitrat, katalizör

To My Family

ACKNOWLEDGMENTS

It is a great pleasure to thank my supervisors Prof. Dr. Naci Sevinç and Prof. Dr. Yavuz A. Topkaya for their valuable guidance, support, suggestions and stimulating advice for the completion of this work. I appreciate the time and effort that Mr. Sevinç has put into this study.

I would like to thank to all of the staff of the Department of Metallurgical and Materials Engineering. Especially, technical assistance of Mr. Necmi Avcı for XRD measurements and Mr. Cengiz Tan for SEM analyses is gratefully acknowledged. I would also like to thank to Mr. İsa Hasar for his help in construction of the tube furnace. Thanks also go to Dr. İbrahim Çam for the valuable discussions and advices.

Technical assistance and interest of the staff of the Research and Development Department of Eti Maden A.Ş. and guidance of Mrs. Selma Tan for the chemical analyses is acknowledged.

This study was supported by the State Planning Organization (ÖYP-DPT) Grant No: BAP-09-11-DPT-2002K120510.

I would like to thank my parents for their support and encouragement through hard times of my study.

Finally, I wish to thank my wife Pınar for her love, understanding and never-ending support. Without her this study could not be accomplished.

TABLE OF CONTENTS

ABSTRACT	iv
ÖZ	vi
DEDICATION	viii
ACKNOWLEDGMENTS.....	ix
TABLE OF CONTENTS	x
LIST OF FIGURES.....	xii
LIST OF TABLES	xviii
CHAPTERS	
I. INTRODUCTION.....	1
II. LITERATURE REVIEW	3
2.1 Phases of Boron Nitride	4
2.2 Properties of Hexagonal BN	6
2.3 Applications of Hexagonal BN.....	8
2.4 Synthesis Methods of Hexagonal BN	11
2.4.1 Reaction of Boric Acid or Boric Oxide with Ammonia.....	14
2.4.2 Reaction of Boric Acid with Nitrogen Containing Organic Materials.....	14
2.4.3 Carbothermic Method	17
III. EXPERIMENTAL SET-UP AND PROCEDURE.....	23
3.1 Experimental Set-Up.....	23
3.3 Materials Used	28
3.3 Experimental Procedure.....	30
IV. RESULTS AND DISCUSSION.....	33
4.1. Results of the Experiments Conducted with Plain (B ₂ O ₃ +C) Mixtures	33

4.2. Role of B ₄ C During Carbothermic Formation of Hexagonal BN.....	50
4.3. Effect of Excess Boric Oxide.....	56
4.4. Effect of Additives.....	61
4.4.1. Effect of Alkaline Earth Metal Oxides and Carbonates, CaCO ₃ , MgO, BaCO ₃	63
4.4.1.1. CaCO ₃ Addition.....	63
4.4.1.2. MgO Addition.....	87
4.4.1.3. BaCO ₃ Addition.....	90
4.4.2. Effect of Transition Metal Oxides.....	92
4.4.2.1. MnO ₂ Addition.....	93
4.4.2.2. Fe ₃ O ₄ Addition.....	95
4.4.2.3. Co ₃ O ₄ Addition.....	97
4.4.2.4. Addition of Cu as Cupric Nitrate.....	98
4.4.3. CaCO ₃ + Cupric Nitrate Addition.....	102
4.4.4 Comparison of the Effect of Additives.....	109
V. CONCLUSION.....	112
REFERENCES.....	119
VITA.....	124

LIST OF FIGURES

Figures	
Figure 2.1. Crystal structures of boron nitride phases.....	5
Figure 2.2. Variation of coefficient of friction of some important lubricants with temperature	8
Figure 2.3. Various h-BN preparation methods	12
Figure 2.4. XRD patterns of the samples obtained at different temperatures, (a) starting material (t-BN), (b) 1000°C, (c) 1300°C, (d) 1600°C, (e) 2000°C	15
Figure 2.5. Free energy change versus temperature plots for the reactions: (1) $B_2O_3(l) + 3C + N_2 = 2BN + 3CO$, (2) $B_2O_3(g) + 3C + N_2 = 2BN + 3CO$, (3) $2B_2O_3(l) + 7C = B_4C + 6CO$, (4) $2B_2O_3(g) + 7C = B_4C + 6CO$, (5) $3B_4C + B_2O_3(g) + 7N_2 = 14BN + 3CO$, (6) $3B_4C + B_2O_3(l) + 7N_2 = 14BN + 3CO$, (7) $B_2O_3(g) + C = 2BO(g) + CO$, (8) $B_2O_3(l) = B_2O_3(g)$, (9) $B_2O_3(l) + C = B_2O_2(g) + CO$, (10) $B_2O_2(g) + 2C + N_2 = BN + 2CO$	20
Figure 3.1. Top and side view drawings of the vertical tube furnace in which the experiments were performed. Dimensions are in millimeters	25
Figure 3.2. Schematic drawing of the experimental set-up.....	26
Figure 3.3. Configuration of the graphite crucible, alumina bar and the upper brass head of the furnace.	27
Figure 3.4. SEM micrograph of activated carbon	29
Figure 4.1. XRD patterns of the products of the experiments conducted with plain B_2O_3+C mixtures for (a) 15 minutes, (b) 30 minutes, (c) 1 hour, (d) 1.5 hours, (e) 2 hours, (f) 2.5 hours, (g) 3 hours. (1) H_3BO_3 , (2) h-BN, (3) B_4C	35
Figure 4.2. Flowsheet of the chemical analysis method employed in this study. .	36

Figure 4.3. XRD patterns of (a) sample obtained in the experiment conducted for 1h, (b) after leaching with water and filtering, (c) after oxidizing sample-(b) at 800°C for 15h and leaching with water. (1) H ₃ BO ₃ , (2) h-BN, (3) B ₄ C.....	37
Figure 4.4. FT-IR patterns of (a) H ₃ BO ₃ , (b) sample obtained in the experiment conducted for 1 hour, (c) after leaching with water and filtering, (d) after oxidizing sample-(c) at 800°C for 15h and leaching with water.	38
Figure 4.5. Variation of the amounts of unreacted activated carbon and boric oxide in the products with duration.	41
Figure 4.6. Variation of the amounts of h-BN and B ₄ C in the products with duration.....	42
Figure 4.7. SEM micrograph of the product of the experiment conducted for 30 minutes.....	44
Figure 4.8. SEM micrograph of the product of the experiment conducted for 1 hour.	45
Figure 4.9. SEM micrograph of the inside surface of the product of the experiment conducted for 1.5 hours.	45
Figure 4.10. SEM micrograph of the product of the experiment conducted for 3 hours.	46
Figure 4.11. Magnified portion of the XRD patterns of the products of the experiments conducted with plain B ₂ O ₃ +C mixtures for (a) 15 minutes, (b) 30 minutes, (c) 1 hour, (d) 1.5 hours, (e) 2 hours, (f) 2.5 hours, (g) 3 hours.	47
Figure 4.12. Variation of mean interplanar spacing and average crystal thickness of the produced h-BN powders with duration of the experiments at 1500°C..	48
Figure 4.13. (a) and (b). B ₄ C rich parts of the product of the experiment conducted for 1 hour.....	51
Figure 4.14. XRD patterns of the products of the experiments conducted with B ₂ O ₃ +C mixtures for (a) 30 minutes, (b) 1 hour and (c) 2.5 hours under argon atmosphere at 1500°C. (*) graphite, (1) H ₃ BO ₃ , (2) B ₄ C.....	52
Figure 4.15. FT-IR pattern of B ₄ C obtained obtained in 2.5 hours from B ₂ O ₃ +C mixtures under argon atmosphere at 1500°C.....	52

Figure 4.16. SEM micrograph of B ₄ C powder obtained in 2.5 hours from B ₂ O ₃ +C mixtures under argon atmosphere at 1500°C.....	53
Figure 4.17. XRD patterns of (a) boron carbide produced in 2.5 hours, (b) after reacting produced boron carbide – boric oxide mixtures under nitrogen at 1500°C for 3 hours. (*) graphite, (1) H ₃ BO ₃ , (2) h-BN, (3) B ₄ C.	54
Figure 4.18. SEM micrograph of the product of the experiment conducted with (produced B ₄ C+B ₂ O ₃) mixtures under nitrogen atmosphere for 3 hours.	55
Figure 4.19. EDX analysis of the points indicated as (1) in Figure 4.18. (Au peaks originating from gold coating of the sample.)	55
Figure 4.20. EDX analysis of the points indicated as (2) in Figure 4.18. (Au peaks originating from gold coating of the sample.)	56
Figure 4.21. Amounts of boron carbide formed in the experiments conducted with 50, 100 and 150 mole% excess boron oxide for 0.25, 0.5 and 1 hour durations.	58
Figure 4.22. XRD patterns showing the effect of excess boron oxide on the boron carbide formed during carbothermic production of h-BN. Experiments were performed with (a) 50, (b) 100 and (c) 150 mole% excess boron oxide for 15 minutes; (d) 50, (e) 100 and (f) 150 mole% excess boron oxide for 30 minutes; (g) 50, (h) 100 and (i) 150 mole% excess boron oxide for 60 minutes. (1) H ₃ BO ₃ , (2) h-BN, (3) B ₄ C.	59
Figure 4.23. Amounts of boron nitride formed in the experiments conducted with 50, 100 and 150 mole% excess boron oxide for 0.25, 0.5 and 1 hour durations.	60
Figure 4.24. Periodic table of the elements. Metallic elements of the used additives in this study are shaded in gray.....	62
Figure 4.25: SEM micrograph of the CaCO ₃ powder	64
Figure 4.26. B ₂ O ₃ – CaO phase diagram [58].	65
Figure 4.27. Change in the amounts of h-BN and B ₄ C in the products of the experiments conducted at 1500°C for 30 minutes with CaCO ₃ additions.	67
Figure 4.28. XRD patterns of the products of the experiments conducted with 0-50 weight% CaCO ₃ addition for 30 minutes at 1500°C. (a) No addition, (b) 5	

wt%, (c) 10 wt%, (d) 20 wt%, (e) 30 wt%, (f) 40 wt%, (g) 50 wt % CaCO ₃ addition. (1) h-BN, (2) B ₄ C, (3) H ₃ BO ₃ , (4) CaB ₂ O ₄	68
Figure 4.29. Amounts of h-BN and B ₄ C in the products of the experiments conducted for 30 minutes to 2 hours at 1500°C with plain and 10 wt% CaCO ₃ added mixtures.....	70
Figure 4.30. XRD patterns of the products of the experiments conducted with plain and 10 wt% CaCO ₃ added mixtures at 1500°C. (a) plain mixture - 30 minutes, (a') CaCO ₃ added mixture - 30 minutes; (b) plain mixture - 1 hour, (b') CaCO ₃ added mixture - 1 hour; (c) plain mixture - 2 hours, (c') CaCO ₃ added mixture - 2 hours. (1) H ₃ BO ₃ , (2) h-BN, (3) B ₄ C.	71
Figure 4.31. SEM micrograph of h-BN formed from plain mixture at 1500°C in 2 hours.	72
Figure 4.32. SEM micrograph of h-BN formed from 10 wt% CaCO ₃ added mixture at 1500°C in 2 hours.	73
Figure 4.33. FT-IR patterns of (a) B ₄ C, (b) h-BN, (c) H ₃ BO ₃ , (d) calcium borate, (e) product obtained from plain B ₂ O ₃ +C mixtures in 30 minutes at 1500°C, (f) product obtained from 10wt% CaCO ₃ added B ₂ O ₃ +C mixtures, (g) product obtained from 30wt% CaCO ₃ added B ₂ O ₃ +C mixtures, (h) product obtained from 50wt% CaCO ₃ added B ₂ O ₃ +C mixtures.	77
Figure 4.34. FT-IR patterns of (a) product obtained from 30wt% CaCO ₃ added B ₂ O ₃ +C mixture in 30 minutes at 1500°C, (b) sample in (a) leached in dilute HCl, (c) sample in (b) oxidized at 800°C and leached with water.	78
Figure 4.35. SEM micrograph of h-BN formed from 10 wt% CaCO ₃ added mixture at 1500°C in 1 hour.	81
Figure 4.36. SEM micrograph of MgO powder.	88
Figure 4.37. XRD patterns of the experiments conducted with 10wt% MgO added B ₂ O ₃ +C mixtures for (a) 30 minutes, (b) 1 hour, (c) 1 hour and leached, (d) 2 hours. (1) h-BN, (2) Mg ₂ B ₂ O ₅ , (3) H ₃ BO ₃ , (4) B ₄ C.....	88
Figure 4.38. B ₂ O ₃ -MgO phase diagram [58].....	89
Figure 4.39. SEM micrograph of BaCO ₃ powder	90

Figure 4.40. XRD patterns of the experiments conducted with 10wt% BaCO ₃ added B ₂ O ₃ +C mixtures conducted for (a) 30 minutes, (b) 30 minutes and leached, (c) 1 hour, (d) 2 hours. (1) h-BN, (2) B ₄ C (3) H ₃ BO ₃	91
Figure 4.41. BaO-B ₂ O ₃ phase diagram [58].....	92
Figure 4.42. SEM micrograph of MnO ₂ powder.....	93
Figure 4.43. XRD patterns of the experiments (a) conducted with 10wt% MnO ₂ added B ₂ O ₃ +C mixtures for 1 hour, (b) after leaching product (a). (1) h-BN, (2) H ₃ BO ₃ , (3) MnB, (4) B ₄ C.	94
Figure 4.44. SEM micrograph of Fe ₃ O ₄ powder.....	95
Figure 4.45. XRD patterns of (a) the experiments conducted with 10wt% Fe ₃ O ₄ added B ₂ O ₃ +C mixtures for 1 hour, (b) after leaching product (a). (1) h-BN, (2) H ₃ BO ₃ , (3) Fe, (4) FeC, (5) B ₄ C.	96
Figure 4.46. SEM micrograph of Co ₃ O ₄ powder	97
Figure 4.47. XRD patterns of (a) the experiments conducted with 10wt% Co ₃ O ₄ added B ₂ O ₃ +C mixtures for 1 hour, (b) after leaching product (a). (1) h-BN, (2) H ₃ BO ₃ , (3) Co, (4) B ₂ CCo ₁₁ , (5) Co ₂ C.	98
Figure 4.48. XRD patterns of (a) product of the experiment conducted with B ₂ O ₃ +C mixtures with 2.5wt% Cu addition (in the form of cupric nitrate) for 1 hour. (b) after leaching product (a). (1) h-BN, (2) H ₃ BO ₃ , (3) B ₄ C, (4) Cu....	99
Figure 4.49. SEM micrograph of the product of the experiment conducted with Cu addition for 30 minutes.....	100
Figure 4.50. SEM micrograph of the h-BN powder obtained by leaching the product of the experiment conducted for 2 hours with Cu addition.	101
Figure 4.51. XRD patterns of (a) product of the experiment conducted for 2 hours with B ₂ O ₃ +C mixtures containing 10wt% CaCO ₃ and 2.5wt% Cu addition (in the form of Cu-nitrate), (b) after leaching product (a). (1) h-BN, (2) H ₃ BO ₃ , (3) Cu.....	102
Figure 4.52. SEM micrograph of the product of the experiment conducted for 30 minutes with 10wt% CaCO ₃ and 2.5wt% Cu addition.	103
Figure 4.53. SEM micrograph of the product of the experiment conducted for 2 hours with 10wt% CaCO ₃ and 2.5wt% Cu addition.....	104

Figure 4.54. SEM micrograph of the product of the experiment conducted for 2 hours with 10wt% CaCO ₃ and 2.5wt% Cu addition (higher magnification).	104
Figure 4.55. SEM micrograph of the product of the experiment conducted for 2 hours with 10wt% CaCO ₃ and 2.5wt% Cu addition (after leaching with 1/1 (v/v) HCl/water solution).....	105
Figure 4.56. SEM micrograph of the product of the experiment conducted for 2 hours with 10wt% CaCO ₃ and 2.5wt% Cu addition (outer surface of the pellet).....	106
Figure 4.57. SEM micrograph of the product of the experiment conducted for 2 hours with 10wt% CaCO ₃ and 5wt% Cu addition.....	107
Figure 4.58. Magnified part of Figure 4.57.....	107
Figure 4.59. SEM micrograph of the product of the experiment conducted for 2 hours with 10wt% CaCO ₃ and 2.5wt% Cu addition after further reaction for an additional 2 hours with 2.5wt% Cu addition, and leaching.....	108
Figure 4.60. Magnified part of Figure 4.59.....	109

LIST OF TABLES

Tables

Table 2.1. Properties of h-BN, graphite, Al ₂ O ₃ and AlN.	7
Table 4.1. Variation of the amounts of boric oxide, boron carbide, boron nitride and unreacted activated carbon in the products with duration.	41
Table 4.2. 2θ, interplanar spacing (d ₀₀₂), broadening data (B _M), and average crystallite size calculated by the Scherrer formula.	48
Table 4.3. Amounts of boron carbide and boron nitride formed in the experiments conducted with 50, 100 and 150 mole% excess boron oxide for 0.25, 0.5 and 1 hour durations.	57
Table 4.4. Change in the amounts of h-BN and B ₄ C in the products of the experiments conducted at 1500°C for 30 minutes with CaCO ₃ additions; and CaO percentages of the (CaO+B ₂ O ₃) system in the pellets at t=0 and t=30 minutes.	66
Table 4.5. Amounts of B ₄ C, h-BN and unreacted C in the products of the experiments conducted for 30 minutes to 2 hours at 1500°C with plain and 10 wt% CaCO ₃ added mixtures.	69
Table 4.6. Average crystal thickness values of h-BN formed from plain and CaCO ₃ added mixtures.	71
Table 4.7. Amounts of h-BN and B ₄ C obtained in the products of the experiments conducted with 10wt% MgO addition.	90
Table 4.8. Amounts of h-BN and B ₄ C obtained in the products of the experiments conducted with 10wt% BaCO ₃ addition.	92
Table 4.9. Amounts of h-BN and B ₄ C formed in the products of the experiments conducted with plain B ₂ O ₃ +C mixtures and compositions with various additives.	111

Table 4.10. Specific surface areas, observed grain sizes in SEM and average crystal thickness of h-BN powders obtained from plain, 2.5wt% Cu added, 10wt% CaCO₃ added, 10wt% CaCO₃ and 2.5wt% Cu added mixtures in 2 hours. 111

CHAPTER I

INTRODUCTION

The oxide ceramics, although being widely utilized today, do not meet some of the present and future technological needs. These materials are being replaced by advanced or high performance materials having desired microstructures and performance properties. Non-oxide ceramics, such as borides, carbides, nitrides and silicides possess high hardness, mechanical strength; corrosion, oxidation and thermal shock resistance. One important flaw is their brittle characteristic. Today these materials are receiving more attention than their oxide counterparts. New processing routes in materials science enable production of these materials cheaply with high efficiency and in high purity [1,2].

Hexagonal boron nitride (h-BN) has a unique place in the wide range of non-oxide advanced ceramics. It has three most important properties: lubricating, refractory and electrical. It is used in high temperature lubrication, as insulators and coolers in electronics and in production of crucibles for molten metal handling, etc [3,4]. Due to its useful properties and wide application field, a significant need has arisen for cheaper and more efficient methods for manufacturing boron nitride. Turkey holds most of the boron reserves in the world; however production of processed materials containing boron is still very limited in Turkey [5,6]. Therefore it is essential to investigate the production methods of advanced ceramics containing boron.

One of the important production techniques of h-BN is carbothermic reduction of boric oxide in nitrogen atmosphere [5]. Studies indicate that B_4C also forms during the initial periods of the reaction which then reacts with B_2O_3 to form h-BN. The role of B_4C , which forms during this process, is not clear in the literature [7]. Additionally, efficiency of h-BN formation, in terms of carbon usage, is low and carbon loss from the system is high [8]. Some additives are known to catalytically affect h-BN formation [9]. The aim of this study is to investigate the role of B_4C in formation of boron nitride by carbothermic reduction and nitridation of boric oxide and to study the catalytic effects of some alkaline earth metal oxides and carbonates, some transition metal oxides and cupric nitrate.

CHAPTER II

LITERATURE REVIEW

Hexagonal boron nitride (h-BN) is one of the important advanced ceramics. Due to its excellent refractory, lubricating and electrical properties it meets the requirements for a wide range of applications [3,4]. Among many techniques, carbothermic reduction of boric oxide in nitrogen atmosphere is reported to be the most widely used one for the industrial production of h-BN [5]. B₄C was reported to be present in the reaction products in the early stages of reaction during production of h-BN by this process [8,10]. One of the concerns of this study is to investigate the role of boron carbide in the carbothermic production of h-BN. The reaction rate and efficiency of carbothermic production was low [8,10]. Therefore, the other aim of this study is to explore the catalytic effects of some alkaline earth metal oxides and carbonates such as CaCO₃, MgO and some transition metal oxides such as Fe₃O₄, MnO₂ additions on the carbothermic formation of h-BN. When the reactions were conducted at or below 1500°C, grain size of the formed h-BN was small in this process. Due to this fact, effect of cupric nitrate addition on the grain growth of h-BN was also examined in this study by adding it into the starting reactant mixture.

In this section, the phases of boron nitride, properties and applications of h-BN will be reviewed. Production techniques of h-BN will be examined while giving emphasis to the carbothermic method.

2.1 Phases of Boron Nitride

Due to the special bonding characteristics of boron and nitrogen, boron nitride (BN) exists in many different structures. Boron and nitrogen are on the right and left of carbon on the periodic table, as a result the BN phases are isoelectric to the corresponding carbon phases. Properties of BN phases are dependent on their crystal structures and show distinct properties from each other. The well-defined crystallographic structures are hexagonal BN (h-BN), rhombohedral BN (r-BN), wurtzitic BN (w-BN), and cubic BN (c-BN). Additionally, amorphous and turbostratic BN (t-BN) structures exist [4]. The crystal structures of these phases are illustrated in Figure 2.1. Turbostratic structure presents a layer structure similar to h-BN while the layers are disordered and they are not aligned in the direction of the c-axis as shown in Figure 2.1 (f). The important BN phases are cubic and hexagonal. h-BN is soft and lubricating however c-BN is hard and abrasive. The atomic structure of c-BN is similar to that of diamond and in fact it is the second hardest material after diamond. c-BN is synthesized from h-BN at high temperatures and pressures ($>1500^{\circ}\text{C}$, $>60\text{kbar}$) [4,11]. Rhombohedral boron nitride (r-BN) is similar to h-BN as shown in Figure 2.1 (e), but it has an ABC type alternating sequence of layers. Wurtzite BN (w-BN), which is a high pressure phase, is another hard phase of BN [4].

Hexagonal BN crystallizes similar to graphite in a layered hexagonal structure and it is often called as `white graphite`. The atomic planes are formed of hexagonal rings built by B and N atoms. The covalent bonds between the atoms forming the ring are very strong (sigma bonding, sp^2 hybridization). However the van der Waals bonding forces between the atomic planes are weak (pi bonding). The easy sliding of these planes due to this weak bonding is the origin of the lubricating nature of h-BN. As can be seen in Figure 2.1 (c and d), the planes are stacked on top of one another without any horizontal displacement; consequently the atoms of B and N are alternating along the c-axis. In graphite, carbon atoms in adjoining layers are not superimposed. The interlayer spacing of h-BN, which is 3.33\AA is

similar to that of graphite, which has an interlayer spacing of 3.35\AA . Hexagonal BN is an electrical insulator and has a white color due to the location of pi-electron at the nitrogen atom which results from the higher electronegativity of the nitrogen atom [4,11]. Consequently, unlike graphite, the electrons are not in the conductivity band and therefore they do not play a role in conductivity or absorbing visible light; whereas graphite, consisting of only carbon atoms, has a black color and it is an electrical conductor.

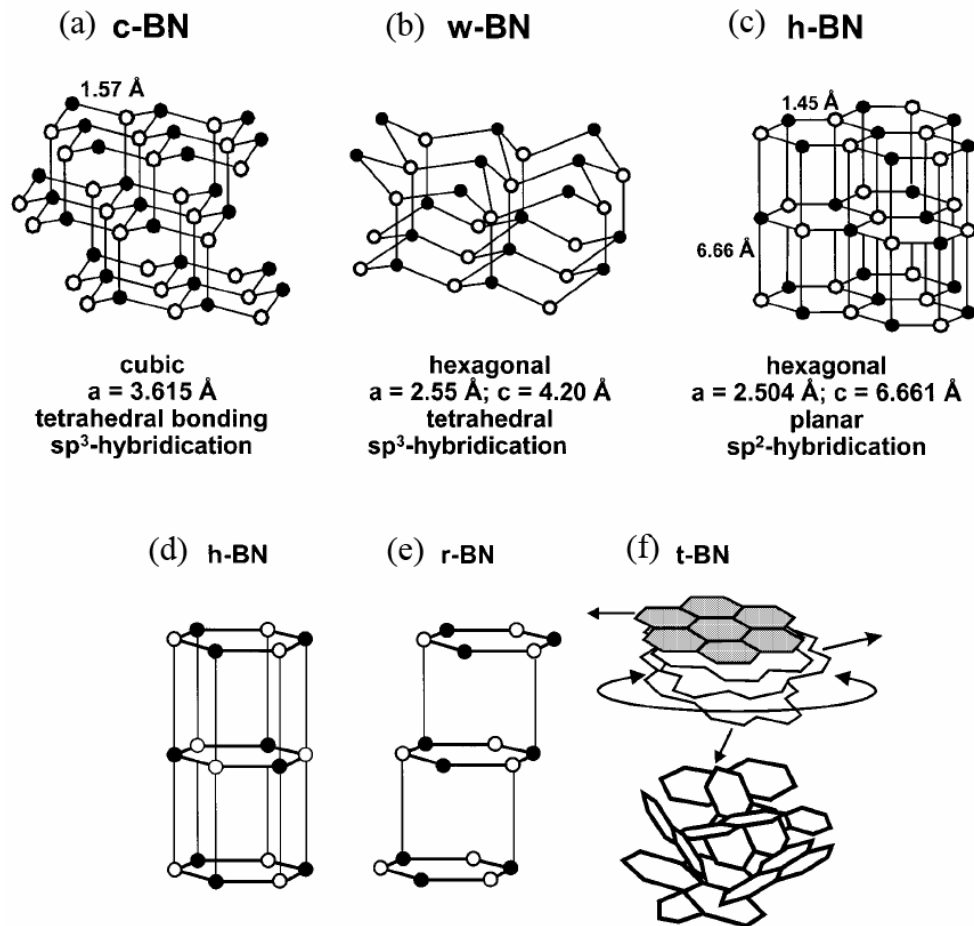


Figure 2.1. Crystal structures of boron nitride phases [4].

2.2 Properties of Hexagonal BN

Hexagonal BN can be produced by numerous different techniques such as carbothermic reduction and nitridation of boric oxide or reaction of urea with boric acid [4]. According to the synthesis method and/or conditions; crystallinity, purity, grain size and shape of h-BN may show variations, which are responsible for the differences in the physical properties. These variations can lead to unreliable mechanical properties and variable oxidation stability. Therefore, processing method and parameters are of utmost importance for the final properties and area of utilization of the produced h-BN powder. For example, h-BN powders with small grain size and high specific surface area are suitable for sintering and producing bulk articles [11], whereas powders with large grains and good crystallinity are suitable for lubrication and have better high temperature properties.

Hexagonal BN has good thermal conductivity, solid lubricity, and good electrical insulation properties. It is stable in air up to 1000°C, in vacuum to 1400°C and in inert atmosphere to 2800°C [4]. However, in some sources there are different data on the high temperature behavior of h-BN. Paine et. al. [11] reported that h-BN sublimates above 2330°C in nitrogen atmosphere. In other sources maximum operating temperature of h-BN is stated as 2000°C or 2400°C [3,12] and sublimation temperature as 3000°C [13]. These differences may have arisen due to variances in purity or degree of crystallinity of investigated h-BN.

Some important properties of h-BN are reported in Table 2.1, in comparison with graphite, alumina (Al_2O_3) and aluminum nitride (AlN). Hexagonal BN has a relatively low theoretical density, 2.27g/cm^3 . It has high thermal conductivity and dielectric strength. Its dielectric constant is about 4 and dielectric strength is almost 4 times higher than alumina. Its thermal shock resistance is very high and thermal expansion is low. Due to these properties, h-BN is starting to take the place of AlN in insulator and cooler parts in electronics. h-BN is not wetted by

many metallic melts such as Al, Cu, Zn, Fe and non-metallic melts such as Si, B and glasses. In addition, it is chemically inert to most of these molten metals and slags. It is quite soft and it can be shaped by hot pressing and machined easily [3,4,12]. However, h-BN is gradually hydrolyzed upon long exposures to moisture. If additives such as SiO₂ or Ca are not used as sintering additives, free B₂O₃ reacting with moisture, can induce surface spalling and cracking [14].

Table 2.1. Properties of h-BN, graphite, Al₂O₃ and AlN [13,15,16,17,18].

(// : parallel to C-axis, ⊥: perpendicular to C-axis)

	h-BN	Graphite	Al ₂ O ₃	AlN
Theoretical Density (g/cm ³)	2.27	2.1-2.2	3.98	3.26
Melting Point (°C)	3000	3700	2015	2200
Hardness knoop (kg/mm ²) Mohs	205 2	2	2000 9	1200
Dielectric Constant	4.2	-	9.7	10
Dielectric Strength (kV/mm)	35	-	9	14
Volume Resistivity (ohm-cm)	1*10 ¹³ (RT) 3*10 ⁴ (1000°C)	109*10 ⁻⁶ (RT) 8- 15*10 ⁻⁴ (1000°C)	1*10 ¹⁶ (14°C) 3*10 ¹³ (300°C)	10 ¹³
Thermal Conductivity at RT (W/m.K)	71 // 121 ⊥	95 // 138 ⊥	17-33	180-220
Thermal Expansion Coefficient (/C*10 ⁶)	0.7 ⊥ 7.5 //	32 ⊥ 46 //	7.1	4.1
Working Temperature (°C) in Air In inert atmosphere In chlorine environment	1000 3000 700	330 1650 -	1700 2000 -	1350

In Figure 2.2 high temperature lubricating behavior of some important lubricants are compared. Due to its stability, h-BN enjoys its low coefficient of friction up to much higher temperatures than the other commercial lubricants [19].

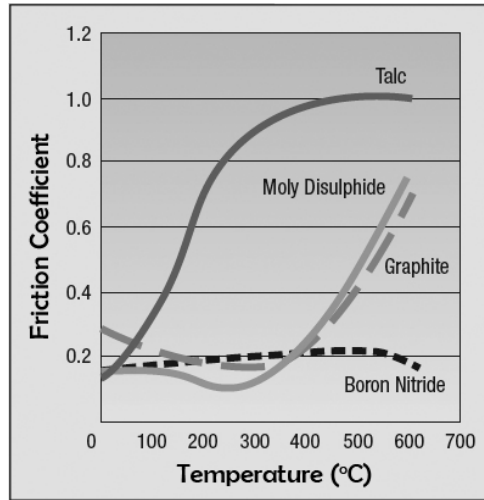


Figure 2.2. Variation of coefficient of friction of some important lubricants with temperature [19].

2.3 Applications of Hexagonal BN

Due to its excellent properties, h-BN finds place in various industrial applications. Most important of them are high temperature lubrication, as crucibles in molten metal handling, as insulators and coolers in electronic circuits, and as additives in other ceramics and polymers. It is possible to utilize h-BN in many forms including hot pressed solids, powders, fibers, in aerosols and as dispersed powders in liquid media [3,4,11,12].

Hexagonal BN powders can be tailored to very specific applications by modifying the process parameters. Hexagonal BN powders produced at high temperatures or by use of some additives exhibit low surface area and coarse grains. This type of

h-BN has good thermal conductivity and lubricating properties, but poor sinterability. On the other hand, fine h-BN particles with irregular grain shape and high dislocation density can be produced under another set of parameters. This powder is ideal for sintering due to its high dislocation density; irregular grain shape and boric oxide content [11].

Hexagonal BN is used as a lubricant in oxidizing atmospheres up to 900°C, which is much higher than the maximum use temperature of graphite (~400°C). It can be used as a solid surface lubricant, as additions into alloys or ceramics or as dispersions in liquid medium having lubricating properties. It is used for reinforcing ceramics and alloys to reduce wear and friction. Thus, self lubricating parts can be obtained [20]. Liquid lubricants, mineral or silicon oils or highly viscous organic components are used with h-BN dispersions for increasing high temperature lubrication properties [4,21,22].

As a surface coating agent, it is mainly employed for its inert, non-sticking and non-oxidizing behavior. In this application, it is used as die coatings in forming processes and casting. Hexagonal BN coatings in molds reduce sticking and reactions between the material and the mold and provide easy releasing. These coatings are used in metal industry, as well as glass, plastic and rubber industry. They extend mold/die life and increase processing speeds. Hexagonal BN coatings can be produced by CVD techniques, as well as spraying, brushing, dipping or pouring [4,15]. Water based coatings of h-BN are used to protect graphite articles from oxidation [15]. Hexagonal BN coatings containing organic or inorganic binders have excellent handleability, however they have lower use temperature and purity as compared to binderless coatings [15].

Pyrolytic boron nitride (PBN), deposited on graphite by high temperature reaction of ammonia and a boron halogenide, has a very high degree of crystal orientation. Crucibles produced by this technique present a thermal conductivity around the

wall of the coating about 40 times higher than through its thickness. Therefore, PBN is used in many leading edge processes as crucible materials [19].

BN can be shaped and sintered into dense bodies by hot pressing (HP) or hot isostatic pressing (HIP). Well crystallized h-BN is very difficult to sinter and requires very high temperatures, therefore for sintering, amorphous or turbostratic BN is used [4,23,24]. MgO or CaO has been added together with boric oxide into h-BN powder in order to improve its sintering characteristics. The purpose of these metal oxides is to reduce the volatility of B_2O_3 in the hot pressing operation [11]. Hexagonal BN ceramics produced by HP show anisotropic mechanical, thermal and electrical properties depending on the hot pressing direction. Due to the high temperature stability and chemical inertness of h-BN, shaped articles are used as molds and crucibles for containment of liquid metals or slags. They are also used as break rings in continuous casting of steel or in the non-ferrous industry [4]. Due to the different sintering additives used, which are necessary for sintering of h-BN at lower temperatures and to higher densities, properties of sintered parts may show differences [11].

In the last decade, h-BN found increasing attention in advanced ceramic composite applications [11]. It can be added into nitride, oxide, boride or carbide ceramics. Addition of h-BN into these ceramics increases machinability, resistance against molten metals [4], thermal shock resistance and decrease elastic modulus [11]. Some important ones of these are SiC/h-BN, Si_3N_4 /h-BN and Al_2O_3 /h-BN [11,15]. These composites find application as nozzles in continuous steel casting [1,4]. TiB_2 -BN composites are used for high temperature applications such as evaporator crucibles and boats. Due to the high electrical conductivity of TiB_2 , these composites can be used for electrodes. More than 70% of world h-BN production is used for producing TiB_2 -BN composites [4]. Before the last decade, the primary application for h-BN was for the construction of high-temperature crucibles and other pressure sintered parts [11].

Combination of high thermal conductivity of h-BN with its excellent electrical insulating and dielectric properties makes it suitable for a variety of applications in electric industry. Hexagonal BN is used as heat sinks and substrates due to its high thermal conductivity and low thermal expansion. Cooling components made of boron nitride added to polymers are used effectively in transferring thermal energy away from electronic circuits, due to high thermal conductivity and electrical insulating nature of boron nitride. Adding boron nitride into plastics is a growing area. Depending on the type of the plastic, in which boron nitride is added, it reduces friction, increases thermal conductivity, reduces thermal expansion and friction coefficient and increases use temperatures [3,22]. Due to its white color and lubricious nature, boron nitride is used even in cosmetics [3].

2.4 Synthesis Methods of Hexagonal BN

BN is not found spontaneously in nature and it has to be produced synthetically. The first synthesis of BN was achieved in 1842 by Balmain by the reaction of boric acid with potassium cyanide. However, the product was not stable and BN did not become a commercial material until 1950s due to the technical difficulties in synthesis methods and high cost of this material [4].

Today, three principal methods are utilized for the production of h-BN in the industrial scale [4,5,11]. According to some sources, reaction of boric acid with ammonia is suggested to be the most widely used method [4,25]. According to some others, carbothermic method is the principal industrial method [5,11]. The other method is the reaction of nitrogen containing substances such as urea or melamine with boron containing substances like boric acid [26,27,28].

Approximately 400 tons of h-BN is produced annually by the manufacturers all around the world. Main manufacturers are in the United States, Japan and some countries of the former Soviet Union and Europe. Its price is 50-150 USD per kg, depending on the purity of the product [4,12].

Below are a figure and a list of the various production reactions and methods of h-BN. The major techniques will be taken on in the following sections. In the present study, carbothermic method has been investigated. Therefore, it will be introduced in more detail.

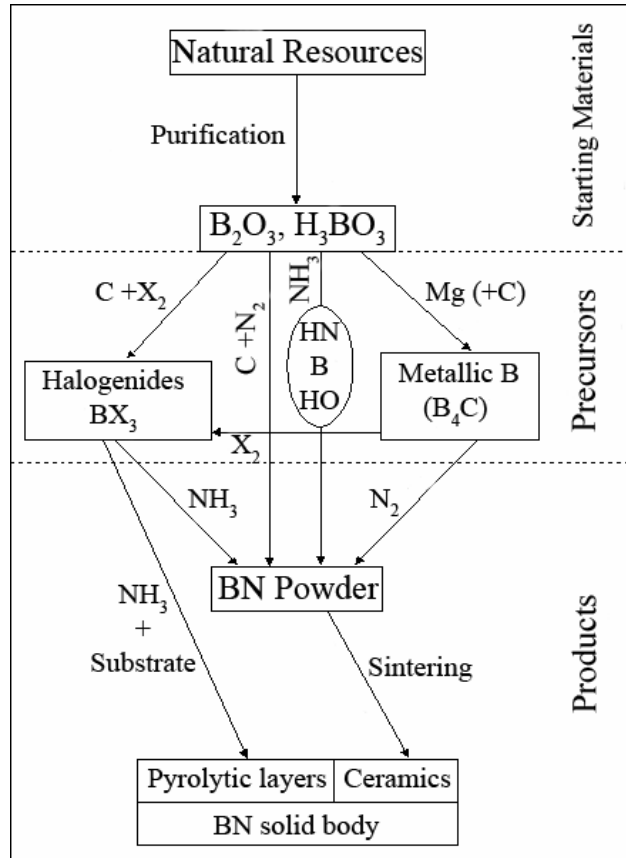


Figure 2.3. Various h-BN preparation methods [29].

- Reaction between elemental boron and nitrogen or ammonia [30].
- Reaction between calcium boride (CaB_6) and boric acid. [31]. These compounds were reacted in nitrogen at temperatures above $1500^\circ C$. Iron boride (FeB) was also reacted instead of calcium boride with ammonia over $1000^\circ C$ in order to form BN [32].

- Reaction of boric acid or boric oxide with ammonia in the presence of an inert carrier such as calcium phosphate or oxide [25].
- Reaction of boric oxide with carbon in nitrogen atmosphere [7,8,10].
- Reaction of boron containing substances such as boric acid, boric oxide or alkali borates with nitrogen containing substances like urea or melamine [26,27,28].
- Deposition of h-BN from gas phase has been performed from B₂H₂-NH₃-H₂ or BCl₃-NH₃-H₂ gas mixtures [33,34]. The gas mixtures can be activated by plasma assisted CVD.
- Pyrolytic boron nitride is manufactured by reacting ammonia with a boron halogenide at temperatures of 2000°C. The resulting BN is vapor deposited on graphite substrates and it can either be removed from the substrate or left as a coating on the graphite [15].
- Hexagonal BN fibers are produced from decomposition of boric acid impregnated cellulose [35].
- In the metallothermic production of boron nitride, sodium or magnesium metal has been used as the reducing agent [36,37]. The reaction with the sodium metal proceeds as:



The metallothermic reactions are initiated by heating to 300°C and the temperature rises to about 800°C due to the exothermic nature of the reactions. The product, containing boric oxide and oxides of the metal is washed with dilute acid for purification. In another metallothermic process, anhydrous borax, Na₂B₄O₇ was reacted with magnesium and ammonia at 650-900°C to yield BN [38]. The crystal structure of the BN produced in the metallothermic studies is not stated in the reported studies but it is known that at relatively low temperatures (<1000°C) mostly turbostratic boron nitride forms [39].

2.4.1 Reaction of Boric Acid or Boric Oxide with Ammonia

Boric acid and ammonia reacts (Reaction (2.2)) in the presence of an inert carrier substance such as calcium phosphate ($\text{Ca}_3(\text{PO}_4)_2$) or CaCO_3 . Generally, temperatures above 900°C are used for this reaction [12,25]. Without the presence of the carrier substance, the reaction is very slow due to the boric oxide melt which has a very low surface area. The grains of the carrier are wetted by the boric oxide melt, thereby the surface area for the reaction is increased. After the reaction, carrier can be removed by leaching with dilute acid solution. Due to the low temperature of the reaction; formed BN has an amorphous structure and contains oxygen impurities. A second treatment above 1500°C under N_2 is necessary to obtain the hexagonal crystal structure of h-BN and to remove the oxygen impurities [4,25].



2.4.2 Reaction of Boric Acid with Nitrogen Containing Organic Materials

Another important method of h-BN production is the reaction of boric oxide, boric acid or alkali borates with nitrogen containing organic compounds such as urea, melamine or amides, cyanides and cyanamides, etc.[12,26,27,28,40]. Reaction of boric oxide with urea is presented below:



After mixing and pre-reacting the starting materials at 300°C , reactions are carried out above 900°C in N_2 . A second treatment is applied above 1500°C in N_2 for removing oxygen impurities and for crystallization after removing the non-reacted materials by washing with methanol or dilute acids [4]. Figure 2.4 shows typical powder X-Ray diffraction (XRD) patterns ($\text{Cu-K}\alpha$) of turbostratic to hexagonal transformation of boron nitride with temperature. Turbostratic starting material

used in this example was produced by thermal decomposition of melamine diborate in flowing nitrogen at 900°C [38]. It is seen in this figure that t-BN, having broad peaks, become more ordered with more intense and narrower peaks upon increasing temperature. The width of h-BN peaks decreases and (10) peak resolves into (100) and (101) peaks, which indicate an increasing of crystallization.

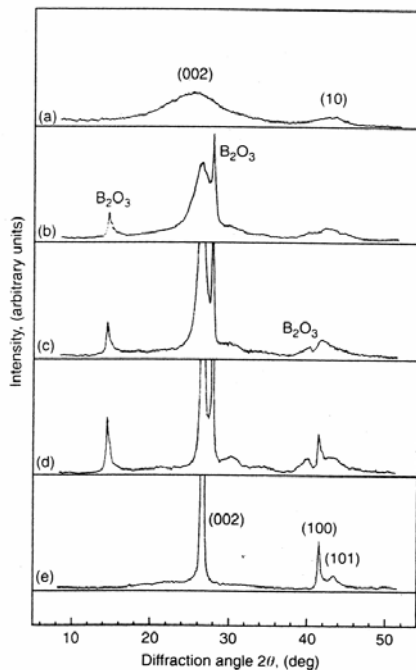


Figure 2.4. XRD patterns of the samples obtained at different temperatures, (a) starting material (t-BN), (b) 1000°C, (c) 1300°C, (d) 1600°C, (e) 2000°C [38].

Crystallization behavior of t-BN, which was produced by the reaction of boric oxide with ammonia, was investigated by Alkoy et. al. [41]. It was found from the experiments performed by holding t-BN in argon atmosphere at 1500°C for ½-5 hours that the rate of crystallization decreased significantly after the first hour. Degree of crystallization was determined from the relative peak heights of the formed h-BN. Variation in the interlayer spacing, d_{002} was also investigated; and it

was stated that the decrease of this value by heat treatments indicated an increase in the ordering of the crystal structure.

In another study concerned with production of h-BN by the reaction of boric acid with nitrogen containing organic compounds, the use of CaCO_3 as a catalyst has been investigated. [42]. It was reported that the addition of CaCO_3 into the starting mixture of melamine and boric acid, yielded h-BN powder with high crystallinity and low specific surface area after firing at 1800-2100°C. Larger grain size and higher crystallinity lead to better lubricating and electrical insulating properties and high temperature stability of h-BN [11,26,43].

The effect of copper on the crystallization of h-BN was studied by Hubacek et. al. [44]. They investigated the crystallization of t-BN with the addition of cupric nitrate. They also investigated nitridation of elemental amorphous boron which was mixed with 15wt% cupric nitrate. These investigations were made considering the facts that many metals of groups IVa –IVb produces graphitization of hard carbons and that crystal structure of graphite resembles h-BN. It was found from the experiments performed by holding the amorphous B or t-BN at 1950-2150°C under nitrogen atmosphere that the grain size and crystallinity of the formed h-BN was immensely improved when Cu was added. It was suggested that Cu accelerates mass transport for the crystal growth of h-BN [44].

In another study of Hubacek et. al. [45], the interaction between Cu and h-BN has been investigated under hot pressing conditions. Two types of t-BN were prepared by the reaction of urea and boric oxide, one of which contained well dispersed Cu atoms formed by dissolution of copper-nitrate. The other t-BN contained metallic Cu in powder form, which was obtained by mechanical mixing. It was found that the t-BN which contained Cu in powder form showed only a slight increase in crystallinity and grain size upon heating to 1950°C. However, the t-BN containing atomically dispersed Cu showed an extensive increase. Therefore, it was

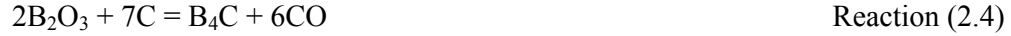
suggested that Cu did not act through a dissolution-crystallization mechanism, since the Cu in powder form was not effective. The mechanism of atomically dispersed Cu was suggested to be due to the interaction of the copper electronic orbitals with (002) planes of h-BN crystals. This interaction provided the growth of h-BN crystal by aligning and adjoining of the crystallites, during which the Cu atom was released.

2.4.3 Carbothermic Method

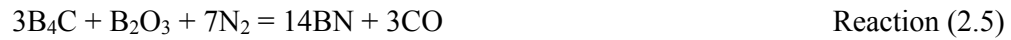
Carbothermic reduction processes have been used in the synthesis of variety of compounds such as carbides, borides and nitrides. During carbothermic reduction, nitridation can be applied in order to produce desired nitrides by conducting the process in a nitrogen atmosphere [1]. If the reactions are carried out in an inert atmosphere such as argon, then carbide products can be obtained. One important advantage of the carbothermic reduction over the metallothermic ones is that the side products such as CO are in gaseous form and are readily removed from the system during the processes. However, the products obtained at the end of the metallothermic reductions mostly need to be leached in acid solutions in order to remove the metal oxide side products.

In the carbothermic production of h-BN, boric oxide is reduced with carbon in the presence of pure nitrogen gas at temperatures above 1200°C [4,8,10,11]. Carbothermic production is stated as the most commonly used industrial technique of h-BN production [5,11].

There have been some studies in order to reveal the reaction mechanism of formation of hexagonal boron nitride by the carbothermic reduction of boric oxide. In the study of Pikalov [7], it was presumed that formation of h-BN took place through separate reduction and nitridation steps. At first formation of boron carbide takes place as the reduction products, by the reaction of boric oxide and carbon (Reaction (2.4)).



Then, by the reaction of boron carbide and boric oxide in the presence of nitrogen, h-BN formation takes place (Reaction (2.5)). It was found that the interaction of boron oxide and carbide in nitrogen took place through the gas phase.



In another study on the carbothermic formation of boron nitride, Bartnitskaya et al. [10] concluded that boron nitride forms through the following general reaction in the zones of contact of the boron suboxide with carbon particles to which nitrogen can penetrate:



Boron carbide was suggested to form according to Reaction (2.4) in regions where the supply of nitrogen is inhibited. Accordingly, the formation of boron carbide in the initial stage of the reaction was explained by the fact that nitrogen could not penetrate the boric oxide melt. Further reaction of boron carbide and oxide in the presence of nitrogen leads to the formation of boron nitride as given in Reaction (2.5).

Yoon and Jha [46] examined the B-N-C-O system and claimed that BO is the boron containing gaseous species in the carbothermic formation of boron nitride. However, it has been shown by Aydoğdu and Sevinç [8] that equilibrium vapor pressure of BO is much lower than that of B_2O_3 at 1500°C and it was concluded that gaseous B_2O_3 is the reacting species.

Aydoğdu and Sevinç [8] studied formation of h-BN by subjecting pellets prepared from B_2O_3 -activated C mixtures to N_2 gas at temperatures ranging from 1100°C to 1500°C for durations ranging from 15 minutes to 4 hours and found the reaction to

be complete in 2 hours at 1500°C and B₄C, in addition to unreacted B₂O₃, unreacted C and BN formed, to exist in the reaction products of the experiments in which h-BN formation was not complete. They found from the results of experiments directed to the mechanism of the reaction by use of different geometrical arrangements that liquid B₂O₃ and solid carbon need not be in contact in the formation of BN from B₂O₃, C and N₂ and concluded the overall Reaction (2.6) to proceed by evaporation of B₂O₃(l) and reaction of B₂O₃(g) with C(s) and N₂(g) on C(s). By thermodynamic analysis based on Reaction (2.5), they showed that either BN(s) or B₄C(s) but not both can exist in the system at equilibrium and that B₄C(s) is unstable in the system when the $P_{CO}^3/P_{N_2}^7$ ratio is less than a critical value at a given temperature which can be calculated to be 6.7×10^{34} for 1500°C by employing the data used by them. They stated the $P_{CO}^3/P_{N_2}^7$ ratio in their experimental system, where there is a continuous flow of N₂ gas, to be expected to be less than the critical ratio when B₄C is expected not to be present in the system and suggested B₄C to form in regions of the pellet where N₂ pressure is too low due to insufficient penetration of nitrogen gas. They concluded that some h-BN forms according to the overall Reaction (2.6), some according to Reactions (2.4) and (2.5) taking place successively and found from experiments conducted by subjecting commercial B₄C – B₂O₃ mixtures to N₂ gas the rate of Reaction (2.5) to be lower than that of Reaction (2.6). While B₄C appears to be a necessary intermediate product according to Pikalov [7], the results of Aydoğdu and Sevinç imply B₄C formation not to be necessary in carbothermic formation of BN. However, due to the fact that the commercial B₄C powder used in their experiments had relatively coarse grain size, they reported that their results were not conclusive [8].

Therefore, in the present study, in order to obtain a more accurate insight about the reaction mechanism, B₄C powder was produced in the same experimental setup that h-BN was produced, but argon gas was used instead of nitrogen. The produced B₄C powder, having similar size and morphology to that forming in nitrogen atmosphere during h-BN production, was mixed with B₂O₃ and reacted

in nitrogen atmosphere in order to produce h-BN according to Reaction (2.5). This investigation was one of the aims of the present study.

Dependence of free energy change of various reactions related to the studied system on temperature is presented in Figure 2.5. This figure was plotted by utilizing the enthalpy and entropy of formation data compiled by Turkdogan [47]. Data for the reactions involving $B_2O_2(g)$ was obtained from Lamoreaux et. al. [48].

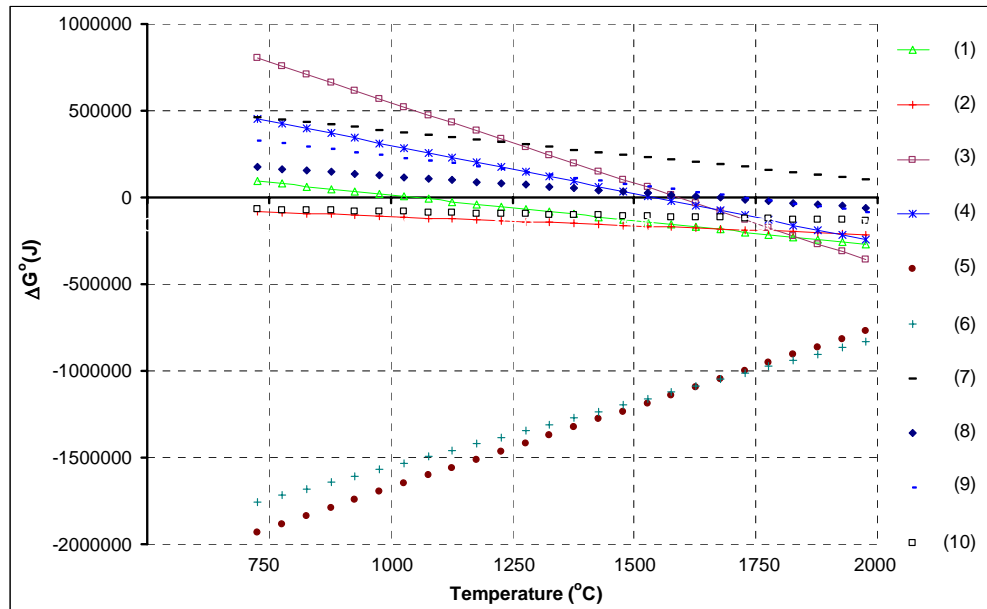


Figure 2.5. Free energy change versus temperature plots for the reactions: (1) $B_2O_3(l) + 3C + N_2 = 2BN + 3CO$, (2) $B_2O_3(g) + 3C + N_2 = 2BN + 3CO$, (3) $2B_2O_3(l) + 7C = B_4C + 6CO$, (4) $2B_2O_3(g) + 7C = B_4C + 6CO$, (5) $3B_4C + B_2O_3(g) + 7N_2 = 14BN + 3CO$, (6) $3B_4C + B_2O_3(l) + 7N_2 = 14BN + 3CO$, (7) $B_2O_3(g) + C = 2BO(g) + CO$, (8) $B_2O_3(l) = B_2O_3(g)$, (9) $B_2O_3(l) + C = B_2O_2(g) + CO$, (10) $B_2O_2(g) + 2C + N_2 = BN + 2CO$

The increase of the demand on h-BN and the requirement of high temperatures in the mentioned production processes have lead to further research on finding ways

to increase the rate and to decrease the temperature of h-BN formation reaction. Studies on the use of catalysts have been reported in the previously mentioned methods of h-BN production. However, in the literature there are only a few studies about the effect of catalysts on the carbothermic formation of h-BN [7,9,10,]. In a study [9], the reaction of boric oxide with carbon and nitrogen has been examined with addition of some catalysts such as metal oxides and carbonates. It was stated from the results of the experiments conducted at 1400°C that when the additives were used the conversion of boron in the starting mixture into h-BN increased. The mechanism of increasing the efficiency of these kind of additives was suggested to be loosening of the B_2O_3+C aggregate during reaction, increasing the surface area for reaction and providing easier N_2 penetration into the system. However, no information was given on the chemical reactions taking place between these additives and the B_2O_3+C mixture.

In another study, catalytic effect of some lithium compounds such as Li_2CO_3 and $LiOH$ on the yield and three-dimensional crystallographic ordering of h-BN was investigated by Bartnitskaya et. al. [49]. It was found from the experiments conducted at 1500°C for 3 hours in nitrogen atmosphere that when Li_2CO_3 was added to the initial boric acid-carbon black mixture at an amount of 12%, the amount of h-BN formed was about twice the amount formed in the experiments without Li_2CO_3 . The crystal structure of the formed h-BN was also seen to be improved by the addition of Li_2CO_3 . A so called catalyst-solvent mechanism was suggested for the role of Li_2CO_3 , in which Li_2CO_3 reacts with B_2O_3 resulting in a lithium borate melt [50,51]. Then, h-BN forms and crystallizes through the formed melt.

The abundance and low cost of $CaCO_3$ make it a suitable catalyst material for the carbothermic production of h-BN. In the present study, catalytic effect of some alkaline earth metal oxides and carbonates, namely $CaCO_3$, MgO and $BaCO_3$ and some transition metal oxides, namely Fe_3O_4 , MnO_2 , Co_3O_4 on the formation of h-

BN by the reaction of boric oxide with carbon under nitrogen atmosphere has been investigated. Emphasis has been given to CaCO_3 .

Positive effect of Cu on grain growth and crystallization of h-BN during its production through urea and boric acid had been reported [44,45]. However, effect of Cu addition on the carbothermic formation of h-BN has not been investigated previously. Therefore, in the present study, in order to examine the effect of Cu on the carbothermic formation of h-BN, Cu was added in the form of cupric nitrate trihydrate ($\text{Cu}(\text{NO}_3)_2 \cdot 3\text{H}_2\text{O}$) alone and also together with CaCO_3 into the starting $\text{B}_2\text{O}_3 + \text{C}$ mixture.

CHAPTER III

EXPERIMENTAL SET-UP AND PROCEDURE

Experiments aiming for the investigation of formation of h-BN were performed by holding activated carbon-boric oxide mixtures in a graphite crucible at 1500°C under nitrogen atmosphere for a determined duration. For this purpose, a vertical tube furnace was utilized. Effects of various additives, namely CaCO₃, MgO, BaCO₃, Fe₂O₃, MnO₂, Co₃O₄ and cupric nitrate were investigated by mixing them with the B₂O₃+C mixtures. In the following sections experimental set-up, materials used and experimental procedure will be given.

3.1 Experimental Set-Up

Preliminary experiments were conducted by reacting activated carbon - boric oxide mixtures at 1500°C under nitrogen atmosphere using the same set up used by Aydoğdu and Sevinç [8] in which similar results were obtained. The furnace in this system was a horizontal tube furnace in which the service life of the furnace tube and the heating elements was rather short due to attack of the boric oxide vapor. In the current study the configuration of the furnace was altered in order to increase the lifetime of the furnace elements and the experiments were conducted in a vertical tube furnace which had an 800mm long mullite tube of 50mm inner and 60mm outer diameters. This furnace was constructed in the present study. Top and side view drawings and dimensions of the furnace are presented in Figure 3.1. The mullite tube was closed at both ends by water-cooled brass heads having

thermocouple insertion, gas inlet and outlet tubes. Nitrogen gas was introduced into the furnace from the bottom and the exit gas was removed from the top. The experimental set-up, used in this study is given schematically in Figure 3.2. Gas flow was adjusted by a flowmeter before entering into the furnace and overflow gas was permitted to exit from the system as shown in Figure 3.2. Temperature of the furnace, kept constant at $\pm 1^\circ\text{C}$ by a digital temperature controller, was measured with an S type thermocouple inserted into the system from the bottom. Before the experiments the furnace was heated to and stabilized at 1500°C .

The graphite crucible with its contents was lowered from the top end of the tube into the hot zone of the furnace by hanging to an alumina bar. The interior of the graphite crucible was lined with a thin ($\sim 0.5\text{mm}$) h-BN layer. The configuration of the graphite crucible, alumina bar and the upper brass head of the furnace is presented in Figure 3.3. A radiation shield was utilized in order to protect the upper brass head from overheating due to the radiated heat from the hot zone as shown in Figure 3.3. The radiation shield was cut in a circular shape in order to fit into the mullite working tube. It was made from a refractory fiber-board which was suitable for use at 1500°C . The position of the shield was adjusted so that it stayed a few cm above the hot zone of the furnace. Another one was inserted from the bottom of the mullite working tube, to protect the bottom brass head.

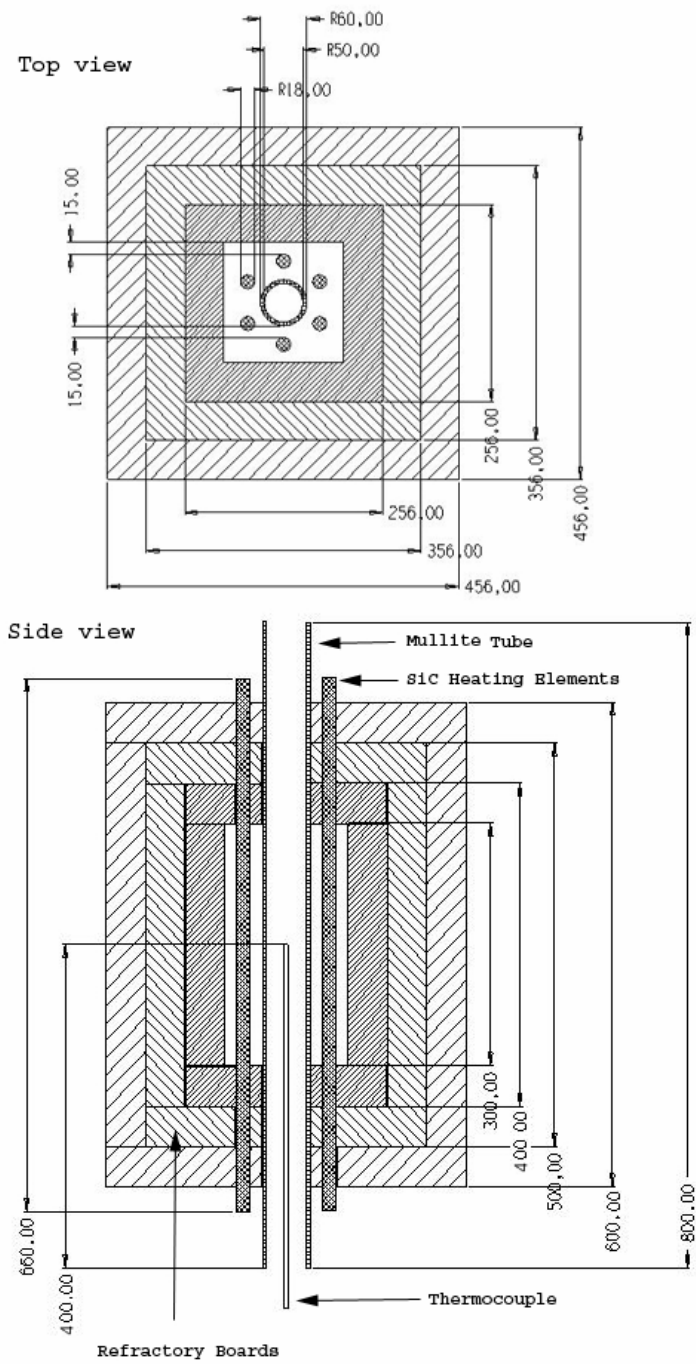


Figure 3.1. Top and side view drawings of the vertical tube furnace in which the experiments were performed. Dimensions are in millimeters.

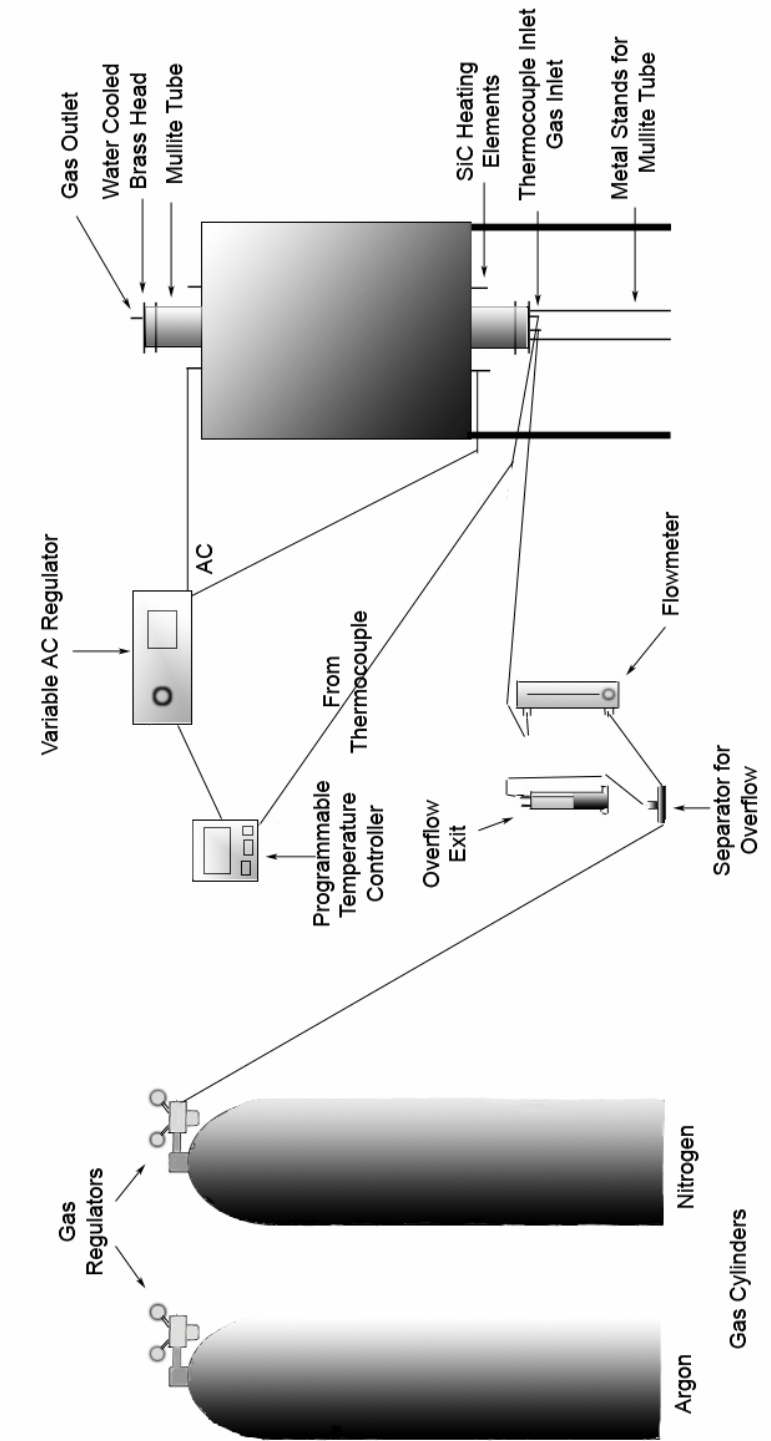


Figure 3.2. Schematic drawing of the experimental set-up.

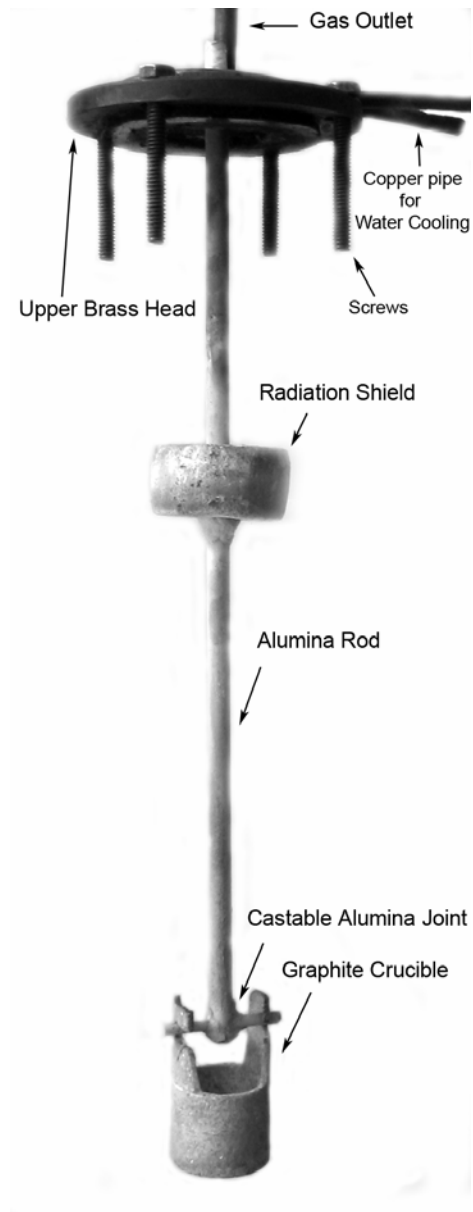


Figure 3.3. Configuration of the graphite crucible, alumina bar and the upper brass head of the furnace.

3.3 Materials Used

The major materials used in this study were activated carbon and boric oxide. Activated carbon (Merck Chemicals) was over 99% purity. Its XRD pattern revealed no peaks indicating that it had an amorphous structure. It was found after complete burning by keeping at 600°C for 40 hours in a muffle furnace that the activated carbon contained 0.3% ash. It is seen from the SEM micrograph of the activated carbon given in Figure 3.4 that its grains did not have a uniform shape and had a wide distribution of particle size. Most particles were in the range of 10-20 microns. There were also particles as large as 50 microns.

Boric oxide was produced by calcination of boric acid (Merck Chemicals) of 99.8% purity at 900°C in an alumina crucible for 1 hour and then by pouring the melt onto the surface of a stainless steel plate. During cooling and solidification, boric oxide separated itself from the surface of the stainless steel plate due to shrinkage. It was then collected and stored as bulk pieces in a closed jar in a desiccator. No other phase was detected by XRD analysis in the produced boric oxide. High purity nitrogen gas (BOS A.Ş.), used in the experiments was of 99.998% purity and contained <30vpm moisture and <50vpm O₂. Argon gas (Habaş A.Ş.), which was used in the production of B₄C, was 99.998% pure and contained 0.9vpm moisture, 2.8vpm N₂, and 1.7vpm O₂.

In order to investigate the effects of various additives, namely CaCO₃, MgO, BaCO₃, Fe₂O₃, MnO₂, Co₃O₄ and cupric nitrate on the carbothermic production of h-BN, they were mixed with the B₂O₃+C mixtures. Identifications, purities and grain sizes of the chemicals that were used in the experiments are presented in Table 3.1.

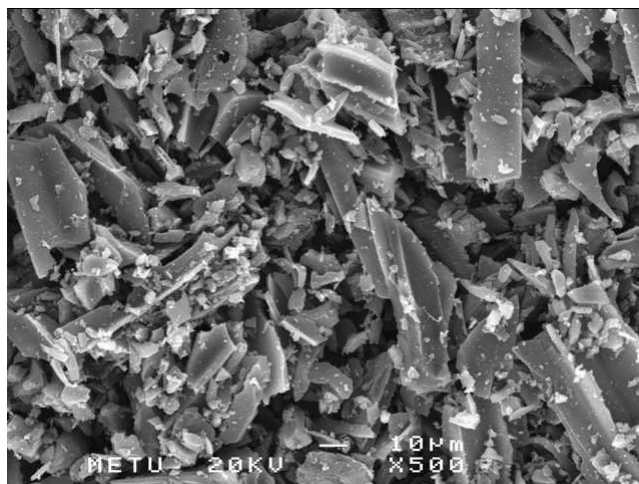


Figure 3.4. SEM micrograph of activated carbon

Table 3.1. Identifications, purities and grain sizes of the chemicals used in the experiments.

Name	Brand	Catalog #	Purity (%)	Grain size (μm)
H_3BO_3	Merck	100165	>99.8	Not specified
Activated C	Merck	102186	>99	<100
HCl (fuming)	Merck	100314	Extra pure 37-38	-
Mannitol ($\text{C}_6\text{H}_{14}\text{O}_6$) (for determination of boric acid)	Merck	105983	Not specified	Not specified
CaCO_3	Merck	102066	>99	About 14
BaCO_3	Aldrich	237108	>99	Not specified
MgO	Merck	105865	>97	Not specified
MnO_2	Aldrich	243442	>99	$63 < x < 250$
Co_3O_4	BDH	1707130	Not specified	Not specified
Fe_3O_4	BDH	1655330	Not specified	Not specified
Cu(II) nitrate pure crystal ($\text{Cu}(\text{NO}_3)_2 \cdot 3\text{H}_2\text{O}$)	Riedel-De Haen	38197	Not specified	Not specified

3.3 Experimental Procedure

Experiments were performed by holding the activated carbon – boric oxide mixtures under nitrogen atmosphere in the hot zone of the tube furnace. Activated carbon - boric oxide mixtures were prepared by grinding and thoroughly mixing in acetone in an agate mortar and pestle. The mixtures contained B_2O_3 100 mole% in excess of the amount calculated in accord with the stoichiometry of Reaction (2.6) to account for loss due to evaporation. In each experiment, a total mixture of 2.5g was used, which consisted of 1.9860g boric oxide and 0.5140g activated carbon.

At the beginning of the experiments, the activated carbon - boric oxide mixture was placed into a graphite crucible. The furnace tube was flushed with N_2 for 5 minutes and the graphite crucible with its contents was lowered from the top end of the tube into the hot zone of the furnace by hanging to the alumina bar. After that, the top end of the tube was closed air tight. Time was taken as zero when the furnace regained its stable state at $1500^\circ C$, which was about 3-5 minutes after the positioning of the sample in the furnace. At the end of the experiments the crucible was quickly removed from the furnace. The crucible and the contents were cooled to room temperature under flow of argon gas in a closed jar. The reaction product was in the form of an aggregate, which was weighed and then cut longitudinally into two pieces. One of the pieces was ground in agate mortar and pestle and subjected to XRD analysis and chemical analysis. The other piece was used for scanning electron microscopy (SEM) examinations on fracture surfaces.

Nitrogen gas flow rates of 50cc/min, 100cc/min, 200cc/min and 400cc/min were tested in the preliminary experiments in order to determine a suitable rate for investigation of the formation of h-BN. It was seen in most of the experiments conducted with 50cc/min N_2 flow rate that there was popping of a flame when the top brass head of the furnace was opened for taking the sample out. Also, the amount of hexagonal boron nitride as well as boron carbide was observed to be less than the amounts obtained at higher flow rates. These results were taken as

indications that there could be a high concentration of carbon monoxide in the system when 50cc/min N_2 flow rate was used, which might have slowed down the reactions. It was observed that nitrogen flow rates above 100cc/min did not have a significant effect on the amount of boron nitride formed. Based on these findings it was decided to use a nitrogen gas flow rate of 200cc/min in the experiments. The BN-coated graphite crucible used to contain the B_2O_3 -activated carbon mixtures had an ID of 2.5 cm, an OD of 3 cm and a depth of 3 cm while the reaction products in aggregate form had depths of 1 to 1.5 cm. Holes close to the circumference of the bottom of the BN-coated graphite crucible used to contain the B_2O_3 -activated C mixtures were drilled in some of the preliminary experiments to have better contacting of N_2 gas with the B_2O_3 -activated C mixtures contained in the crucible and to find if the unoccupied volume above the reaction mix in the crucible to have any effect on the reaction. This geometry was found not to have a significant effect on the quantity of BN and B_4C forming but resulted in higher evaporation loss of B_2O_3 . All of the experiments reported were conducted by subjecting B_2O_3 -activated C mixtures, contained in a BN-coated graphite crucible having no holes at the bottom, to nitrogen gas introduced into the system at a flow rate of 200cc/min.

Boron carbide formation experiments were performed by the same procedure as h-BN formation, but argon atmosphere was used instead of nitrogen. In order to investigate the conversion of B_4C into h-BN, the produced B_4C was then mixed with boric oxide, the amount of which was 150% more than the stoichiometric amount according to Reaction (2.5). The mixture was reacted under nitrogen atmosphere at $1500^\circ C$ for 3 hours and the reaction products were examined.

Effect of various additives, namely $CaCO_3$, MgO , $BaCO_3$, Fe_2O_3 , MnO_2 , Co_3O_4 and cupric nitrate was investigated by mixing them with the B_2O_3+C mixtures and performing the experiments as described above. The emphasis was on $CaCO_3$ (Merck Chemicals) and it was added at amounts of 5-50 wt% of the initial B_2O_3+C mixtures. Durations of the experiments were 30 minutes to 2 hours.

Addition of Cu was in the form of cupric-nitrate, $(\text{Cu}(\text{NO}_3)_2 \cdot 3\text{H}_2\text{O})$. It was added to yield the amount of Cu corresponding to 2.5 and 5 wt% of the $\text{B}_2\text{O}_3+\text{C}$ mixtures. The amount of other additives was fixed at 10wt% of the $\text{B}_2\text{O}_3+\text{C}$ mixtures.

Reaction products were analyzed by a Rigaku Multiflex Powder X-Ray diffractometer with $\text{Cu-K}\alpha$ radiation in the 2θ range of 10° to 80° with 0.02° steps at a rate of $2^\circ/\text{min}$. XRD data was processed and phases were identified by the Qualitative Analysis Program. It is a software embedded in the computer of the XRD device, where smoothing, background subtraction, $\text{K}\alpha_2$ elimination and phase identification operations were performed on the XRD patterns. Grain size and morphology were examined by a Jeol JSM 6400 scanning electron microscope (SEM). FT-IR analyses were performed with a Varian-1000 model unit after mixing the powders with KBr. The amounts of the constituents of the products were determined by following a method, which is very similar to the method used by Aydođdu and Sevinç [8]. The method will be explained in detail in the Results and Discussion section.

Specific surface area measurements of the produced h-BN powders, which were obtained in pure form after the described chemical analysis, were performed by Brunauer-Emmet-Teller method in liquid nitrogen in a BET specific surface area analyzer (Carlo Erba, Sorptomatic 1900). Before the measurements, powders were subjected to ultrasonic vibration in water bath for 30 minutes in order to break up the soft agglomerates.

CHAPTER IV

RESULTS AND DISCUSSION

In this study, experiments were performed with plain B_2O_3+C mixtures and with B_2O_3+C mixtures containing additives; in order to investigate the formation of h-BN by carbothermic reduction and nitridation of B_2O_3 . In this section, first, results of the experiments conducted with plain mixtures will be presented. B_4C was observed to be present in the reaction products of the experiments for which h-BN formation was not complete. B_4C is known [8] to be unstable under the experimental conditions. Experiments were conducted to clarify the role of B_4C . Results of the experiments performed with the aim of gaining information about the role of boron carbide in this process will be shown and discussed. Amount of B_2O_3 in the reaction mix was also varied in the experiments. Findings related to the effect of excess boric oxide amount on the carbothermic production of h-BN will be presented. Finally, results pertaining to the effects of various additives on this process will be given.

4.1. Results of the Experiments Conducted with Plain (B_2O_3+C) Mixtures

Experiments were conducted in order to investigate the formation of hexagonal boron nitride and to determine the duration for the completion of the reaction. In the initial runs the weight of boric oxide in the activated carbon-boric oxide mixtures was 50 mole % in excess of the amount, calculated in accord with the stoichiometry of Reaction (2.6) to account for loss of boric oxide by vaporization.

This quantity of boric oxide was found more than adequate for completion of h-BN formation in the preliminary experiments conducted in the horizontal furnace used by Aydoğdu and Sevinç [8], but the products of experiments conducted in the vertical furnace described before were found to contain boron carbide and h-BN but no boric oxide at 1500°C for durations longer than 2 hours. It is known that some boron carbide forms in carbothermic production of h-BN according to Reaction (2.4), which is then converted into h-BN by reacting with boric oxide and nitrogen according to Reaction (2.5) [46,52]. Reaction (2.5) is known to proceed in the presence of N₂ gas until at least one of B₄C or B₂O₃ is completely used [8]. Presence of B₄C but absence of B₂O₃ in the reaction products stated above indicated that 50 mole% excess boric oxide was not sufficient and that more boric oxide would be necessary for complete conversion of B₄C into h-BN. The higher loss of boric oxide was attributed to the vertical position of the furnace used in the current study. Later experiments were conducted with activated carbon-boric oxide mixtures having 100 mole% excess boric oxide.

Formation of h-BN was followed by powder XRD analysis. The XRD patterns of the products of the experiments conducted with 100 mole% excess boric oxide for 15 minutes – 3 hours are given in Figure 4.1. Hexagonal BN phase (ICDD card # 34-0421) was identified in the XRD patterns and it was seen that B₄C peaks (ICDD card # 35-0798) were present up to 2 hours. The relative peak heights of the products in the XRD patterns indicate that the amount of h-BN increases with increasing duration and the amount of B₄C is high in the early stages of reaction. H₃BO₃ peaks, present in these XRD patterns are due to the formation of H₃BO₃ by hydration of unreacted amorphous B₂O₃ in the reaction products during specimen preparation for the XRD analyses.

The amounts of the constituents of the products were determined by following a method, which is very similar to the method used by Aydoğdu and Sevinç [8]. The method is schematically shown in Figure 4.2 and explained below.

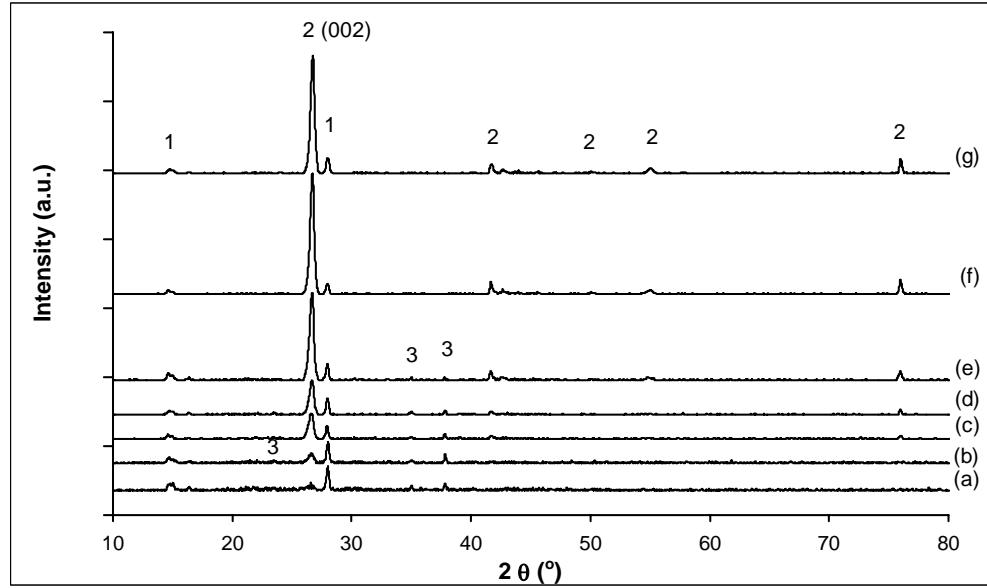


Figure 4.1. XRD patterns of the products of the experiments conducted with plain B_2O_3+C mixtures for (a) 15 minutes, (b) 30 minutes, (c) 1 hour, (d) 1.5 hours, (e) 2 hours, (f) 2.5 hours, (g) 3 hours. (1) H_3BO_3 , (2) h-BN, (3) B_4C .

The product of each experiment was ground in an agate mortar and pestle. In the products, only boric oxide was soluble in water. Therefore, the product was dissolved in water and filtered. Solid to liquid ratio in the leaching operations was 1/100 in weight. The steps of the analysis method were followed by XRD and FT-IR analysis. It is seen in Figure 4.3 (b) and 4.4 (c) that after leaching with water, boric oxide is completely removed from the products and taken into the filtrate. Amount of unreacted boric oxide, $W_{B_2O_3}$, was determined volumetrically by titrating the filtrate with 1N NaOH solution [53].

1N NaOH solution was prepared by dissolving 40g of solid NaOH in 1 liter of deionized water. Then, the NaOH solution was factorized by titrating it with sodium hydrogen phthalate. Before titration of the filtrate, which was obtained by leaching and filtering of the experimental product, mannitol ($C_6H_{14}O_6$) was added

into the filtrate, in order to form a complex with H_3BO_3 in the solution. Phenolphthalein ($C_{20}H_{14}O_{14}$) was added as the indicator. NaOH solution was added dropwise into the filtrate until a pink color was obtained. Volume of the spent 1N NaOH solution until the turning point was recorded and used in the calculation of boric oxide according to the following equation [53]:

$$\%B_2O_3 = \frac{0.003482 \times \text{Factor of NaOH solution} \times \text{Volume of spent NaOH (ml)}}{\text{Weight of dissolved product in water (g)}} \times 100 \quad \text{Equation (4.1)}$$

The residue containing boron carbide, boron nitride and unreacted carbon was placed in a small alumina boat and oxidized at 800°C in a muffle furnace for 15 hours, as a result of which boron carbide was completely converted into boric oxide and unreacted carbon was completely burned. It was found in a previous study [8] that boron carbide gets oxidized but h-BN does not at 800°C . It is seen in Figure 4.3 (c) and 4.4 (d) that after oxidizing at 800°C for 15 hours and 2nd leaching with water, boron carbide is completely removed and pure h-BN is obtained. The presence of activated C could not be followed by XRD due to its amorphous structure. However, due to the fact that the oxidation temperature of C ($\sim 450^\circ\text{C}$) is much lower than 800°C , no C is expected to remain in the samples after 15 hours oxidation at 800°C . The absence of C was verified from visual observations of the product after oxidation, when it became completely white in color.

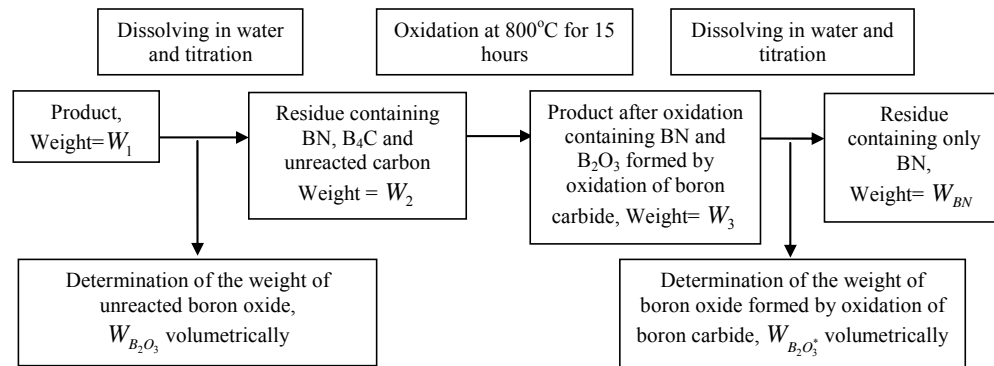


Figure 4.2. Flowsheet of the chemical analysis method employed in this study.

The oxidized products were weighed and dissolved in water and then filtered. Amount of boric oxide, $W_{B_2O_3^*}$, which was formed by the oxidation of boron carbide was determined volumetrically by titrating the filtrate with 0.5N NaOH solution, from which the amount of boron carbide was calculated by use of the equation: $W_{B_4C} = W_{B_2O_3^*} / 139.24 \times 55.25$. The final product contained only h-BN. Amount of boron nitride was calculated by subtracting the amount of boric oxide, $W_{B_2O_3^*}$, formed by the oxidation of boron carbide from the weight of the products after oxidation: $W_{BN} = W_3 - W_{B_2O_3^*}$. Calculated weight of boron nitride was also verified by weight of the final product. Amount of unreacted carbon was calculated by subtracting the weight of boron carbide and boron nitride from the weight of the product before oxidation: $W_C = W_2 - W_{B_4C} - W_{BN}$.

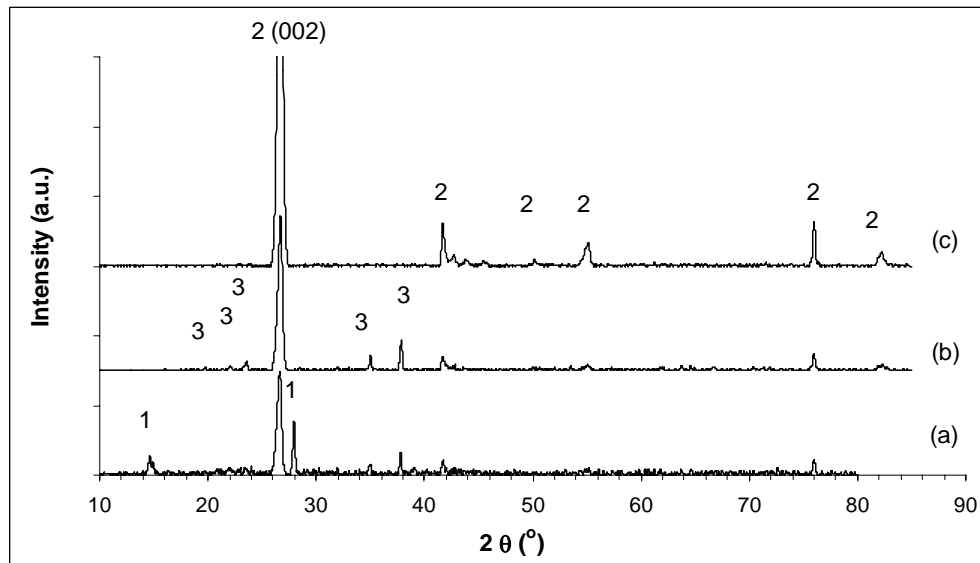


Figure 4.3. XRD patterns of (a) sample obtained in the experiment conducted for 1h, (b) after leaching with water and filtering, (c) after oxidizing sample-(b) at 800°C for 15h and leaching with water. (1) H_3BO_3 , (2) h-BN, (3) B_4C .

Due to the fact that the method consists of successive weighing, leaching and filtering steps, and sample sizes are very small, small errors in weighing steps may lead to magnified errors in the relative amounts of the constituents of the reaction products. Therefore, amounts of the constituents in the reaction products determined by the method should be regarded as approximate.

According to FT-IR measurements, H_3BO_3 has 4 main peaks at wavenumber of 825, 1203, 1490, 3230 cm^{-1} [54]. The FT-IR pattern of the product of the experiment conducted for 1 hour is presented in Figure 4.4 (b). It is seen in Figure 4.4 (c) that after leaching the product with water, the peaks pertaining to H_3BO_3 are removed and only peaks at 817, 1095, 1404 cm^{-1} remain. After oxidising at 800°C for 15 hours and leaching again with water, the peak at 1095 cm^{-1} , which is known to belong to B_4C [54] disappears and only the peaks belonging to h-BN [54] remain (Figure 4.4 (d)).

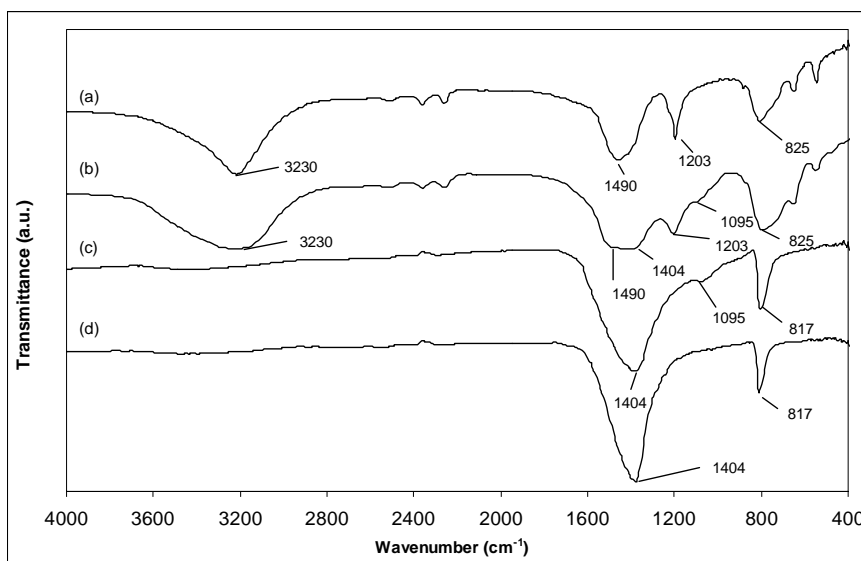


Figure 4.4. FT-IR patterns of (a) H_3BO_3 , (b) sample obtained in the experiment conducted for 1 hour, (c) after leaching with water and filtering, (d) after oxidizing sample-(c) at 800°C for 15h and leaching with water.

In all the filtering operations performed during the analysis steps, Whatman #42 filter paper was used, which is the slowest filter paper and specifically used for filtering fine crystalline particles. A vacuum pump with a funnel was used in the filtering system to speed up the process. No solid particle passed to the filtrate, which would cause blurring and difficulties in the titration process. All of the titrations and analysis of the samples were conducted twice in parallel. The values from two analyses were compared and repeated if they were inconsistent. The average of the two values was reported, if the two analyses were consistent with each other.

For the analyses of the samples containing additives such as oxides or carbonates of some alkaline earth metals or some transition metals; the first leaching step was performed with 1/1 (v/v) HCl(Merck, 37%)/water solution instead of pure water. Consequently, acid soluble additives and unreacted boric oxide was removed. Latter steps were similar to the procedure applied for the products obtained without additives.

Amounts of the constituents of the products of the experiments conducted with 100 mole% excess boric oxide for durations in the range of 15 minutes – 3 hours at 1500°C are presented in Table 4.1 and Figures 4.5 and 4.6. It is seen from the results that the amounts of unreacted activated carbon and boric oxide decreased with increasing duration. Amount of h-BN in the reaction products increased with time and was constant after 2.5 hours. Amount of boron carbide in the reaction products increased in the first 30 minutes and then decreased. This behavior may be as a result of two competing reactions. The first one is Reaction (2.4), where B_4C formation occurred and the second is Reaction (2.5), where consumption of B_4C took place. It can be inferred from Figure 4.6 that rate of formation of B_4C was higher by Reaction (2.4) in the initial stages, i.e. up to 30 minutes, most probably due to the high concentration of carbon in the reactants. As the amount of carbon decreased, the rate of Reaction (2.5) became higher than Reaction (2.4) and consumption of B_4C dominated, resulting in a decrease in the amount of B_4C

after the first half hour. It can be suggested therefore that the overall formation of h-BN took place by two parallel reactions. Some of the total h-BN formed by Reaction (2.6), where boric oxide was directly reduced by carbon in the presence of nitrogen in order to form h-BN. Additionally, some of it formed as a result of combination of Reactions (2.4) and (2.5), where B₄C first formed from boric oxide and carbon and simultaneously converted into h-BN.

Efficiency of h-BN formation was calculated from the chemical analysis data according to the following equation:

$$\text{Efficiency \%} = \frac{\text{Amount of carbon utilized in formation of h-BN}}{\text{Amount of carbon in the starting mixture}} \times 100 \quad \text{Equation (4.2)}$$

It can be seen from the results of the chemical analyses given in Table 4.1 and Figures 4.5 and 4.6 that some unreacted carbon remained at the end of 2 hours. At this stage, it was calculated that 56% of the initial C was consumed in h-BN formation. As the reaction continued, it was seen that all of the C was consumed in 3 hours and 63% of initial C was utilized. These results indicate that there was a considerable loss of carbon from the system, the main reason of which was given as physical loss. Physical loss takes place due to the C being carried away with the furnace gases [8].

Table 4.1. Variation of the amounts of boric oxide, boron carbide, boron nitride and unreacted activated carbon in the products with duration.

Duration (h)	B ₂ O ₃ (g)	B ₄ C (g)	h-BN (g)	Unreacted C (g)
0	1.99	0	0	0.51
0.25	1.46	0.12	0.04	0.33
0.5	1.22	0.15	0.09	0.20
1	0.83	0.10	0.23	0.18
1	0.60	0.12	0.24	0.13
1.5	0.67	0.10	0.30	0.08
2	0.29	0.03	0.40	0.05
2	0.20	0.03	0.41	0.04
2.5	0.10	0.01	0.45	0.04
3	0.13	0	0.45	0

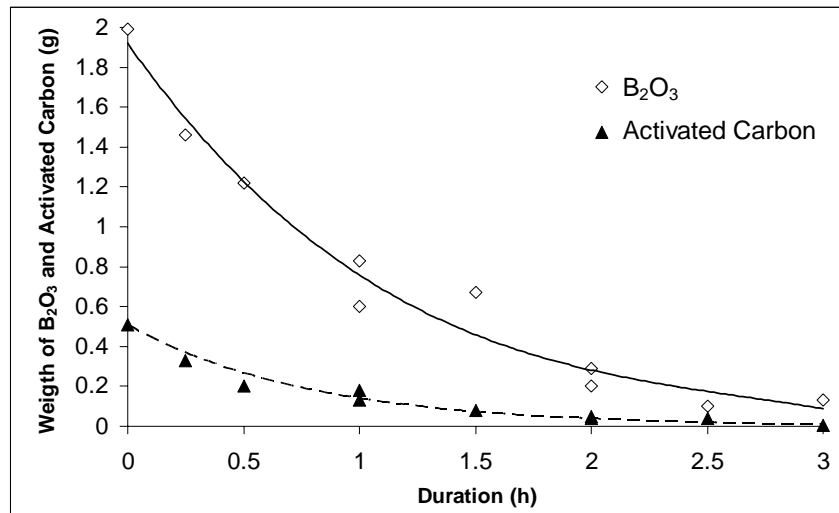


Figure 4.5. Variation of the amounts of unreacted activated carbon and boric oxide in the products with duration.

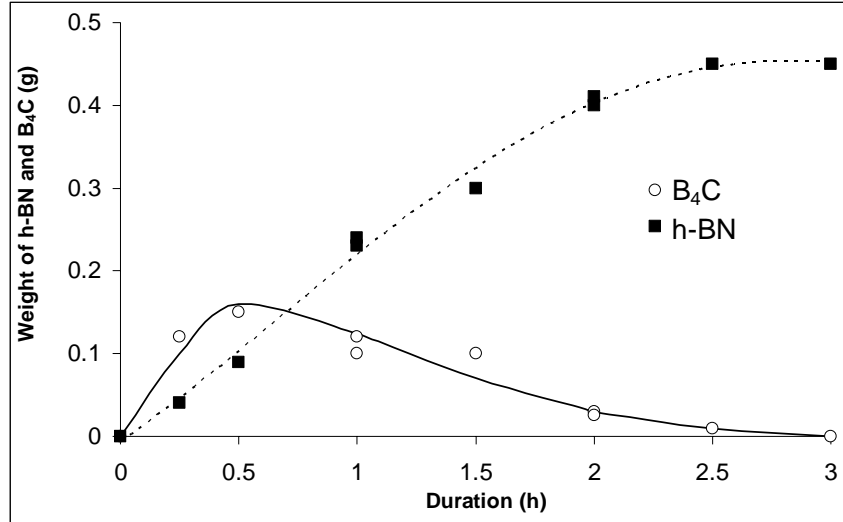


Figure 4.6. Variation of the amounts of h-BN and B₄C in the products with duration.

Aydođdu and Sevinç [8] found from the results of experiments directed to the mechanism of the reaction by use of different geometrical arrangements that liquid B₂O₃ and solid carbon need not be in contact in the formation of BN from B₂O₃, C and N₂ and concluded the overall Reaction (2.6) to proceed by evaporation of B₂O₃(l) and reaction of B₂O₃(g) with C(s) and N₂(g) on C(s). It was shown that gaseous B₂O₃ is the important boron containing intermediate gaseous species in the formation reaction of h-BN [8,18]. Lamoreaux et. al. [48] suggested that under reducing conditions vapor pressure of B₂O₂(g) becomes important at high temperatures (>1300°C). Thermodynamic calculations similar to those in the studies of Aydođdu and Sevinç [8,18] were made in order to determine the equilibrium gas composition of the system including B₂O₂(g). By simultaneous solution of the following possible reactions in the system it was found that at equilibrium $P_{CO} = 0.8579$ atm, $P_{B_2O_3} = 0.1319$ atm, $P_{B_2O_2} = 0.0100$ atm, $P_B = 1.524 \times 10^{-10}$ atm, $P_{N_2} = 7.34 \times 10^{-5}$ atm and $P_{BO} = 1.24 \times 10^{-4}$ atm.



ΔG° values of the Reactions (2), (4) and (5) were calculated in Joules from the data compiled by Türkdoğan [47]. ($\Delta G_2^\circ = 2,025,980 - 763T$, $\Delta G_4^\circ = -820,780 + 235.43T$ and $\Delta G_5^\circ = 1,106,840 - 473.42T$). $\Delta G_3^\circ = 359,995 - 186.2T$ was taken from the study of Yoon and Jha [46]. $\Delta G_1^\circ = 652,587.7 - 328.55T$ was calculated from the data given in Türkdoğan[47] and Lamoreaux et.al. [48].

Equilibrium vapor pressure of $\text{B}_2\text{O}_3(\text{g})$ is seen to be about one order of magnitude higher than that of $\text{B}_2\text{O}_2(\text{g})$ and about 3 orders of magnitude higher than that of $\text{BO}(\text{g})$. These results suggest that the important boron containing intermediate gaseous species in the formation of h-BN in the system at 1500°C is $\text{B}_2\text{O}_3(\text{g})$.

From the SEM and visual observations it was revealed that the products had irregular shape and were in the form of porous solid aggregates. The solidified B_2O_3 phase was holding the products together. SEM micrograph of the product of the experiment conducted for 30 minutes is presented in Figure 4.7. According to the chemical analyses given in Figure 4.6, amount of B_4C is higher than that of h-BN in this stage (first 30 minutes). In addition, the amount of B_4C in the system takes its highest value in this stage of the reaction. It is seen in Figure 4.7 that there is a continuous matrix of solidified B_2O_3 phase, in which chunky and faceted B_4C grains are embedded. There are also C particles which look as if they are covered with B_2O_3 . Hexagonal BN grains could not be seen due to their very

small sizes, since this micrograph is of an early stage of reaction. The liquid B_2O_3 phase, which is evident in Figure 4.7 is believed to be responsible for the formation of B_4C by preventing the penetration of N_2 gas into the aggregate [8,10]. It may be thought that carbon particles help preventing the coalescence of the B_2O_3 phase and create voids for the penetration of the N_2 gas, by acting like a support phase.

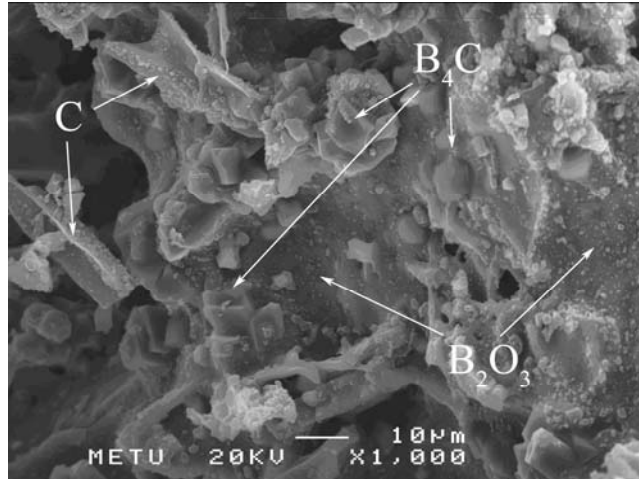


Figure 4.7. SEM micrograph of the product of the experiment conducted for 30 minutes.

Chemical analyses reveal that amount of C, B_4C and B_2O_3 decreases after the first half hour, and amount of h-BN increases until the end of the reaction. Amount of B_2O_3 decreases due to its consumption by reacting with C and N_2 ; and also due to evaporation [8]. In the SEM micrograph of the product of the experiment conducted for 1 hour given in Figure 4.8 it is seen that there is still a high amount of B_4C in the structure. This observation is in accord with the chemical analyses.

SEM micrograph of the product of the experiment conducted for 1.5 hours is presented in Figure 4.9. It was revealed from SEM observations that smooth

surfaces of solidified B_2O_3 phase are present on the inside surfaces of the aggregate. It is highly probable that these surfaces limit the penetration of N_2 gas.

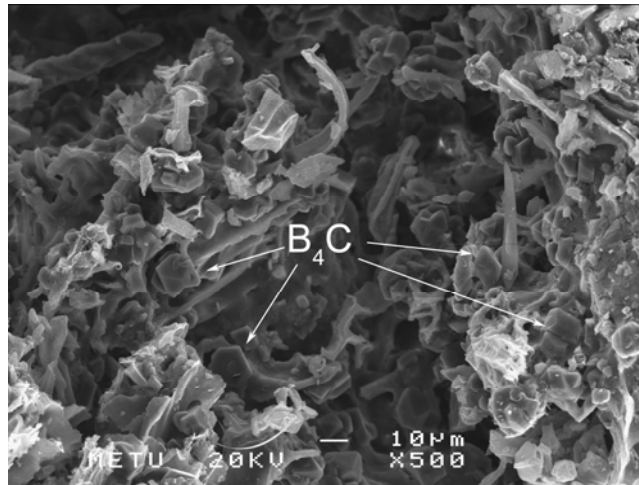


Figure 4.8. SEM micrograph of the product of the experiment conducted for 1 hour.

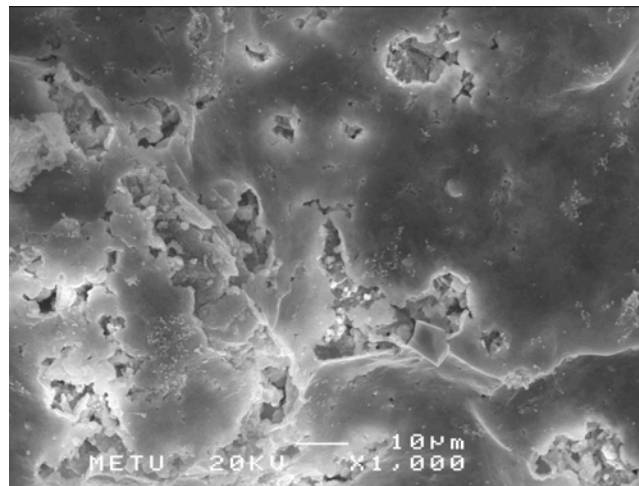


Figure 4.9. SEM micrograph of the inside surface of the product of the experiment conducted for 1.5 hours.

At the end of 3 hours, all of the C and formed B_4C were consumed and reaction ended. The product consisted of formed h-BN and some unreacted B_2O_3 . SEM micrograph of the product of the experiment conducted for 3 hours is given in Figure 4.10. It is observed in this micrograph that h-BN particles forming by reaction of gaseous B_2O_3 and nitrogen gas on C(s) [8] has a thin, flaky structure; and the particle size is about $0.49 \pm 0.09 \mu$. Grain average diameter was determined by averaging at least 30 grains and calculating the standard deviation.

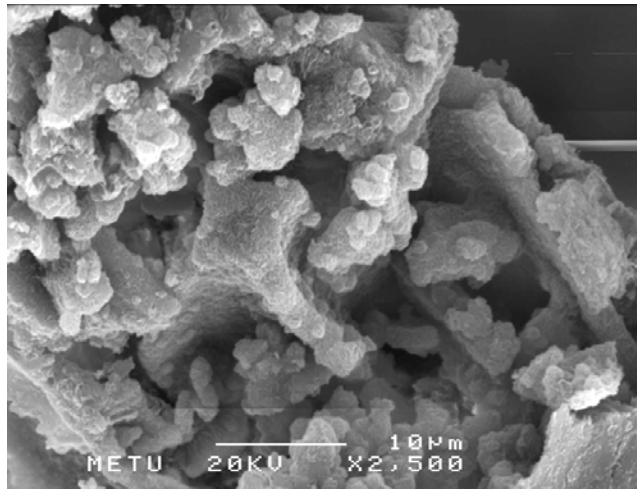


Figure 4.10. SEM micrograph of the product of the experiment conducted for 3 hours.

The specific surface area of the h-BN powder obtained in 2 hours was determined as $31.7 \text{ m}^2/\text{g}$. This result indicates that the formed h-BN had a very small grain size. From the SEM images, the average diameter of the grains was measured as $0.36 \pm 0.08 \mu$.

The formation of h-BN crystals with duration has been investigated by XRD analyses. For this purpose, the changes in the interplanar spacing and thickness of the formed h-BN crystals have been examined. A magnified portion of Figure 4.1

is presented in Figure 4.11, where the peak belonging to the (002) plane of h-BN is presented.

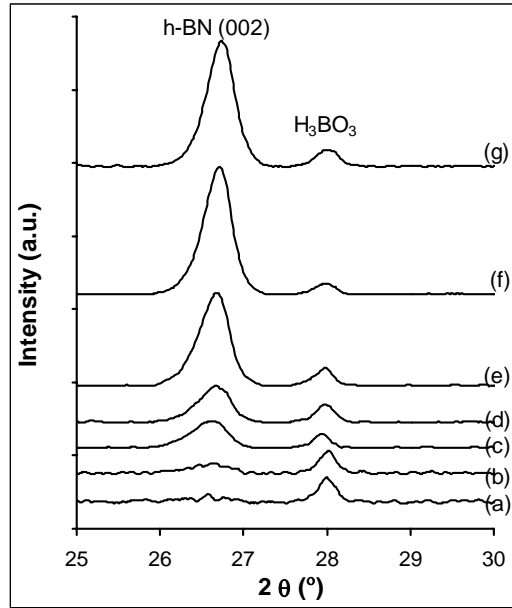


Figure 4.11. Magnified portion of the XRD patterns of the products of the experiments conducted with plain B_2O_3+C mixtures for (a) 15 minutes, (b) 30 minutes, (c) 1 hour, (d) 1.5 hours, (e) 2 hours, (f) 2.5 hours, (g) 3 hours.

Mean interplanar spacings, d_{002} of h-BN powders were determined by the Bragg's law according to the following equation [55]:

$$n\lambda = 2.d.\text{Sin}\theta \quad \text{Equation (4.3)}$$

where n is an integer (taken as 1), λ is the wavelength of the X-rays ($\lambda=1.54056\text{\AA}$ for Cu- $K\alpha$ radiation), d is the mean interplanar spacing in \AA , θ is the diffraction angle. Mean interplanar spacing values of (002) planes, d_{002} of the produced h-BN are presented in Table 4.2 and in Figure 4.12. It was stated by Alkoy et. al. that the decrease in the d_{002} value indicated the ordering in the crystal

structure of h-BN [41]. It is seen that the d_{002} of the h-BN decreases from 3.35\AA to 3.33\AA with increasing duration of the experiments at 1500°C . 3.33\AA is the typical interplanar spacing value for well crystallized of h-BN [44].

Table 4.2. 2θ , interplanar spacing (d_{002}), broadening data (B_M), and average crystallite size calculated by the Scherrer formula.

Duration	2θ value of (002) peak ($^\circ$)	d_{002} (\AA)	B_M ($^\circ$)	Average crystallite size, L_c , (nm)
15 minutes	26.58	3.35	0.62	13.57
30 minutes	26.66	3.34	0.56	15.13
1 hour	26.64	3.34	0.48	17.90
1.5 hours	26.68	3.34	0.44	19.74
2 hours	26.68	3.34	0.4	22.02
2.5 hours	26.72	3.33	0.38	23.39
3 hours	26.74	3.33	0.38	23.39

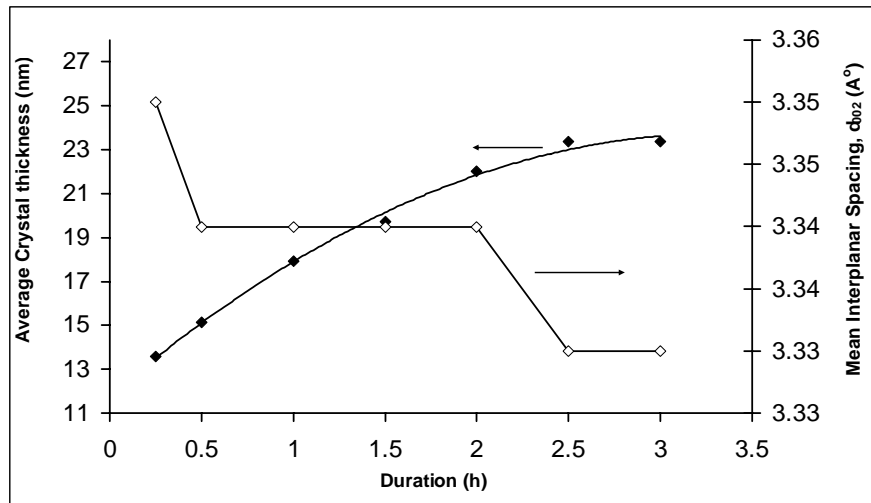


Figure 4.12. Variation of mean interplanar spacing and average crystal thickness of the produced h-BN powders with duration of the experiments at 1500°C .

Scherrer formula was used to calculate the average crystal thickness, L_c of particles by using the broadening of the peaks on the XRD pattern. L_c is defined as the mean height of a pack of parallel and crystallographically connected hexagonal layers. Relatively crude measurements can be done in the range of 0-500Å with the Scherrer formula given below [55,56].

$$L_c = \frac{0.9\lambda}{B \cdot \cos\theta_B} \quad \text{Equation (4.4)}$$

where, L_c is the average thickness of the crystal, λ is the wavelength (1.54056 Å, for CuK α), θ_B is the Bragg angle (26.78° for (002) plane of h-BN).

B is the line broadening, in radians, by reference to a standard, so that

$$B^2 = B_M^2 - B_s^2 \quad \text{Equation (4.5)}$$

where B_s is the width of the standard material in radians and B_M is the measured value of the full width at half maximum of the peak on the XRD pattern. B_M values, determined from peaks of the (002) planes on the XRD patterns of the produced h-BN powders, are presented in Table 4.2. In the current measurements a peak of a silicon standard at 2 theta of 28.41° was used to determine B_s , which had a width of 0.15°.

Average crystallite thickness values of the produced h-BN powders, calculated by the Scherrer formula, are presented in Table 4.2 and in Figure 4.12. It is seen that the average crystallite thickness increases with increasing duration of the experiments at 1500°C. This was expected, since increasing duration causes the growth of the grains and the crystallites in the grains.

4.2. Role of B₄C During Carbothermic Formation of Hexagonal BN

As reported in the previous section according to the observations made on SEM micrographs, the reaction products were in the form of solid aggregates which were kept together by the solidified boric oxide and in which some small and large pores existed. It was observed by visual examination of these aggregates that B₄C formation mostly took place in the core and bottom regions of the pellets. It can be suggested from this observation that B₄C formed at points where nitrogen gas could not penetrate into the aggregate and where N₂ partial pressure was too low for h-BN formation. This observation may be taken as an indication that B₄C may not be a necessary intermediate product in the carbothermic production of h-BN under nitrogen atmosphere.

SEM micrographs of boron carbide rich parts of the products of the experiments conducted for 1 hour are given in Figure 4.13 (a) and (b). It can be seen that boron carbide forming in the system had various shapes such as whisker like formations as in Figure 4.13 (a) and blocky - angular grains as in Figure 4.13 (b).

In order to investigate the conversion of B₄C into h-BN by Reaction (2.5), B₄C was produced in the same experimental conditions that h-BN formation was studied, but under argon atmosphere. Experiments were performed for 30 minutes, 1 and 2.5 hours. XRD patterns of the products obtained in these experiments and FT-IR pattern of the product of the experiment conducted for 2.5 hours are presented in Figures 4.14 and 4.15, respectively. Characteristic peak of B₄C at 1095cm⁻¹ given in Figure 4.15 is in accord with the data in the literature [54]. Produced boron carbide phase was clearly detected by XRD and FT-IR analysis. It was also realized from this XRD pattern that some graphite might have been formed by the graphitization of activated carbon. Similar results were observed in other studies [57].

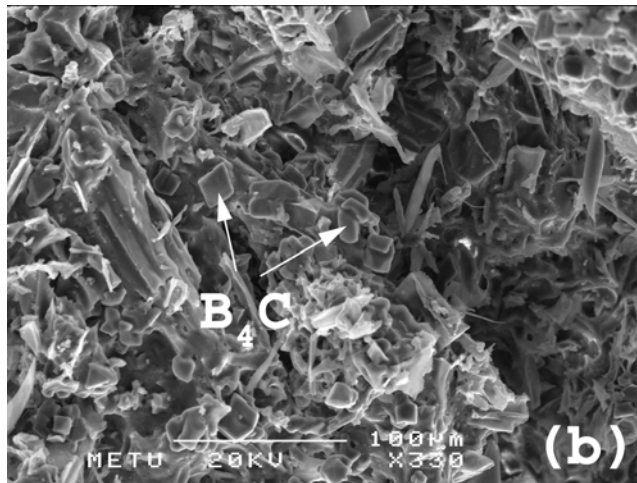
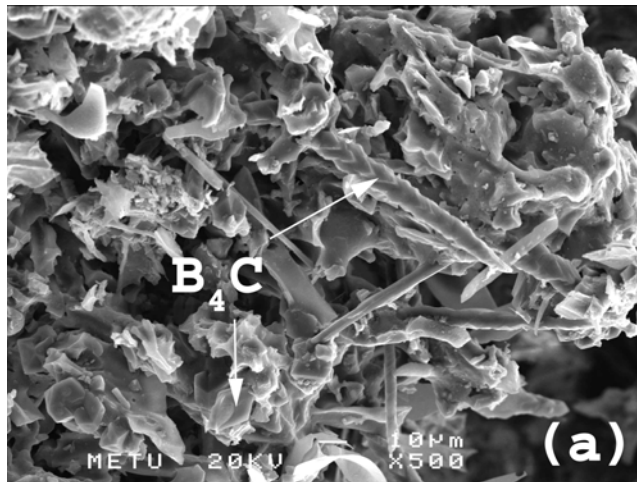


Figure 4.13. (a) and (b). B_4C rich parts of the product of the experiment conducted for 1 hour.

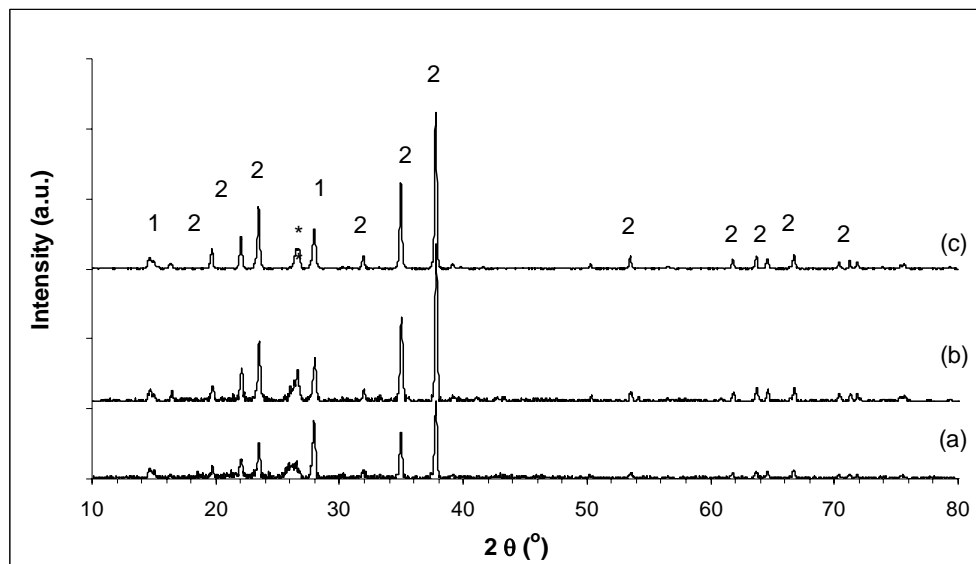


Figure 4.14. XRD patterns of the products of the experiments conducted with $\text{B}_2\text{O}_3+\text{C}$ mixtures for (a) 30 minutes, (b) 1 hour and (c) 2.5 hours under argon atmosphere at 1500°C . (*) graphite, (1) H_3BO_3 , (2) B_4C .

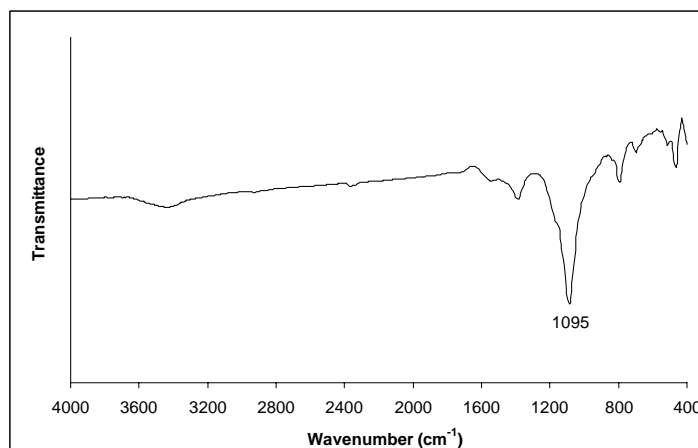


Figure 4.15. FT-IR pattern of B_4C obtained in 2.5 hours from $\text{B}_2\text{O}_3+\text{C}$ mixtures under argon atmosphere at 1500°C .

SEM micrograph of the boron carbide powder produced by reacting activated carbon – boric oxide mixtures under argon at 1500°C for 2.5 hours is given in Figure 4.16. A mixed morphology of boron carbide grains was observed. There were some rod-like or whisker-like formations, also blocky and angular grains of 2-7 microns were present. It was realized from SEM examinations that the size and morphology of the B₄C grains produced under argon were comparable to those formed during h-BN formation.

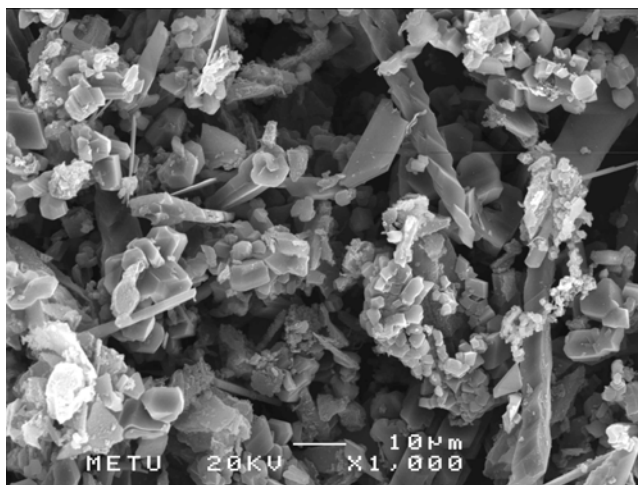


Figure 4.16. SEM micrograph of B₄C powder obtained in 2.5 hours from B₂O₃+C mixtures under argon atmosphere at 1500°C.

The produced boron carbide was mixed with boric oxide, the amount of which was 150% more than the stoichiometric amount according to Reaction (2.5) and the mixture was reacted under nitrogen atmosphere for 3 hours. It can be seen in the XRD pattern given in Figure 4.17 (b) that h-BN was formed; however boron carbide phase was also present with h-BN, indicating that the conversion of boron carbide into h-BN was not complete. This indicates that reaction of boron carbide and boric oxide under nitrogen (Reaction 2.5) in order to form h-BN requires longer durations than 3 hours.

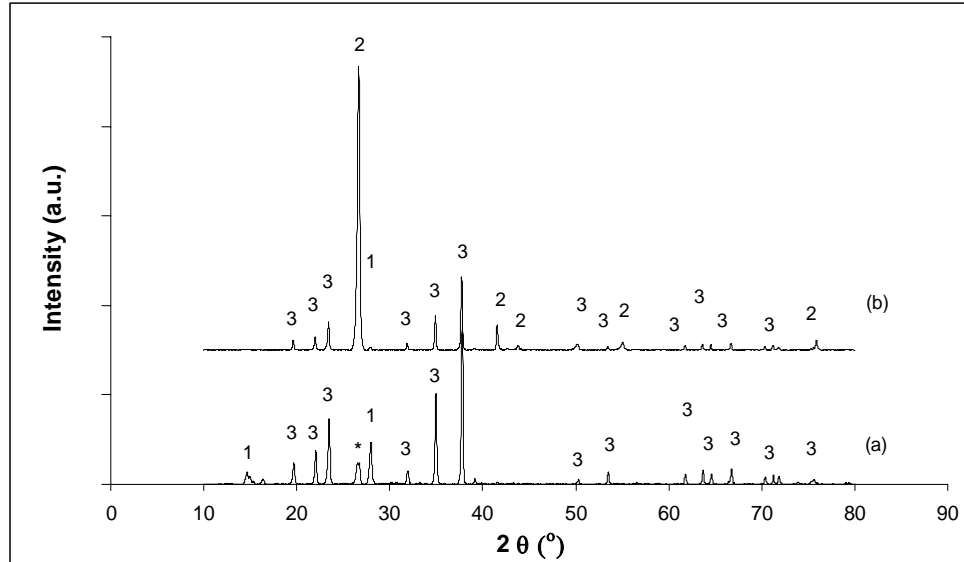


Figure 4.17. XRD patterns of (a) boron carbide produced in 2.5 hours, (b) after reacting produced boron carbide – boric oxide mixtures under nitrogen at 1500°C for 3 hours. (*) graphite, (1) H₃BO₃, (2) h-BN, (3) B₄C.

SEM micrograph of the product of the experiment conducted by reacting boron carbide – boric oxide mixtures at 1500°C for 3 hours under nitrogen atmosphere is given in Figure 4.18. Unreacted B₄C grains could be distinguished from its bulky and faceted morphology in the reaction products. It was inferred from the boron and nitrogen peaks in the energy dispersive analysis by X-ray (EDX) given in Figure 4.19 that the points indicated as (1) in Figure 4.18 are h-BN. The results of EDX analysis from the points indicated as (2) in Figure 4.18 is presented in Figure 4.20. It is seen that B, C and N signals are received from these points. The presence of B and both C and N at these points can be taken as an indication that these points are B₄C, which were transforming into h-BN when the experiment was stopped.

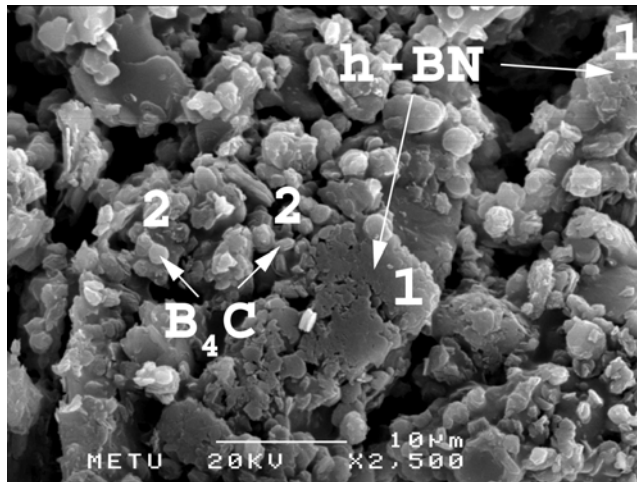


Figure 4.18. SEM micrograph of the product of the experiment conducted with (produced $B_4C+B_2O_3$) mixtures under nitrogen atmosphere for 3 hours.

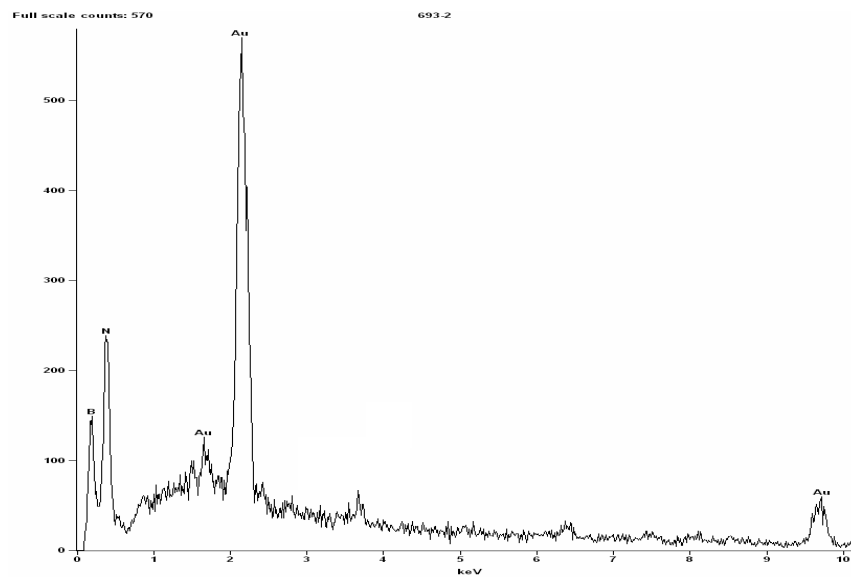


Figure 4.19. EDX analysis of the points indicated as (1) in Figure 4.18. (Au peaks originating from gold coating of the sample.)

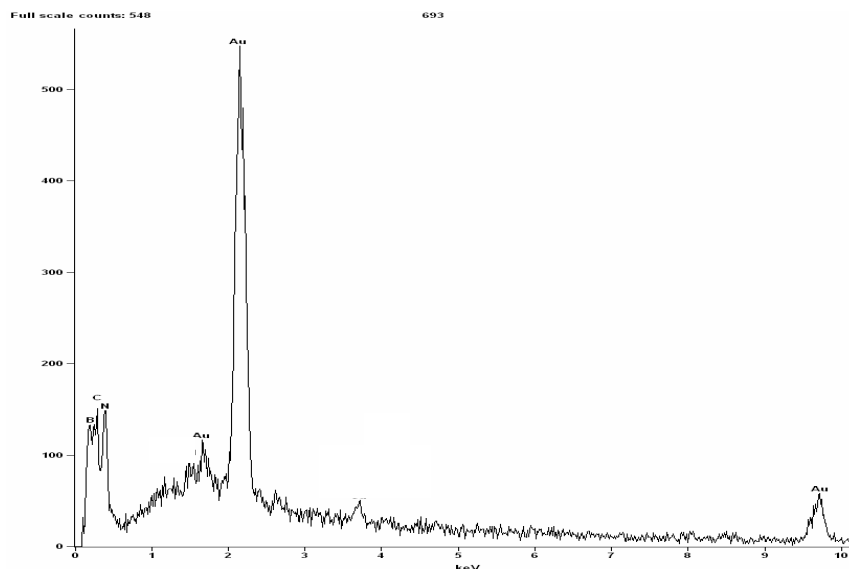


Figure 4.20. EDX analysis of the points indicated as (2) in Figure 4.18. (Au peaks originating from gold coating of the sample.)

Therefore, it could be concluded that formation of h-BN from boron carbide by Reaction (2.5) was slower than formation of h-BN from carbon by Reaction (2.6). This result may be taken as an indication that boron carbide is not a necessary intermediate product in formation of hexagonal boron nitride and that formation of boron carbide slows the rate of formation of boron nitride.

4.3. Effect of Excess Boric Oxide

In order to investigate the effect of excess boric oxide on the formation of h-BN and formation and consumption of B_4C in the carbothermic production of h-BN, experiments were performed with 3 different activated carbon – boric oxide compositions containing 50, 100, 150 mole% excess boric oxide for 15, 30 and 60 minutes at 1500°C . These durations were selected since B_4C formation was

observed to take place mostly at the initial stages of catbothermic production of h-BN.

The amounts of B_4C , formed in the products of the experiments conducted with all 3 compositions are presented in Table 4.3 and in Figure 4.21 as a function of duration. It is seen that when 100 and 150 mole% excess B_2O_3 were used, the amount of B_4C formed in the products reaches its highest amount in the first half hour, and then starts to decrease. When 50 mole% excess B_2O_3 was used, the highest amount was reached in 15 minutes. Additionally, amount of B_4C was seen to increase with decreasing excess amount of B_2O_3 in the starting mixture. These results indicate that the rate of formation of B_4C increases with the increase in C concentration in the starting mixture. This finding is in agreement with the explorations which were made in Section 4.1 about the increase of the B_4C amount in the first half hour and then decrease.

Table 4.3. Amounts of boron carbide and boron nitride formed in the experiments conducted with 50, 100 and 150 mole% excess boron oxide for 0.25, 0.5 and 1 hour durations.

Excess B_2O_3 Amount →	50%		100%		150%	
	B_4C (g)	h-BN (g)	B_4C (g)	h-BN (g)	B_4C (g)	h-BN (g)
Duration (h) ↓						
0	0	0	0	0	0	0
0.25	0.18	0.03	0.12	0.04	0.05	0.02
0.5	0.17	0.08	0.15	0.09	0.10	0.06
1	0.16	0.17	0.10	0.23	0.05	0.25
1			0.12	0.24		

The XRD patterns of the experiments conducted with 50, 100 and 150 mole % excess B_2O_3 for 15, 30 and 60 minutes are presented in Figure 4.22. The results of the chemical analyses are in accord with the XRD analyses, in which the relative

heights of the B_4C peaks decrease with increasing B_2O_3 amount in the starting mixture. Taking into account the fact that equal amounts of carbon were used for varying amounts of B_2O_3 in the initial B_2O_3+C mixtures, the increase in B_2O_3 amount could have either inhibited the formation of B_4C (Reaction 2.4) or enhanced the conversion of B_4C into h-BN (Reaction 2.5) or both. It is not likely for the increase in the amount of B_2O_3 to slow down Reaction (2.4), since it is a reactant. Therefore, it is more likely that the increase in the amount of B_2O_3 favored Reaction (2.5) and increased conversion of B_4C to h-BN.

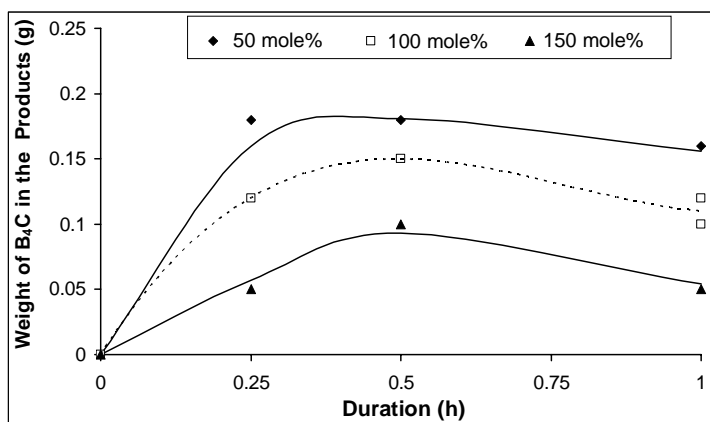


Figure 4.21. Amounts of boron carbide formed in the experiments conducted with 50, 100 and 150 mole% excess boron oxide for 0.25, 0.5 and 1 hour durations.

The amounts of h-BN formed from the mixtures containing 50, 100 and 150 mole% excess B_2O_3 are presented as a function of duration in Table 4.3 and Figure 4.23. It can be seen that when 50 mole % excess B_2O_3 was used, the amount of h-BN in the first half hour is similar to the ones obtained with higher B_2O_3 amounts. However, it was much less at the end of 1 hour. Furthermore, when 50 mole % excess B_2O_3 was used, the amount of B_4C was much higher than the compositions containing higher B_2O_3 and the decrease in the amount of B_4C with increasing duration was lower as observed in Figure 4.21. These results can

be attributed to the insufficient amount of B_2O_3 , due to which the rate of formation of h-BN and consumption of B_4C decreased.

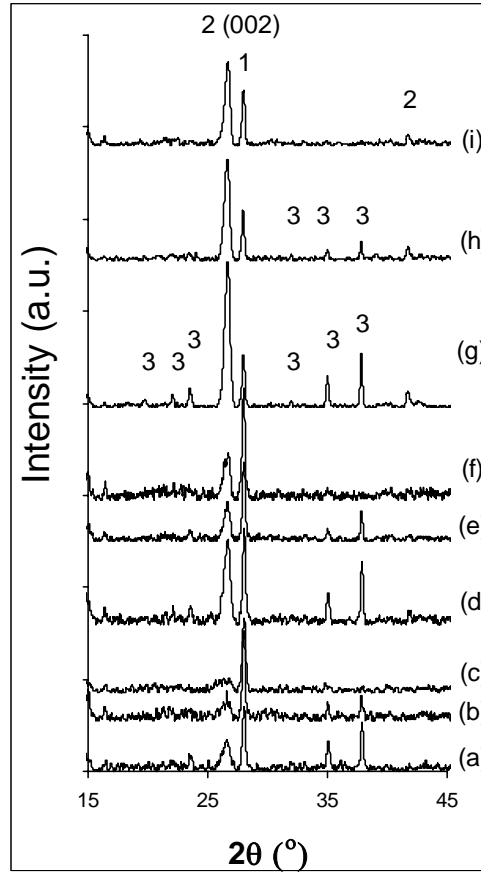


Figure 4.22. XRD patterns showing the effect of excess boron oxide on the boron carbide formed during carbothermic production of h-BN. Experiments were performed with (a) 50, (b) 100 and (c) 150 mole% excess boron oxide for 15 minutes; (d) 50, (e) 100 and (f) 150 mole% excess boron oxide for 30 minutes; (g) 50, (h) 100 and (i) 150 mole% excess boron oxide for 60 minutes. (1) H_3BO_3 , (2) h-BN, (3) B_4C .

When 150 mole % excess B_2O_3 was used, it was seen in the first hour that the amount of h-BN was lower than the compositions containing less amount of B_2O_3 .

It was found previously that h-BN forms on carbon particles by the reaction of carbon with gaseous B_2O_3 and nitrogen [8]. Therefore, for formation of h-BN activated carbon should be in contact with $B_2O_3(g)$ and $N_2(g)$. It can be suggested that increasing the amount of boric oxide most probably causes the formation of too much of liquid boric oxide phase, which can possibly prevent the contact of gaseous boric oxide and nitrogen with carbon particles, thereby hindering the growth of h-BN crystals. At the end of 1 hour it is seen that the amount of h-BN formed from the mixtures containing 100 and 150 mole% excess B_2O_3 are similar. This may be attributed to the increase in the rate of h-BN formation in the 150 mole% B_2O_3 containing composition due to the decrease in B_2O_3 concentration by vaporization loss. The fact that the increase in the B_2O_3 amount did not have a significant effect on the amount of h-BN forming at the end of 1 hour is not unexpected as C is the limiting reactant in the system.

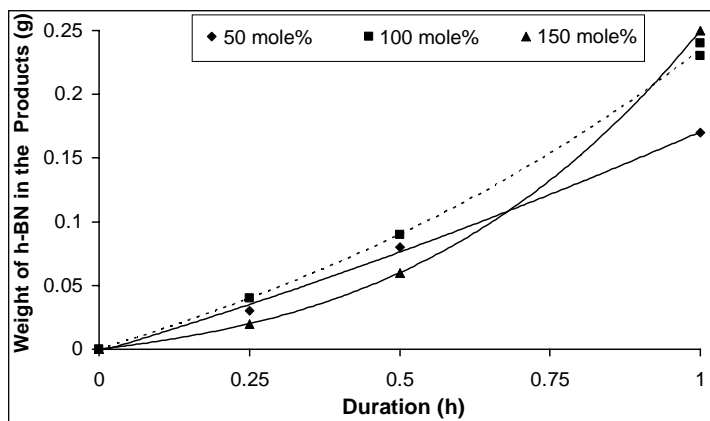


Figure 4.23. Amounts of boron nitride formed in the experiments conducted with 50, 100 and 150 mole% excess boron oxide for 0.25, 0.5 and 1 hour durations.

The (002) peaks of h-BN in the reaction products are seen to take a more diffused and broader form with increasing boric oxide content from the XRD patterns given in Figure 4.22. It can therefore be inferred that increasing the amount of excess boric oxide results in a decrease in the crystal size of the h-BN [55]. This

effect of excess boric oxide on the crystal size may be due to the interaction of excess boric oxide and carbon as explained above.

4.4. Effect of Additives

Formation of h-BN from plain B_2O_3+C mixtures was investigated and the results were presented in Section 4.1. In that part, some drawbacks of this process were stated.

Firstly, it was shown that the efficiency of the Reaction (2.6) was 63% in terms of carbon utilization in 3 hours, which is low. There is a considerable carbon loss, as mentioned in the results of the experiments conducted with plain B_2O_3+C mixtures. Therefore, it is important to increase the efficiency of the carbothermic production of h-BN process.

Secondly, in the early stages of the reaction formation of a high amount of B_4C takes place. It was shown that B_4C retards the completion of the reaction, since the formation of h-BN from B_4C was shown to be slower than formation from C. Therefore, reduction of the amount of B_4C is important for the increase of the rate of this process and the purity of the formed h-BN.

Positive effects of some catalysts have been suggested in the formation of h-BN from urea and boric acid and in carbothermic formation, as stated in Chapter II [49,50]. Hence, in this part of the study the effect of addition of some alkaline earth metal oxides and carbonates namely: $CaCO_3$, MgO , $BaCO_3$; and some transition metals and oxides namely: MnO_2 , Fe_3O_4 , Co_3O_4 and cupric nitrate has been investigated.

As mentioned in the results of the experiments conducted with plain mixtures, grain size of the produced h-BN by the carbothermic method was seen to be very small. It was stated that better lubricating and high temperature properties are

obtained with large grained h-BN powders [43]. In order to increase the grain size of the produced h-BN, effect of addition of CaCO₃ and cupric nitrate together was investigated. In the final part of this section results pertaining to these experiments will be presented.

The metallic elements of the used additives are shown in the periodic table given in Figure 4.24. These additives were mixed with B₂O₃+C mixtures and reactions were carried out in the same fashion as with the plain mixtures. In the following section, results related to the addition of alkaline earth metal oxides and carbonates will be presented. In this section, emphasis will be on the effect of CaCO₃ addition. Then, results of the transition metal oxide additions and cupric nitrate will be given.

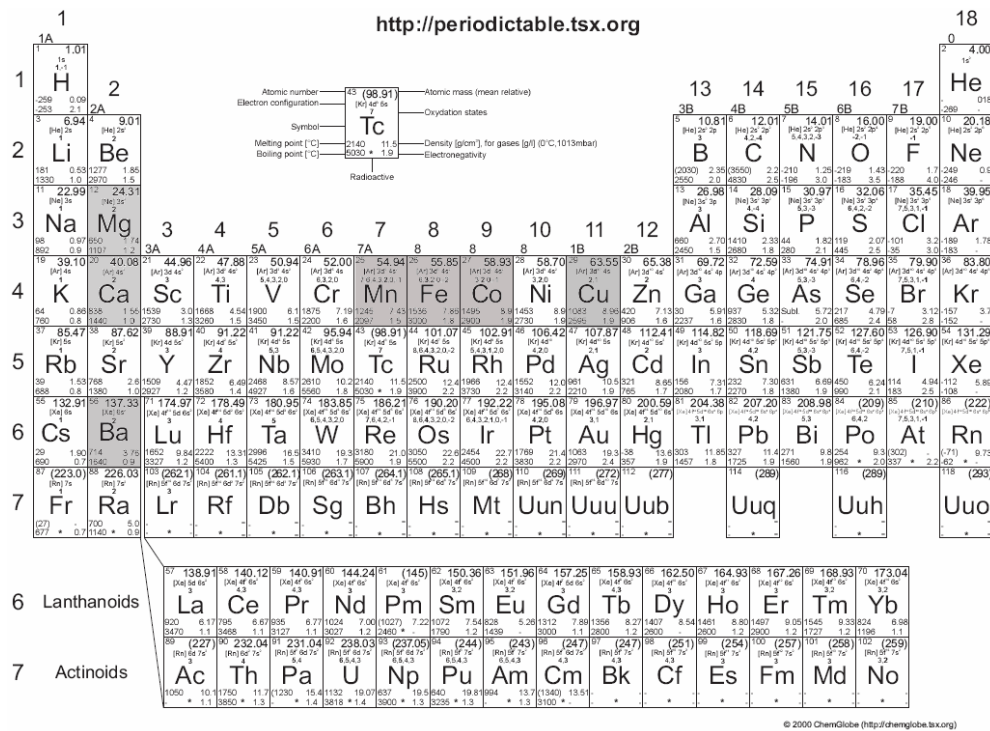


Figure 4.24. Periodic table of the elements. Metallic elements of the used additives in this study are shaded in gray.

As mentioned before, effect of CaCO_3 addition was investigated in more detail due to its abundance, low cost and possibility to provide a high catalytic activity. The optimum amount of CaCO_3 was determined and this value was used for the addition of all other additives, in order to be able to compare their catalytic effect.

4.4.1. Effect of Alkaline Earth Metal Oxides and Carbonates, CaCO_3 , MgO , BaCO_3

In this section, effect of addition of some alkaline earth metal oxides and carbonates namely: CaCO_3 , MgO , BaCO_3 will be investigated. Emphasis will be on the effect of CaCO_3 addition.

4.4.1.1. CaCO_3 Addition

Samples containing CaCO_3 were prepared by mixing and grinding B_2O_3 , C and CaCO_3 powders in an agate mortar and pestle in acetone. It was seen from the SEM micrograph given in Figure 4.25 that CaCO_3 powder used in the experiments had rhombohedral shaped grains and its grain size was in the range of 3-10 microns. XRD analysis indicated that CaCO_3 had rhombohedral crystal structure.

Initial experiments were performed in order to determine the optimum amount of CaCO_3 to be added into the activated carbon – boric oxide mixtures. The duration for these experiments was selected by considering two issues. First, as mentioned in the introduction part, B_4C also forms as an undesired side product together with h-BN during carbothermic production of h-BN. It was observed in this study and also in previous studies [8] that at 1500°C the amount of B_4C in the reaction products increases in the first 30 minutes and then decreases by reacting with boric oxide and nitrogen; suggesting that formation of B_4C mainly takes place in the first 30 minutes. Therefore, in order to observe the effect of CaCO_3 addition on formation of B_4C , duration of 30 minutes at 1500°C was suitable. Secondly;

the reaction products had to be analyzed at an intermediate stage before complete consumption of the reactants, to examine the effect of CaCO_3 on the formation of h-BN. Duration of 30 minutes could serve well for both of these purposes.

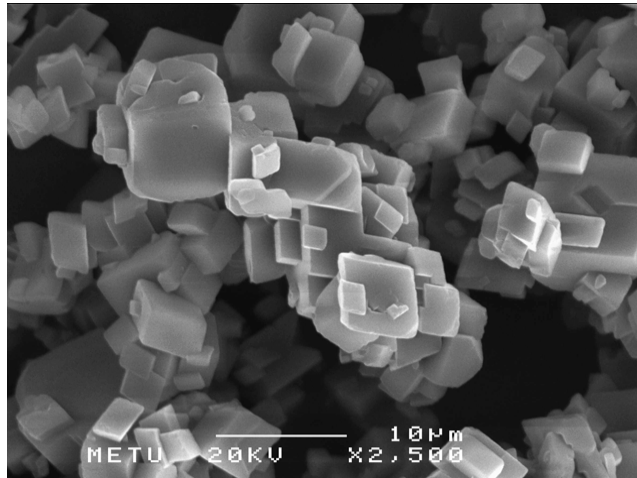


Figure 4.25: SEM micrograph of the CaCO_3 powder

Addition of CaCO_3 is expected to result in formation of calcium borates in view of the phase diagram given in Figure 4.26 [58]. In order to determine if calcium borates were soluble in dilute HCl, two B_2O_3 -CaO mixtures containing 20 and 35 wt% CaO, respectively, were prepared and kept in a platinum crucible at 1150°C for 2 hours. It is known from the phase diagram given in Figure 4.26 that calcium borate melt forms above 1100°C for these compositions. After removing from the furnace and cooling, the platinum crucible with its contents was placed into a 1/1 (v/v) HCl/water solution. It was found that both of the compositions were completely soluble in dilute HCl and it was concluded that it was possible to remove calcium borates by leaching in this solution. The leaching duration in the chemical analysis method used was fixed at 15 hours for all the products obtained with additives.

The chemical analyses for the determination of the amounts of the constituents of the products were performed similar to the method explained previously according to Figure 4.2. The only difference was in the first leach; 1/1 (v/v) HCl/water (dilute HCl) solution was used as the leachant instead of water. This leach served the purpose of removing ($B_2O_3 + CaO$) from the pellet. On the basis of the assumption that no CaO is lost from the system, the overall composition of the ($B_2O_3 + CaO$) system could be determined.

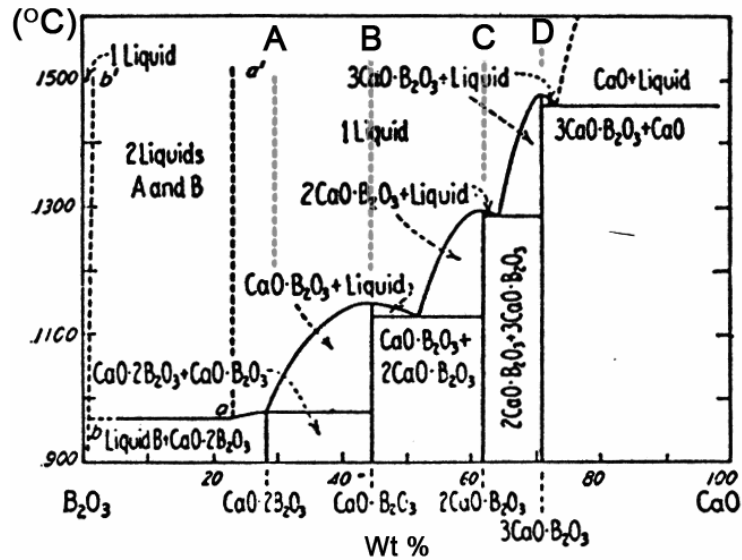


Figure 4.26. $B_2O_3 - CaO$ phase diagram [58].

The quantities of B_4C and h-BN in the reaction products of the experiments conducted for 30 minutes at $1500^\circ C$ with activated carbon – boric oxide mixtures containing 0 – 50 wt% $CaCO_3$ additions, are presented in Table 4.4 and in Figure 4.27. In the same table CaO percentages of the ($CaO + B_2O_3$) system in the pellets at $t=0$ and $t=30$ minutes are also given. The amounts of h-BN in all of the reaction products obtained from pellets containing $CaCO_3$ are seen to be higher than that obtained from plain mixtures. It is seen that amount of h-BN increases with addition of $CaCO_3$ up to an amount of 10 wt% of the activated carbon-boric oxide

mixture and decreases afterwards. It can be concluded from this figure that the positive effect of CaCO_3 on carbothermic formation of h-BN is the highest at 10 wt%. 5-10 wt% CaCO_3 addition is effective in reducing the amount of B_4C in the reaction products. The decrease in the amount of h-BN and increase in the amount of B_4C in the reaction products of the experiments conducted with higher additions of CaCO_3 than 10 wt% reveals that higher amounts of CaCO_3 is not as beneficial for this process.

Table 4.4. Change in the amounts of h-BN and B_4C in the products of the experiments conducted at 1500°C for 30 minutes with CaCO_3 additions; and CaO percentages of the $(\text{CaO}+\text{B}_2\text{O}_3)$ system in the pellets at $t=0$ and $t=30$ minutes.

CaCO_3 %	Amounts in the Products (g)		CaO (wt%) in $(\text{B}_2\text{O}_3+\text{CaO})$	
	h-BN	B_4C	t=0 min	t=30 min
0	0.09	0.15	0	0
5	0.15	0.08	3.4	5.2
10	0.26	0.11	6.6	10.8
10	0.23	0.10	6.6	10.8
20	0.21	0.14	12.4	19.6
30	0.16	0.16	17.5	26.1
40	0.13	0.16	22.0	30.8
50	0.15	0.17	26.1	35.9

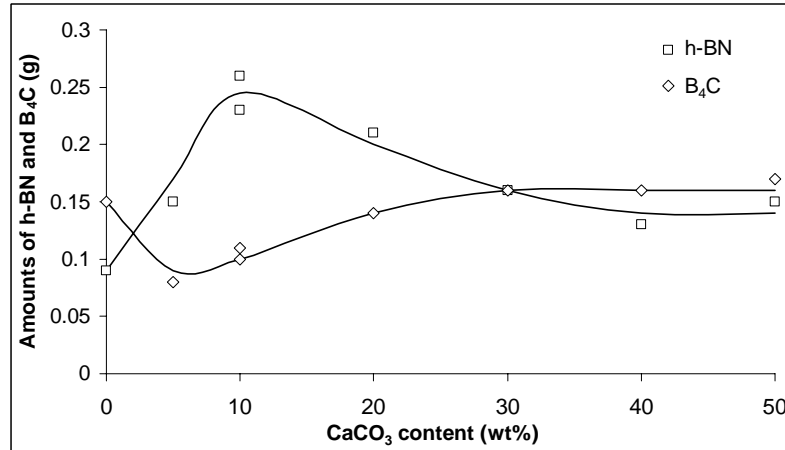


Figure 4.27. Change in the amounts of h-BN and B₄C in the products of the experiments conducted at 1500°C for 30 minutes with CaCO₃ additions.

Relative heights of the peaks of the phases appearing in the XRD patterns presented in Figure 4.28 are in accord with the results of the quantitative chemical analysis. It can be discerned from these patterns that the h-BN peaks attain the highest values with 10 wt% CaCO₃ addition and B₄C peaks attain their lowest values at 5 wt% CaCO₃ addition. H₃BO₃ peaks, present in these XRD patterns are due to the formation of H₃BO₃ by hydration of unreacted amorphous B₂O₃ in the reaction products during specimen preparation for the XRD analyses, therefore their heights are proportional to the amount of B₂O₃ in the reaction products. It is seen in Figure 4.28 that H₃BO₃ peaks become gradually shorter up to 20 wt% CaCO₃ and then fade away, indicating that all of the B₂O₃ was consumed upon addition of 30 wt% CaCO₃ or more.

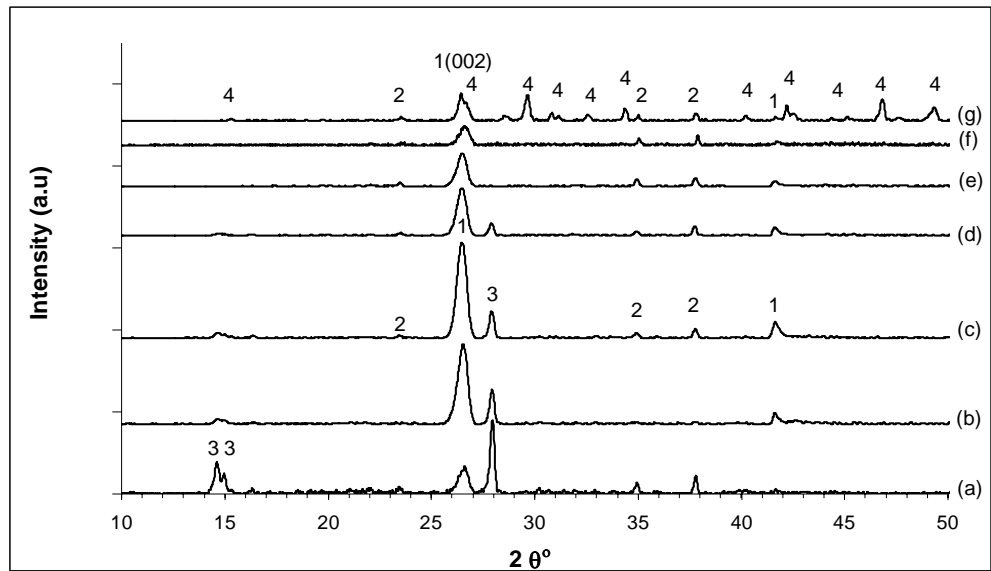


Figure 4.28. XRD patterns of the products of the experiments conducted with 0-50 weight% CaCO_3 addition for 30 minutes at 1500°C . (a) No addition, (b) 5 wt%, (c) 10 wt%, (d) 20 wt%, (e) 30 wt%, (f) 40 wt%, (g) 50 wt % CaCO_3 addition. (1) h-BN, (2) B_4C , (3) H_3BO_3 , (4) CaB_2O_4 .

10 wt% CaCO_3 addition was found to be the optimum value to keep the amount of B_4C as low as possible and h-BN as high as possible in the reaction products. Therefore, experiments aiming for the investigation of the catalytic effect of CaCO_3 for longer durations at 1500°C were performed with 10 wt% CaCO_3 additions. The quantities of h-BN and B_4C formed in the experiments conducted for 30 minutes to 2 hours at 1500°C with plain and 10 wt% CaCO_3 added mixtures are presented in Table 4.5 and in Figure 4.29.

Table 4.5. Amounts of B₄C, h-BN and unreacted C in the products of the experiments conducted for 30 minutes to 2 hours at 1500°C with plain and 10 wt% CaCO₃ added mixtures.

Duration (h)	Plain B ₂ O ₃ +C Mixtures			10 wt% CaCO ₃ added B ₂ O ₃ +C Mixtures		
	B ₄ C (g)	h-BN (g)	Unreacted C (g)	B ₄ C (g)	h-BN (g)	Unreacted C (g)
0	0	0	0.51	0	0	0.51
0.25	0.12	0.04	0.33			
0.5	0.15	0.09	0.20	0.10	0.23	0.18
0.5				0.11	0.26	0.14
1	0.10	0.23	0.18	0.05	0.44	0.07
1	0.12	0.24	0.13	0.07	0.50	0.06
1.5	0.10	0.30	0.08			
2	0.03	0.40	0.05	0.01	0.59	0.01
2	0.03	0.41	0.04	0	0.60	0
2				0.01	0.58	0
2.5	0.01	0.45	0.04			
3	0	0.45	0			

It can be seen that the quantity of h-BN forming in the mixtures containing CaCO₃ as additive were significantly larger than those containing no CaCO₃. CaCO₃ addition is also seen from Figure 4.29 to decrease the quantity of B₄C in the reaction products. The XRD patterns of these experiments given in Figure 4.30 are in accord with the results of the quantitative analysis, where it can be observed that the B₄C peaks of the samples obtained without CaCO₃ addition are higher than the ones with additions. Efficiency of h-BN formation was calculated from the chemical analysis data. It was found that all of the C was consumed in 2h when CaCO₃ was added and 83% of C in the initial mixture was used in formation of h-BN. On the other hand, some unreacted carbon remained at the end of 2h when no CaCO₃ was used and 56% of the C was consumed in h-BN formation. In

these experiments, all of the C was consumed in 3 hours and 63% of initial C was utilized. These results indicate that addition of 10wt%CaCO₃ increases the reaction rate and reduces the loss of carbon. Carbon loss, taking place during carbothermic production of h-BN was also reported in other studies [8].

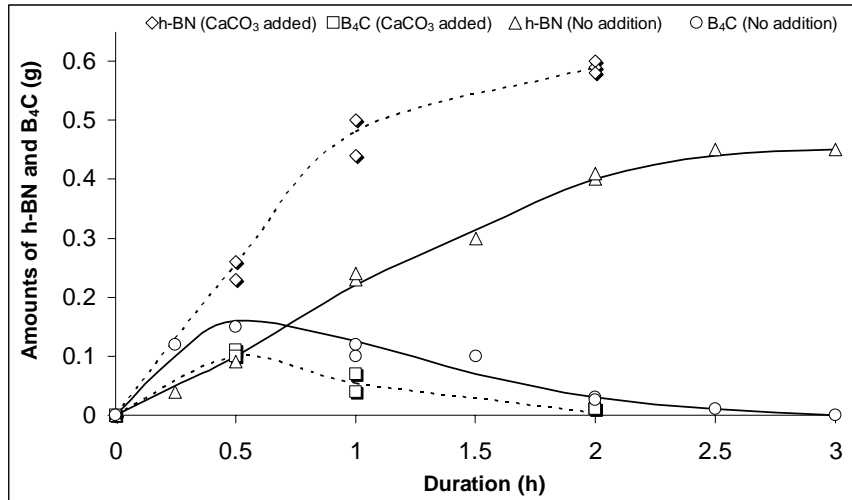


Figure 4.29. Amounts of h-BN and B₄C in the products of the experiments conducted for 30 minutes to 2 hours at 1500°C with plain and 10 wt% CaCO₃ added mixtures.

In order to investigate the effect of CaCO₃ addition on the growth of h-BN crystallites, average crystal thickness values in the c-axis direction, L_c , of the formed h-BN were calculated by the Scherrer formula. L_c is defined as the mean height of a pack of parallel and crystallographically connected hexagonal layers. In this calculation, full width at half maximum (FWHM) values of the peaks originating from (002) planes of h-BN ($2\theta=26.7^\circ$), presented on the XRD patterns given in Figure 4.30 were utilized. The calculated L_c values of the h-BN formed in the experiments conducted for 30 minutes to 2 hours at 1500°C with plain and CaCO₃ added mixtures are presented in Table 4.6. It is seen that addition of

CaCO₃ results in a moderate increase in the average crystal thickness of the formed h-BN powder.

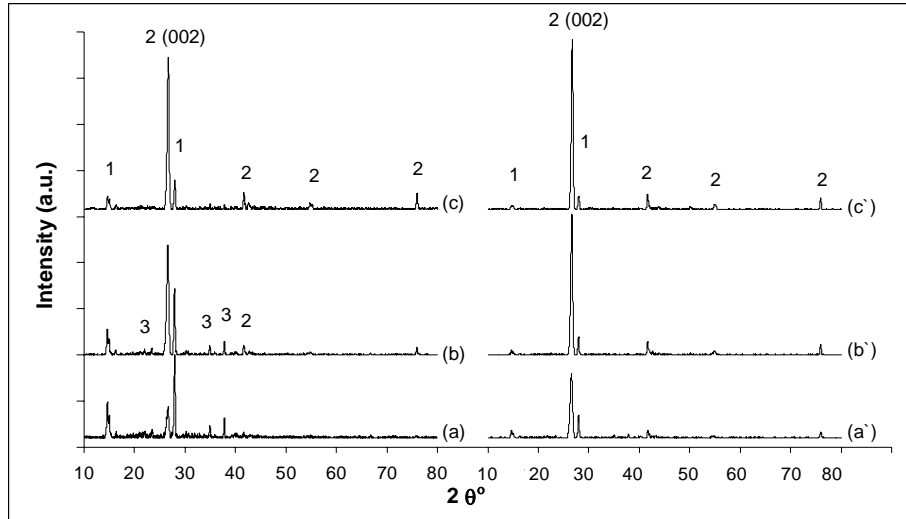


Figure 4.30. XRD patterns of the products of the experiments conducted with plain and 10 wt% CaCO₃ added mixtures at 1500°C. (a) plain mixture - 30 minutes, (a') CaCO₃ added mixture - 30 minutes; (b) plain mixture - 1 hour, (b') CaCO₃ added mixture - 1 hour; (c) plain mixture - 2 hours, (c') CaCO₃ added mixture - 2 hours. (1) H₃BO₃, (2) h-BN, (3) B₄C.

Table 4.6. Average crystal thickness values of h-BN formed from plain and CaCO₃ added mixtures.

Duration of Experiment	Average Crystal thickness, L _c (nm)	
	Plain mixture	CaCO ₃ added
30 minutes	15.13	16.55
1 hour	17.90	21.14
2 hours	22.02	23.85

SEM micrographs of reaction products formed in the experiments conducted for 2 hours at 1500°C with plain and CaCO₃ added mixture are presented in Figures 4.31 and 4.32, respectively. These micrographs were taken from the spots inside the reaction products where definite grain structures could be visualized. It is measured on SEM micrographs that average grain diameter of h-BN formed in 2 hours from plain mixtures is 0.36±0.08μm and addition of CaCO₃ increases the grain diameter to 0.70±0.14μm. The effect of CaCO₃ addition is seen to be that of formation of individual h-BN particles having separate surfaces with definite edges instead of a merged polycrystalline form observed in the h-BN produced without CaCO₃ additions. The results of the BET specific surface area measurements are in accord with the observations made on the SEM micrographs. The specific surface area of the h-BN powder formed in the experiments conducted for 2 hours with plain mixtures was determined as 31.7m²/g; whereas the specific surface area of the h-BN powder obtained in the same experimental conditions with 10 wt% CaCO₃ added mixture was 21m²/g. This result indicates that CaCO₃ has a positive function on the growth of h-BN grains.

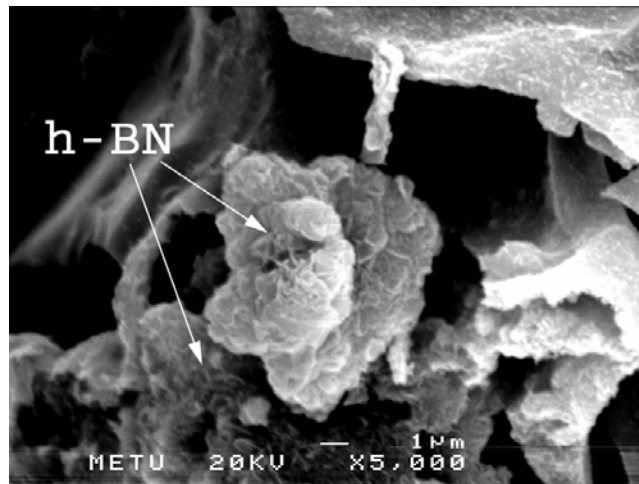


Figure 4.31. SEM micrograph of h-BN formed from plain mixture at 1500°C in 2 hours.

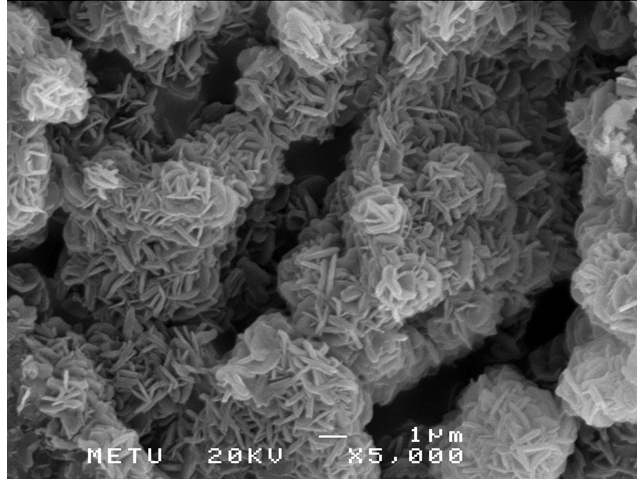
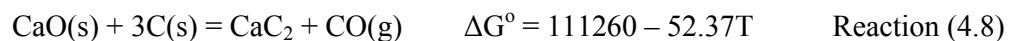
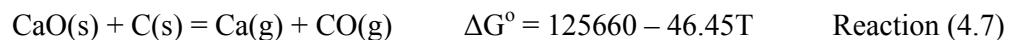


Figure 4.32. SEM micrograph of h-BN formed from 10 wt% CaCO₃ added mixture at 1500°C in 2 hours.

No peaks related to any Ca-containing species are seen on the XRD patterns of the reaction products of the mixtures into which CaCO₃ has been added. No CaCO₃ peak is expected to be present on the XRD patterns as CaCO₃ decomposes in accord with the following reaction above a certain temperature.



As the normal calcination temperature of CaCO₃ is 902°C [47] and as the experimental temperature is 1500°C, there should not remain any CaCO₃ in the reaction products. The fact that there are no CaO peaks on the XRD patterns may be taken as an indication that CaO has undergone a reaction during the experiments. The possibilities are reduction of CaO with carbon and formation of elemental calcium or CaC₂ in accord with the following reactions:

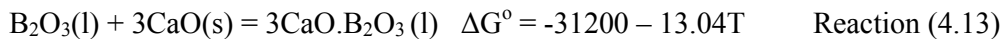
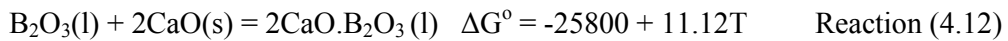
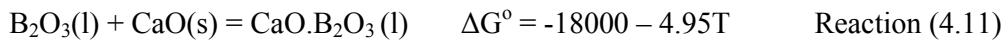
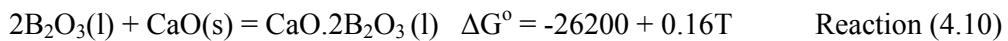


or formation of calcium borate in accord with the reaction:



The equilibrium constant of Reaction (4.7), $K_{4.7} = P_{\text{Ca}} \cdot P_{\text{CO}}$, is 3.65×10^{-6} at 1500°C . This low equilibrium constant indicates that Reaction (4.7) may take place only under very low pressures and is not expected to take place under the experimental conditions used. The equilibrium constant of Reaction (4.8), $K_{4.8} = P_{\text{CO}}$, is 6.45×10^{-3} at 1500°C which again may be taken as an indication that this reaction also does not take place in the system. If either or both of Reactions (4.7) and (4.8) had taken place, carbon loss from the system would have increased. The fact that CaCO_3 addition has resulted in a decrease of carbon loss also favors the conclusion that Reactions (4.7) and (4.8) do not take place in the system.

B_2O_3 - CaO phase diagram shown in Figure 4.26 shows that B_2O_3 and CaO form the compounds $\text{CaO} \cdot 2\text{B}_2\text{O}_3$, $\text{CaO} \cdot \text{B}_2\text{O}_3$, $2\text{CaO} \cdot \text{B}_2\text{O}_3$ and $3\text{CaO} \cdot \text{B}_2\text{O}_3$ in the solid state and there is no solid phase in the system at 1500°C for CaO contents less than $\sim 80\%$. Standard free energy of formation of the compounds $\text{CaO} \cdot 2\text{B}_2\text{O}_3$, $\text{CaO} \cdot \text{B}_2\text{O}_3$, $2\text{CaO} \cdot \text{B}_2\text{O}_3$ and $3\text{CaO} \cdot \text{B}_2\text{O}_3$ indicate that all of these reactions are possible in the system:



So it is likely that a $m\text{CaO} \cdot n\text{B}_2\text{O}_3$ compound has formed during heating of the reaction mix to 1500°C . If such a compound has formed during heating it would

melt and exist in the liquid state at 1500°C. If such a compound has not formed during heating then CaO originating from calcination of CaCO₃ is expected to dissolve in liquid B₂O₃. In either case, then, B₂O₃ and CaO will exist in the liquid state (either as a single liquid or as two immiscible liquids) for CaO contents less than ~80%. When the pellet is cooled to room temperature at the end of the experiment the liquid (or liquids) will solidify. There will be B₂O₃ and CaO.2B₂O₃ phases at room temperature if the overall composition is to the left of A, CaO.2B₂O₃ and CaO.B₂O₃ phases if the overall composition is between A and B, CaO.B₂O₃ and 2CaO.B₂O₃ phases if the overall composition is between B and C, 2CaO.B₂O₃ and 3CaO.B₂O₃ phases if the overall composition is between C and D and 3CaO.B₂O₃ and CaO phases if the overall composition is to the right of D as seen in Figure 4.26. B₂O₃ (H₃BO₃) peaks are seen in the XRD patterns of the pellets into which 20% or less CaCO₃ has been added which indicates that the overall composition of the CaO-B₂O₃ melt is to the left of A in these pellets; the CaO contents given in Table 4.4 verify this indication. Quantity of B₂O₃ is expected to decrease with increasing addition of CaCO₃ in these pellets. The results presented in Figure 4.28 are in accord with this expectation. CaO.2B₂O₃ is also expected to be present in these pellets but no peaks related to this compound are seen on the XRD patterns given in Figure 4.28. This may be due to CaO.2B₂O₃ solidifying in amorphous state as rate of cooling is very fast. CaO.B₂O₃ peaks are observed in Figure 4.28 to be present on the XRD pattern of the pellets into which CaCO₃ higher than 40% have been added. There are no B₂O₃ (H₃BO₃) peaks on the XRD patterns of the pellets containing 30% or more CaCO₃. These results indicate that the overall composition of the CaO-B₂O₃ melt in these pellets is to the right of A. CaO.B₂O₃ phase is also expected to be present but no peaks related to this compound are seen on the XRD patterns given in Figure 4.28. It appears therefore, that CaO.B₂O₃ has solidified in amorphous state in these pellets also.

It was seen in the XRD patterns of the products obtained by reacting 20wt% CaO-80wt% B₂O₃ mixture and 35wt% CaO-65wt% B₂O₃ mixture at 1250°C and then

by cooling in air that both of the compositions were in amorphous structure. The product containing 35wt% CaO did not present any B_2O_3 (H_3BO_3) peaks, however B_2O_3 (H_3BO_3) peaks were present in the XRD pattern of the product obtained from 20wt%CaO-80wt% B_2O_3 mixture. These results are in agreement with the previous statements and the phase diagram given in Figure 4.26.

Due to the fact that amorphous calcium borate phases could not be detected by XRD analysis of the pellets containing less than 40% $CaCO_3$, FT-IR analyses were utilized. In order to distinguish the FT-IR peaks of the constituents of the products, FT-IR patterns of each constituent was determined separately in its pure form. B_4C used for this purpose was produced by the reaction of boric oxide and carbon under argon (Figure 4.33 (a)). It has a characteristic peak at 1095 cm^{-1} . h-BN was produced by carbothermic method and was purified by leaching and oxidation of the impurities (Figure 4.33 (b)) [8]. Hexagonal-BN has peaks at 817 and 1404 cm^{-1} . The pattern of H_3BO_3 given in Figure 4.33 (c) belongs to a commercial boric acid (Merck Chemicals). It has peaks at 825 , 1203 , 1490 , 3230 cm^{-1} . The patterns of h-BN, B_4C , and H_3BO_3 are in agreement with the data in the literature [11,54]. Calcium borate was produced by reacting 35wt% CaO - 65wt% B_2O_3 mixture (Figure 4.33 (d)) at 1150°C . Due to the lack of FT-IR data on calcium borate in the literature, data obtained in the current study is used for the interpretation of product phases in the experiments.

In Figures 4.33 (e-h), FT-IR patterns of the products obtained from the experiments conducted at 1500°C for 30 minutes with 0, 10, 30 and 50 wt% $CaCO_3$ additions are presented. The peaks of h-BN, H_3BO_3 and calcium borate at $1404\text{-}1490\text{cm}^{-1}$ overlap and make it difficult to make interpretations based on these peaks. In the sample produced without addition of $CaCO_3$, presence of h-BN and H_3BO_3 was detected (Figure 4.33 (e)). With addition of 10wt% $CaCO_3$ a peak at 1420 cm^{-1} was observed and with increasing $CaCO_3$ contents, the hump at 1000 cm^{-1} appeared indicating the presence of calcium borate phase (Figure 4.33 (g)). The consumption of B_2O_3 during formation of calcium borate can be followed

from the disappearance of the O-H peak at 3230 cm^{-1} and also the peak at 1203 cm^{-1} , which belong to H_3BO_3 [54].

Peaks belonging to B_4C are relatively small in Figures 4.33 (e) and 4.33 (f); and are not distinguishable in Figures 4.33 (g) and 4.33 (h). They may be masked by the other compounds.

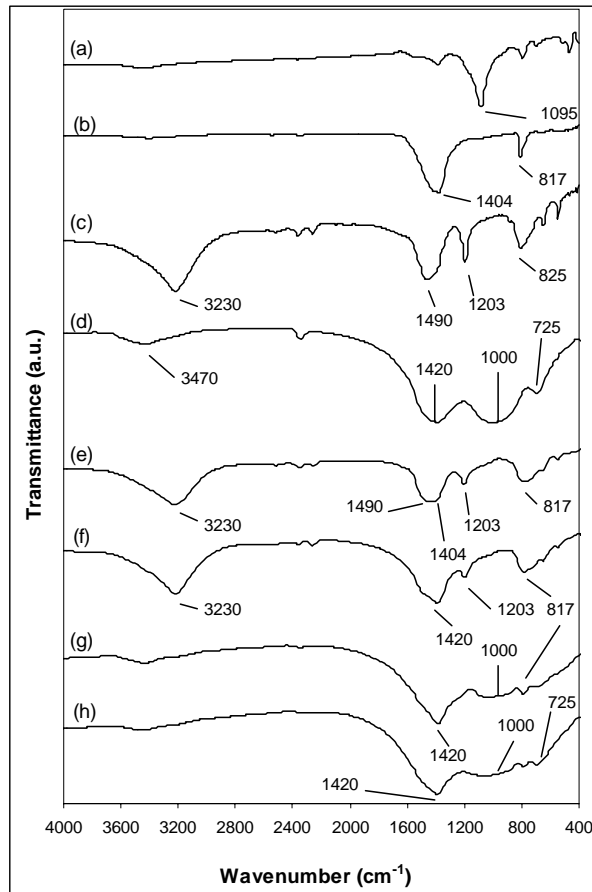


Figure 4.33. FT-IR patterns of (a) B_4C , (b) h-BN, (c) H_3BO_3 , (d) calcium borate, (e) product obtained from plain $\text{B}_2\text{O}_3+\text{C}$ mixtures in 30 minutes at 1500°C , (f) product obtained from 10wt% CaCO_3 added $\text{B}_2\text{O}_3+\text{C}$ mixtures, (g) product obtained from 30wt% CaCO_3 added $\text{B}_2\text{O}_3+\text{C}$ mixtures, (h) product obtained from 50wt% CaCO_3 added $\text{B}_2\text{O}_3+\text{C}$ mixtures.

In Figure 4.34 (b) it is seen that after leaching the sample containing 30wt% CaCO_3 with dilute HCl , the peaks belonging to calcium borate are removed and B_4C peak is revealed. After holding the sample at 800°C in air for oxidation and leaching with water, B_4C was removed and only h-BN remained (Figure 4.34 (c)).

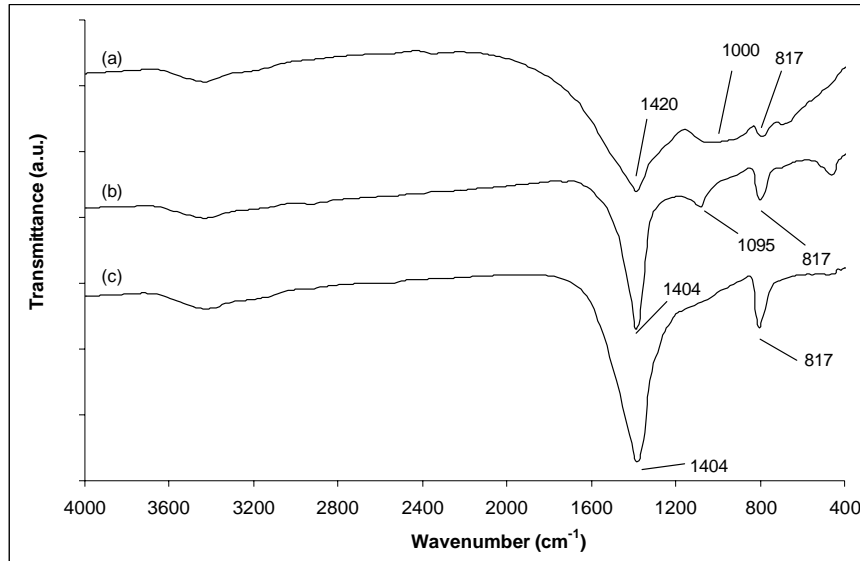


Figure 4.34. FT-IR patterns of (a) product obtained from 30wt% CaCO_3 added $\text{B}_2\text{O}_3+\text{C}$ mixture in 30 minutes at 1500°C , (b) sample in (a) leached in dilute HCl , (c) sample in (b) oxidized at 800°C and leached with water.

Addition of CaCO_3 into ($\text{B}_2\text{O}_3+\text{C}$) mixtures for the proportions in the 5-50wt% range increases the quantity of h-BN formed. It is known [8] that carbothermic formation of h-BN in $\text{B}_2\text{O}_3+\text{C}$ mixtures subjected to N_2 gas takes place by reaction of $\text{B}_2\text{O}_3(\text{g})$ and $\text{N}_2(\text{g})$ on solid C. B_4C also forms [8] during the process which slows the h-BN formation as discussed in the previous sections. If this mechanism does not change with addition of CaCO_3 into $\text{B}_2\text{O}_3+\text{C}$ mixtures, CaCO_3 should somehow be favoring of h-BN formation. B_4C forms during carbothermic h-BN formation in regions of the pellet into which N_2 can not penetrate. Hexagonal BN formation is expected to be accelerated by easing the

access of $N_2(g)$ into the pellet. Accordingly, h-BN formation is expected to be favored by increased porosity of the pellet. Reaction products of the pellets containing lower than 20 wt% $CaCO_3$ were observed to be more porous than those of the plain pellets. Based on this observation, $CaCO_3$ is concluded to increase the porosity of the pellets for additions less than 20%. The effect of $CaCO_3$ in favoring the h-BN formation may therefore be due to increasing the porosity of the pellets. The increase in porosity of the pellet with addition of $CaCO_3$ may be due to $CO_2(g)$ evolution from the system associated with calcination of $CaCO_3$. This can not be the only reason, however, as porosity has been observed to be high with $CaCO_3$ additions up to 20% but low for higher additions. The properties like the viscosity, density, etc. of the liquid calcium borate existing in the system during the reaction also appears to affect the porosity of the pellets.

As stated above two liquids, a' and b' (essentially pure B_2O_3), exist in the system at $1500^\circ C$ (Figure 4.26) for CaO contents of the CaO- B_2O_3 melts less than a' when the activity of B_2O_3 as the standard state is about unity. With the increase in the amount of $CaCO_3$ addition until the CaO content of the CaO- B_2O_3 melt reaches a', B_2O_3 activity remains unchanged but the quantity of B_2O_3 existing in the system decreases. Consequently, ΔG of Reaction (2.6), $B_2O_3(l) + C(s) + N_2(g) = 2BN(s) + 3CO(g)$ and equilibrium vapor pressure of $B_2O_3(l)$ remain unchanged but due to the decrease in the quantity of $B_2O_3(l)$ in the system, rate of evaporation of $B_2O_3(l)$ decreases which decreases the rate of reaction. So, with $CaCO_3$ addition, porosity of the pellet increases (up to 20 wt%) which increases the rate of Reaction (2.6) but the rate of evaporation of $B_2O_3(l)$ decreases which decreases the rate of reaction. Depending on the relative importance of these opposing factors, rate of formation of h-BN may increase or decrease. For $CaCO_3$ additions up to 10wt% the increase in rate of the Reaction (2.6) due to increased porosity of the pellet appears to outweigh the decrease in the rate of the reaction due to decreased rate of evaporation of $B_2O_3(l)$. For $CaCO_3$ additions more than 10wt%, the opposite appears to be true.

For larger CaCO_3 additions when the overall composition of the $\text{CaO-B}_2\text{O}_3$ melt is to the right of a' in Figure 4.26, there is no $\text{B}_2\text{O}_3(l)$ in the system and the liquid existing in the system is a calcium borate in which activity of B_2O_3 is less than 1. Under these conditions ΔG of Reaction (2.6) becomes less negative and equilibrium vapor pressure of B_2O_3 becomes less than that of pure $\text{B}_2\text{O}_3(l)$. Reaction (2.6) thus becomes less favorable which explains the decrease in the rate of formation of h-BN with the increase in CaCO_3 addition; the decrease in the porosity of the pellet also acts in the direction of decreasing rate of formation of h-BN.

Another reason for the increase in rate of formation of h-BN when CaCO_3 is added into $\text{B}_2\text{O}_3+\text{C}$ mixtures could be that a different additional mechanism becomes operative with addition of CaCO_3 . Bartnitskaya et. al. studied the effect of Li_2CO_3 addition to h-BN formation by different methods like subjecting $\text{B}_2\text{O}_3-\text{C}$ mixtures, boric acid-carbamide mixtures to $\text{N}_2(g)$ or ammonia gas [49,50]. They have found Li_2CO_3 to favorably affect h-BN formation and h-BN crystallinity and have suggested h-BN to crystallize from the lithium borate melt. A similar mechanism may apply in formation of h-BN from $\text{B}_2\text{O}_3+\text{C}+\text{CaCO}_3$ mixtures subjected to N_2 gas.

A SEM micrograph of the product pellet which was obtained from the experiment conducted at 1500°C for 1h with 10wt% CaCO_3 addition is given in Figure 4.35. It is known from the presence of unreacted carbon and remaining boric oxide in this sample that reaction was not complete and formation of h-BN grains are in progress. It is seen from this figure that the h-BN grains are embedded in a solidified continuous matrix phase (pointed with arrows). The h-BN grains seem to be growing out from the matrix phase.

In accord with the discussion above, two liquids, a' (calcium borate) and b' (essentially pure B_2O_3) are expected to be present in the system at 1500°C for CaCO_3 additions less than 40%. For 40% and 50% CaCO_3 additions there is a

single liquid calcium borate in the system. As the different additional mechanism applies when CaCO_3 is added into the $\text{B}_2\text{O}_3+\text{C}$ mixture, the matrix phase through which the h-BN grains grow is expected to be the liquid calcium borate phase.

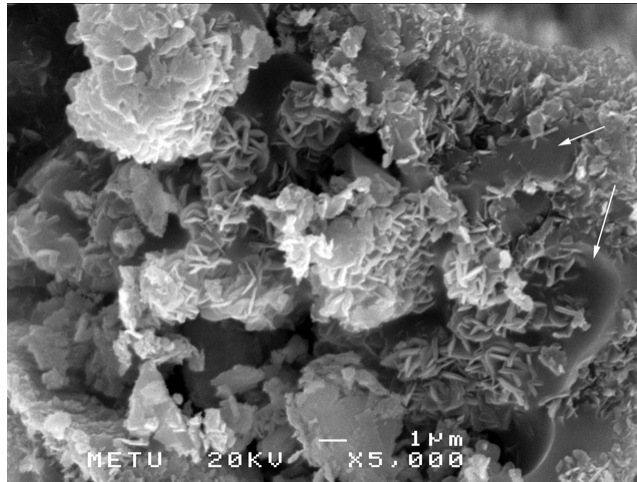


Figure 4.35. SEM micrograph of h-BN formed from 10 wt% CaCO_3 added mixture at 1500°C in 1 hour.

Nitrogen is soluble in oxide melts (slags) and the nitrogen solubility depends on slag basicity for given O_2 and N_2 pressures and temperature. Slag basicity depends on the relative proportions of basic and acidic oxides in the slag. A basic oxide like CaO dissolves in oxide solution in accord with the reaction [59]:



thereby providing O^{2-} ions to the solution. An acidic oxide like B_2O_3 consumes O^{2-} during dissolution in oxide solutions. When sufficient O^{2-} ions are present in the system B_2O_3 is expected to form $(\text{BO}_3)^{3-}$ according to:



A slag composed of basic and acidic oxides is basic when the O^{2-} provided by basic oxides exceeds the O^{2-} need of the acidic oxides when there will remain free O^{2-} in the system. When the O^{2-} need of the acidic oxide for formation of simple anions like $(BO_3)^{3-}$ in Reaction (4.15) exceeds the O^{2-} provided by the basic oxides, the slag will be acidic when the acidic oxides like B_2O_3 form more complicated anions like $(B_2O_5)^{4-}$, $(B_3O_7)^{5-}$, etc. by polymerization (chain formation, network formation) reactions like:



Nitrogen dissolution in basic slags is governed by Reaction (4.18) [59].



The equilibrium constant of Reaction (4.18) is:

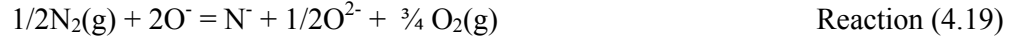
$$K_{4.13} = \frac{a_{N^{3-}} \times P_{O_2}^{3/4}}{P_{N_2}^{1/2} \times a_{O^{2-}}^{3/2}} = \frac{\gamma_{N^{3-}} \times (\%N) \times P_{O_2}^{3/4}}{P_{N_2}^{1/2} \times a_{O^{2-}}^{3/2}} \quad \text{Equation (4.6)}$$

Activities and activity coefficients of single ions in slags can not be determined. Rearranging Equation (4.6), the relation

$$C_{N^{3-}} = K_{4.13} \times \frac{a_{O^{2-}}^{3/2}}{\gamma_{N^{3-}}} = (\%N) \times \frac{P_{O_2}^{3/4}}{P_{N_2}^{1/2}} \quad \text{Equation (4.7)}$$

is obtained where the right hand side, defined as the nitride capacity $C_{N^{3-}}$, can experimentally be determined.

Nitrogen dissolution in acidic slags is more complicated as nitrogen has been observed [60,61] and is considered [59] to be combined to the acidic oxide anions. Fruehan [62] has suggested nitrogen dissolution in acidic slags to be governed by the reaction:



where O^- and N^- are non-bridging oxygen and non-bridging nitrogen, respectively. The equilibrium constant of Reaction (4.19) is:

$$K_{4.14} = \frac{a_{N^-} \times a_{O^{2-}}^{1/2} \times P_{O_2}^{3/4}}{P_{N_2}^{1/2} \times a_{O^-}^2} = \frac{\gamma_{N^-} \times (\%N) \times a_{O^{2-}}^{1/2} \times P_{O_2}^{3/4}}{P_{N_2}^{1/2} \times a_{O^-}^2} \quad \text{Equation (4.8)}$$

Rearranging Equation (4.8), the relation

$$C_{N^-} = K_{4.14} \times \frac{a_{O^-}^2}{\gamma_{N^-} \times a_{O^{2-}}^{1/2}} = (\%N) \times \frac{P_{O_2}^{3/4}}{P_{N_2}^{1/2}} \quad \text{Equation (4.9)}$$

is obtained where the right hand side, defined as the incorporated nitride capacity, C_{N^-} , can experimentally be determined. The right hand side of Equations (4.7) and (4.9) in the definitions of $C_{N^{3-}}$, referred to as free nitride capacity, and C_{N^-} are identical. Nitride capacity, whether defined by Equation (4.7) or by Equation (4.9) is seen to depend on the composition of the oxide melt at a given temperature. Considering $a_{O^{2-}}$ to be a measure of the basicity of the slag, $C_{N^{3-}}$ is seen to increase while C_{N^-} is seen to decrease with the increase in slag basicity. Accordingly, nitride capacity defined as:

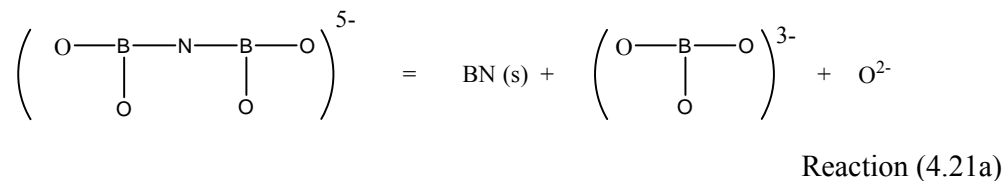
$$C_N = (\%N) \times \frac{P_{O_2}^{3/4}}{P_{N_2}^{1/2}} \quad \text{Equation (4.10)}$$

is expected to decrease with increase in slag basicity in acidic slags and to increase with the increase in slag basicity in basic slags. Nitride capacities of several oxide melts have been measured. The results are not always in accord with the above stated expectations. It should be definite, however, that the nitride capacity of a slag of a given composition be a constant at a given temperature.

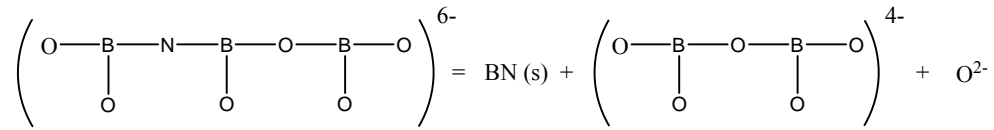
Hexagonal BN is soluble in oxide melts and its solubility depends on composition. Wakasugi [63] determined solubility of h-BN in several B₂O₃-basic oxide binary systems and found h-BN solubility to increase with the increase in the concentration of the basic oxide up to 0.1-0.2 mole fraction of the basic oxide and to decrease with further increase in the concentration of the basic oxide. For a given slag composition h-BN solubility should be a constant at a given temperature. Nitrogen dissolved in B₂O₃ containing oxide melts may result in formation of h-BN if the solubility product of h-BN is exceeded. What the reactions for dissolution of h-BN in oxide melts or for formation of h-BN from oxide melts are not known. The studies of Bartnitskaya et al. [49,50] do not give a clue as to the possible h-BN formation reaction as they do not explicitly state the mechanism of crystallization of h-BN from the borate melt. One possible reaction for formation of h-BN from nitrogen and B₂O₃ containing oxide melts may be:



If, as suggested by Martinez and Sano [59], and Min and Fruehan [62]; nitrogen is considered to be incorporated into the borate anions, reactions like Reactions (4.21) and (4.22) etc. may result in formation of h-BN.



which in condensed form can be written as:



Reaction (4.22a)

which in condensed form can be written as:



Two liquids, a' and b' exist in the system at 1500°C for 5, 10, 20 and 30% CaCO₃ additions while a single calcium borate exists in the system at 1500°C for 40% and 50% CaCO₃ additions as stated above (Figure (4.26)). In the two liquids region thermodynamic properties of the calcium borate represented by a' in Figure (4.26) are independent of composition and as such nitride capacity, activities of several species etc. do not change with change in the quantity of CaCO₃ added. Driving force of Reactions (4.20), (4.21) and (4.22) will accordingly be independent of composition. If a certain amount of h-BN is considered to crystallize in a given time from a certain quantity of calcium borate (a') phase, the total quantity of h-BN crystallizing in the system should increase with increase in the quantity of the calcium borate phase. As CaCO₃ added to the reaction mix increases the quantity of calcium borate (a') phase, the quantity of h-BN forming in the system in a given time is expected to increase with CaCO₃ addition. That the increase in the quantity of h-BN with the increase in the quantity of CaCO₃ added continues up to 10% addition may be taken as an indication that crystallization of h-BN from the calcium borate phase is not the only mechanism of h-BN formation and that some h-BN forms by reaction of gaseous B₂O₃ with N₂(g) on carbon [8], the rate of which was explained before to decrease with increase in the quantity of CaCO₃ added.

For 40% and 50% CaCO_3 additions there is a single calcium borate melt in the system, the composition of which is to the right of a'. Thermodynamic properties like the nitride capacity, activities of several species etc. of this calcium borate phase depend on composition. Equilibrium vapor pressure of B_2O_3 in the system will be less than that of pure $\text{B}_2\text{O}_3(\text{l})$ when the rate of formation of h-BN by reactions of gaseous B_2O_3 with $\text{N}_2(\text{g})$ on carbon should be less than that for plain ($\text{B}_2\text{O}_3+\text{C}$) mixtures. That more h-BN forms for 40% and 50% CaCO_3 additions compared to plain ($\text{B}_2\text{O}_3+\text{C}$) mixtures may be taken as an indication that some h-BN forms by crystallization from the borate melt. With increase in the quantity of CaCO_3 added, the basicity of the borate melt will increase which is expected to decrease the activity of the borate anions making Reactions (4.20), (4.21) and (4.22) less favorable.

Reactions (4.20), (4.21) and (4.22) do not use C for formation of h-BN. C is nevertheless probably necessary, however, as dissolution of nitrogen in the calcium borate melt in accord with Reactions (4.18) and (4.19) and also formation of h-BN with Reactions (4.20), (4.21) and (4.22) are favored by low O_2 pressures which is provided by C.

Quantity of h-BN forming in a given reaction depends on the quantity of C in the reaction mix as C is the limiting reactant for the overall reaction $\text{B}_2\text{O}_3 + 3\text{C} + \text{N}_2 = 2\text{BN} + 3\text{CO}$ (Reaction (2.6)). Quantity of carbon in the ($\text{B}_2\text{O}_3+\text{C}$) mixtures and ($\text{B}_2\text{O}_3+\text{C}+\text{CaCO}_3$) mixtures were the same. The same amount of h-BN is therefore expected to form in different runs if the carbon loss from the system does not vary from run to run. As stated before, the quantity of h-BN forming in the mixtures containing CaCO_3 as additive were significantly larger than those containing no CaCO_3 . This may be taken as an indication that some h-BN forms according to Reaction (2.6) which uses C and some according to Reactions (4.20), (4.21) and (4.22) which do not consume C, on the conditions that C loss from the system does not change with addition of CaCO_3 .

Bartnitskaya et. al. [49,50] found in their study on h-BN formation from boric acid+carbamide mixtures that more C remains present at a given temperature while more h-BN forms when Li_2CO_3 is added to the reaction mechanism. This result may also be taken as an indication that some h-BN forms without use of C when Li_2CO_3 is added to the reaction mixture when a lithium borate is expected to form.

In the experiments performed with CaCO_3 addition, 10wt% CaCO_3 addition was found to be the optimum. Therefore, the amount of addition of all other additives was fixed at 10wt%, in order to be able to compare their catalytic effect with CaCO_3 .

4.4.1.2. MgO Addition

With the aim of investigating the effect of MgO on the carbothermic formation of h-BN, experiments were performed for 30 minutes, 1 and 2 hours with 10wt% MgO added $\text{B}_2\text{O}_3+\text{C}$ mixtures. SEM micrograph of the MgO powder used in the experiments is presented in Figure 4.36. It is seen that there are large agglomerate-like particles size of which is as large as 70-100 μm . However, there are also small particles in the range of 10 μm .

XRD patterns of the products of the experiments conducted for 30 minutes, 1 hour and 2 hours with 10wt% MgO addition are presented in Figure 4.37. It is seen that $\text{Mg}_2\text{B}_2\text{O}_5$ ($2\text{MgO}.\text{B}_2\text{O}_3$) forms by the reaction of MgO with B_2O_3 . After leaching with 1/1 (v/v) HCl/water solution for 15 hours, the $\text{Mg}_2\text{B}_2\text{O}_5$ phase could be removed (Figure 4.37 (c)). According to the phase diagram of B_2O_3 -MgO system given in Figure 4.38, $\text{MgO}.\text{B}_2\text{O}_3$ may also be expected to form. Due to the fast cooling rate of the sample, it may be in amorphous structure and not be detected by the XRD analyses.

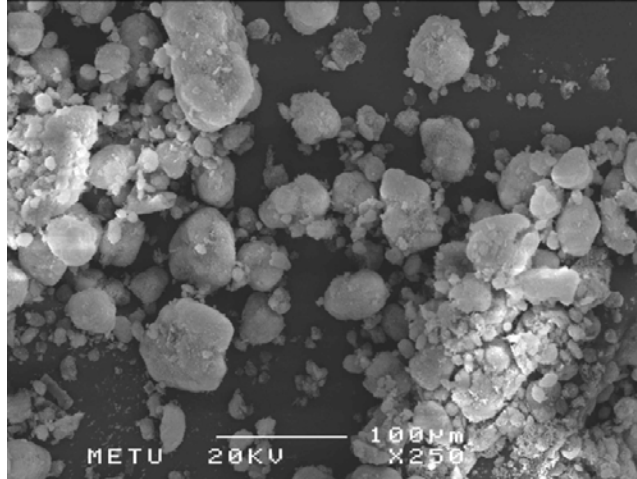


Figure 4.36. SEM micrograph of MgO powder.

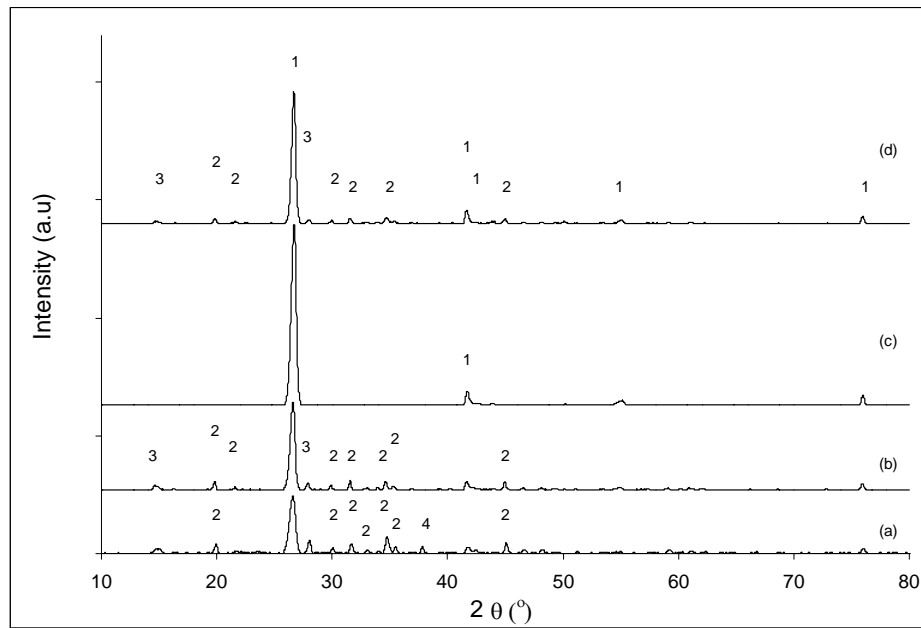


Figure 4.37. XRD patterns of the experiments conducted with 10wt% MgO added B_2O_3+C mixtures for (a) 30 minutes, (b) 1 hour, (c) 1 hour and leached, (d) 2 hours. (1) h-BN, (2) $Mg_2B_2O_5$, (3) H_3BO_3 , (4) B_4C .

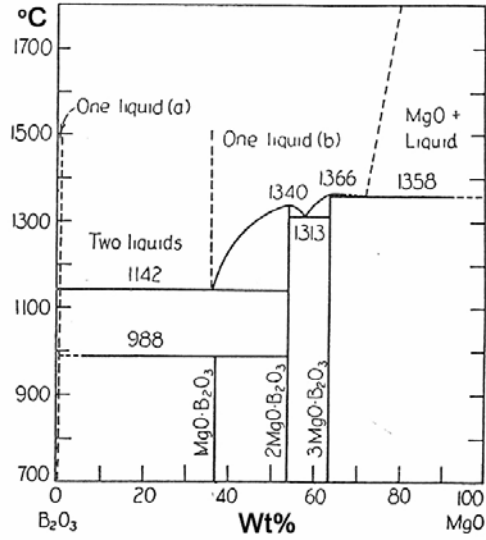


Figure 4.38. B₂O₃-MgO phase diagram [58].

According to chemical analysis given in Table 4.7, amounts of h-BN and B₄C are very similar to the results obtained with CaCO₃ addition. Hexagonal BN amount is considerably higher than the ones obtained from plain B₂O₃+C mixtures and that of B₄C is lower. MgO, therefore, affects h-BN formation in a way similar to CaO (CaCO₃). This is not an unexpected result considering that the reaction product of the (B₂O₃+C) mix into which MgO was added was observed to be more porous than the reaction products of the plain mixes and also considering that MgO is a basic oxide.

The possibility of the increase in the porosity of the pellet due to CO₂(g) evolution from the system as a result of the decomposition of CaCO₃, which was mentioned in the previous section, may therefore not be valid; since there is no CO₂(g) evolution in the MgO added system, however similar porous structure and similar increase in the rate and amount of h-BN formation to those obtained in CaCO₃ added samples are observed.

Table 4.7. Amounts of h-BN and B₄C obtained in the products of the experiments conducted with 10wt% MgO addition.

Duration	Amount of h-BN formed (g)	Amount of B ₄ C formed (g)
30 minutes	0.22	0.13
1 hour	0.46	0.06
2 hours	0.63	0.02

4.4.1.3. BaCO₃ Addition

The effect of BaCO₃ addition was investigated by reacting 10wt% BaCO₃ added B₂O₃+C mixtures for 30 minutes, 1 and 2 hours at 1500°C. From the SEM micrograph presented in Figure 4.39, BaCO₃ powder is seen to be composed of rod-like grains. Their thickness is about 1µm and length is 3-4µm. Presence of some agglomerates, formed from these small grains can be deduced from Figure.4.39.

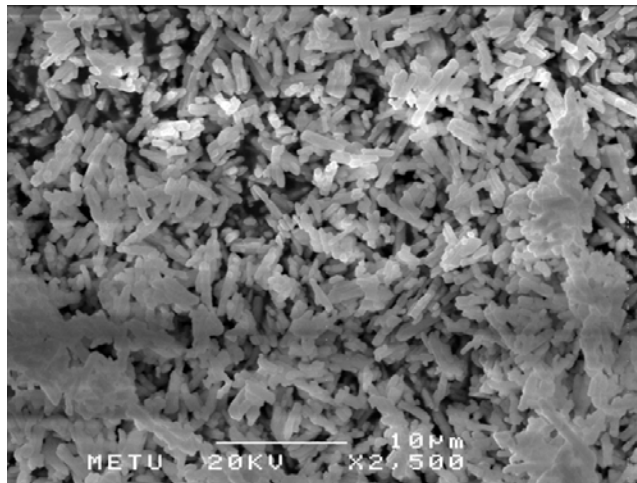


Figure 4.39. SEM micrograph of BaCO₃ powder

Similar to CaCO_3 , BaCO_3 decomposes into BaO and CO_2 . Normal decomposition temperature is 1431°C [47]. XRD patterns of the products of the experiments conducted with 10wt% BaCO_3 added $\text{B}_2\text{O}_3+\text{C}$ mixtures are presented in Figure 4.40. Unreacted BaO or any crystalline phase containing Ba was not detected by the XRD analyses. This finding is similar to CaCO_3 addition. According to the phase diagram given in Figure 4.41, $\text{BaO}\cdot 4\text{B}_2\text{O}_3$ phase would be expected in the reaction products. However, most probably similar to the case in CaCO_3 addition, due to the very fast cooling rate, this phase is in amorphous structure.

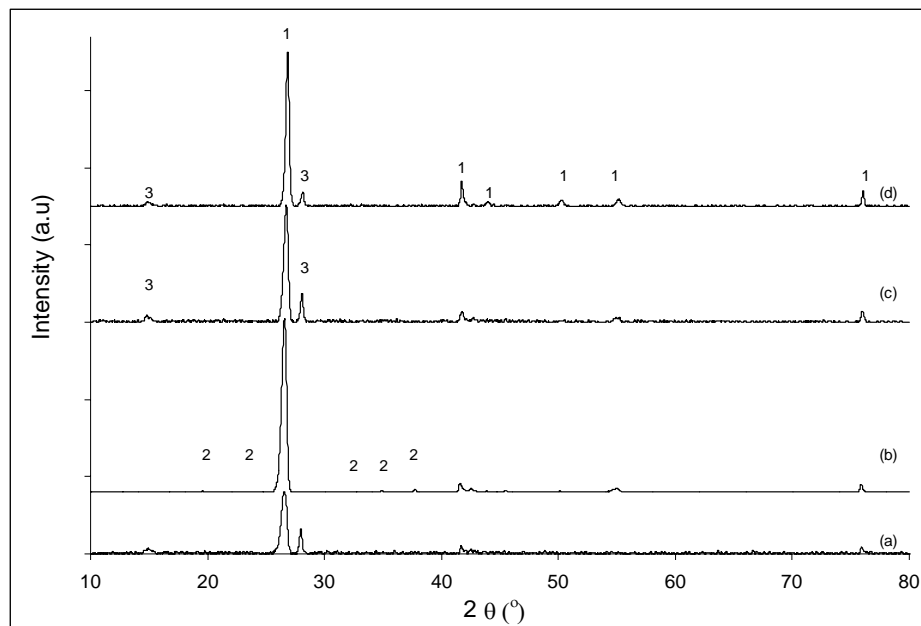


Figure 4.40. XRD patterns of the experiments conducted with 10wt% BaCO_3 added $\text{B}_2\text{O}_3+\text{C}$ mixtures conducted for (a) 30 minutes, (b) 30 minutes and leached, (c) 1 hour, (d) 2 hours. (1) h-BN, (2) B_4C (3) H_3BO_3 .

According to chemical analysis given in Table 4.8, amounts of h-BN and B_4C are similar to the results obtained with CaCO_3 and MgO addition. Explanations similar to CaO should apply to BaO .

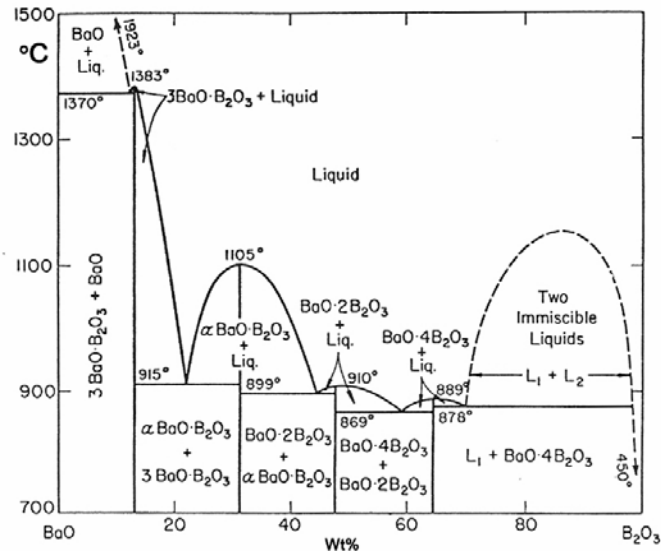


Figure 4.41. BaO-B₂O₃ phase diagram [58].

Table 4.8. Amounts of h-BN and B₄C obtained in the products of the experiments conducted with 10wt% BaCO₃ addition.

Duration	Amount of h-BN formed (g)	Amount of B ₄ C formed (g)
30 minutes	0.19	0.11
1 hour	0.41	0.06
2 hours	0.62	0.02

4.4.2. Effect of Transition Metal Oxides

In this part of the study, effect of addition of some transition metal oxides such as MnO₂, Fe₃O₄, Co₃O₄ and cupric nitrate have been investigated.

4.4.2.1. MnO₂ Addition

The MnO₂ powder used in the experiments was composed of quite large grains which were in the range of 50-100µm as seen from the SEM micrograph in Figure 4.42. The MnO₂ grains had irregular shapes with faceted edges.

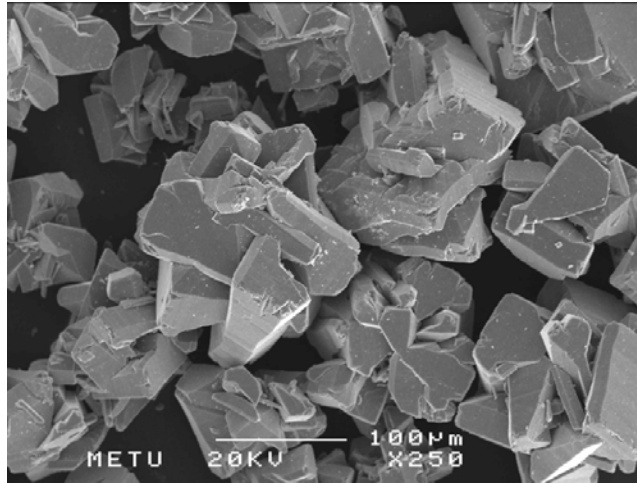


Figure 4.42. SEM micrograph of MnO₂ powder

XRD pattern of the product obtained from the experiment conducted with MnO₂ added B₂O₃+C mixture for 1 hour is given in Figure 4.43 (a). It can be seen in this pattern that no unreacted MnO₂ was left and a high amount of MnB has formed. It can be inferred that MnO₂ and B₂O₃ are reduced by C and MnB formed according to the following reaction:



The reaction product was leached with 1/1 (v/v) HCl/water solution, and it was seen from the XRD pattern given in Figure 4.43 (b) that almost all of the MnB could be leached out in the standard duration of leaching which was applied for all products (15 hours). However, it can be inferred from the minute amount of MnB

remained in the product that MnB is more difficult to remove by leaching than CaB_2O_4 or $\text{Mg}_2\text{B}_2\text{O}_5$. Thus, it requires longer duration or higher acid concentration for leaching.

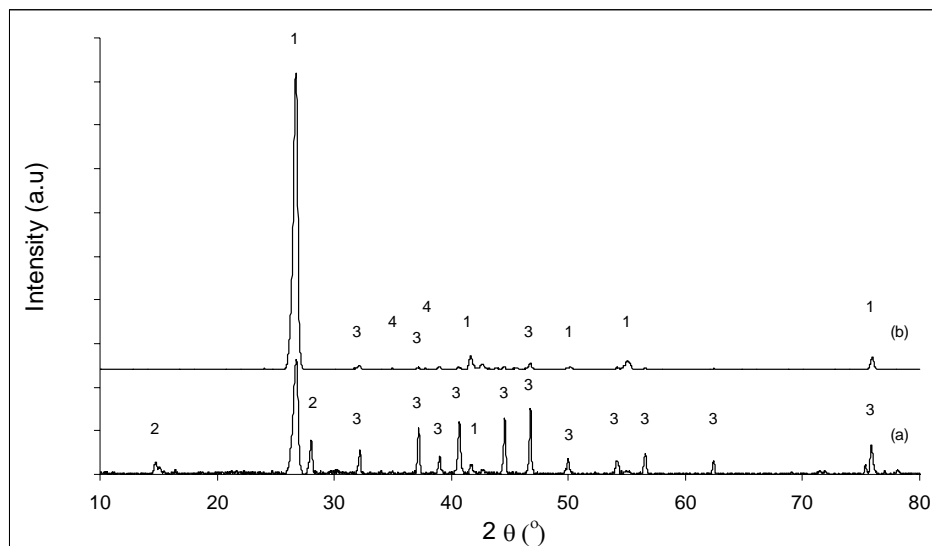


Figure 4.43. XRD patterns of the experiments (a) conducted with 10wt% MnO_2 added $\text{B}_2\text{O}_3+\text{C}$ mixtures for 1 hour, (b) after leaching product (a). (1) h-BN, (2) H_3BO_3 , (3) MnB, (4) B_4C .

It was found by the chemical analyses that the amount of formed h-BN in 1 hour (0.22g) is the similar to the ones formed from plain $\text{B}_2\text{O}_3+\text{C}$ mixtures. This result indicates that there has not been a positive effect of MnO_2 addition on increasing the amount of h-BN. However, amount of formed B_4C was reduced to 0.07g from 0.10g with addition of MnO_2 . MnB remaining in the products after leaching may cause an error in the determination of the amounts of B_4C and h-BN by the employed chemical analysis method. However, due to its amount being very low as inferred from the XRD analyses, the error can be ignored.

Due to the fact that MnO_2 has not provided an increase in the amount of h-BN formed, it can be concluded that MnO_2 is not useful as a catalyst in this process. Furthermore, formation of MnB takes place which, in addition to difficulty of removal by leaching, causes loss of B from the system.

4.4.2.2. Fe_3O_4 Addition

The SEM micrograph of Fe_3O_4 which was used in the experiments is given in Figure 4.44. It can be seen in this figure that Fe_3O_4 powder was composed of sub-micron sized grains. Although the size of the grains was quite small, they did not tend to form agglomerates.

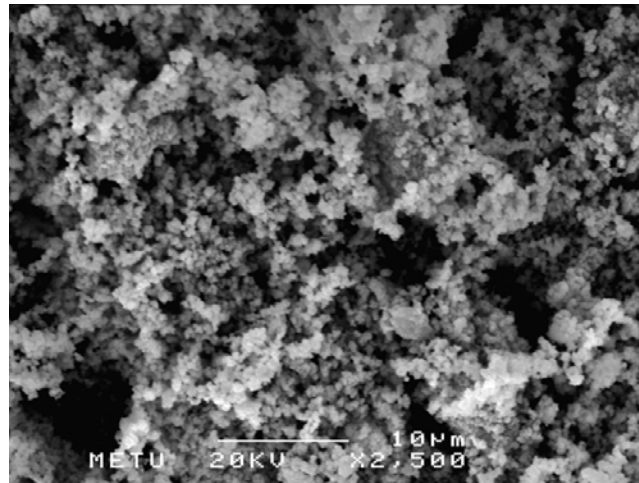


Figure 4.44. SEM micrograph of Fe_3O_4 powder

It was seen from the XRD pattern (Figure 4.45) of the product of the experiment conducted with 10 wt% Fe_3O_4 addition for 1 hour that metallic Fe was formed, due to the reduction of Fe_3O_4 , by the overall reaction:



FeC was also detected by the XRD analyses. From the XRD analysis performed after leaching the product it was inferred that Fe could be removed but FeC could not be removed from the products (Figure 4.45 (b)). According to the chemical analyses, 0.31g h-BN and 0.09g B₄C formed. The effect of the minute amount of the second phase, namely FeC on the chemical analysis is ignorable due to its very low amount as seen in the XRD pattern. Amount of h-BN (0.31g) is moderately higher than the amount formed from plain mixtures (0.23g), but lower than that obtained with CaCO₃ additions (0.44g). The amount of B₄C was lower than without additions and similar to the amount formed with previously used additives.

Consequently, although Fe₃O₄ provides some increase in the amount of h-BN, FeC forming can not be leached out from the produced h-BN. Therefore, it can be suggested that Fe₃O₄ is not a suitable material to be used as a catalytic additive in the carbothermic production of h-BN.

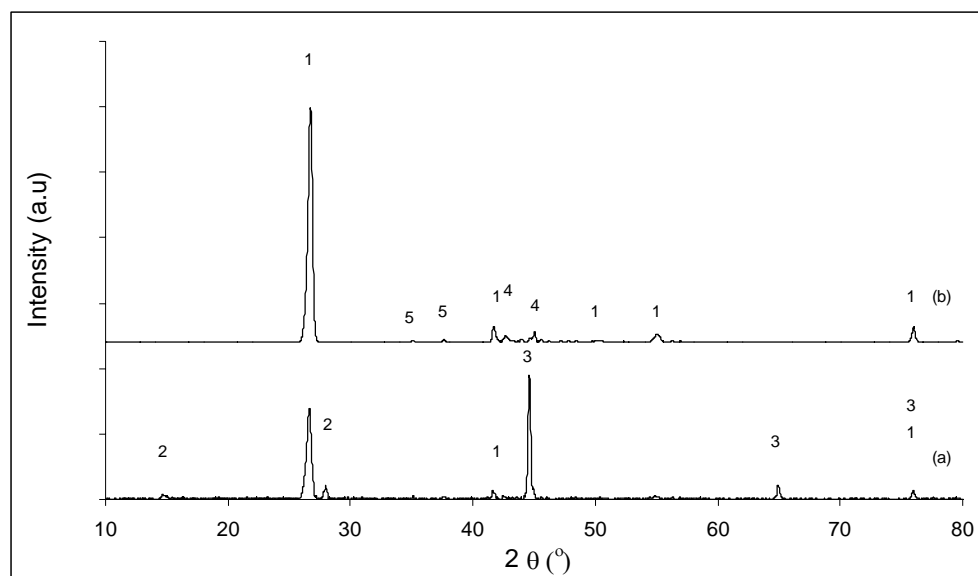


Figure 4.45. XRD patterns of (a) the experiments conducted with 10wt% Fe₃O₄ added B₂O₃+C mixtures for 1 hour, (b) after leaching product (a). (1) h-BN, (2) H₃BO₃, (3) Fe, (4) FeC, (5) B₄C.

4.4.2.3. Co₃O₄ Addition

From the SEM micrograph given in Figure 4.46 it is seen that the Co₃O₄ grains had sub-micron size. There are some grains having a few micron size, which seem like agglomerates composed of small grains.

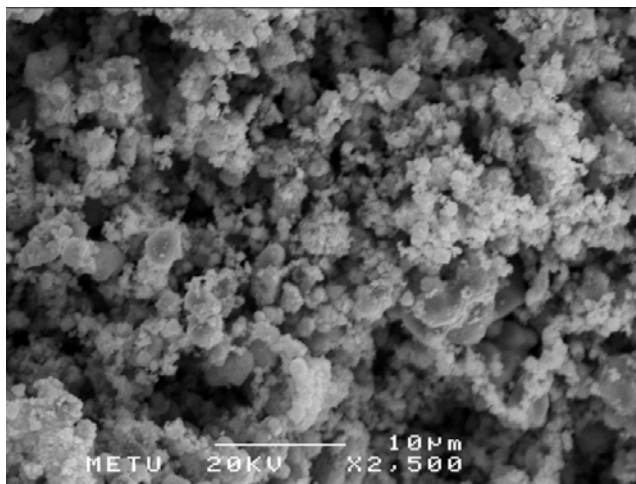


Figure 4.46. SEM micrograph of Co₃O₄ powder

It is found from the XRD pattern of the product obtained from the experiment conducted with 10 wt% Co₃O₄ addition for 1 hour that Co₃O₄ is reduced to metallic Co (Figure 4.47 (a)). Upon leaching, the formed Co could only be partially removed from the products (Figure 4.47 (b)). In addition to Co, presence of Co₂C and B₂CCo₁₁ were also seen together with formed h-BN in the reaction products. From the XRD pattern of the leached product, it can be seen that Co₂C and B₂CCo₁₁ could not be leached from the products at all. Therefore, it can be concluded that the usage of Co₃O₄ as a catalyst in the carbothermic production of h-BN is not suitable. For this reason amounts of the h-BN and B₄C could not be determined due to the high amount of unleachable secondary phases in the

products. Presence of secondary phases would lead to incorrect results in the chemical analyses.

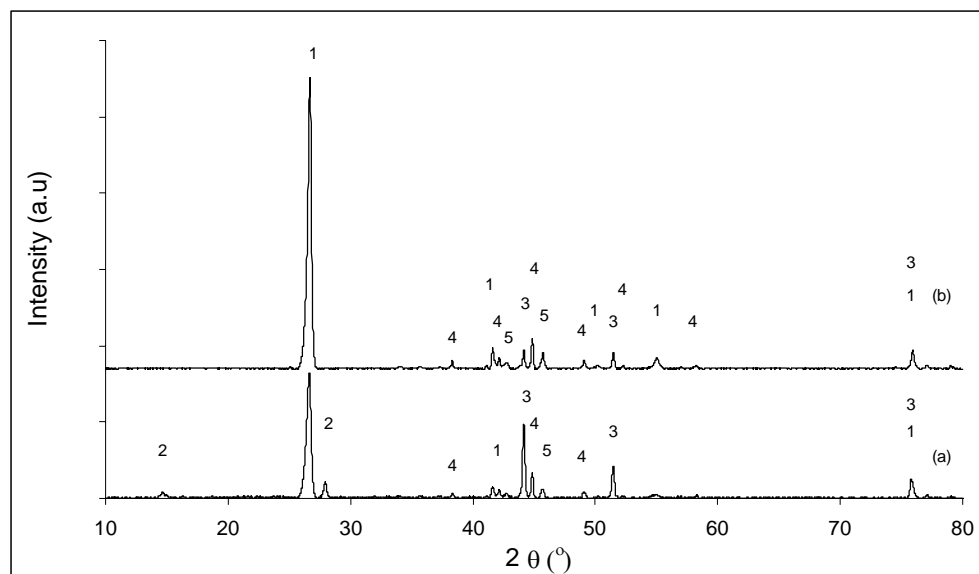


Figure 4.47. XRD patterns of (a) the experiments conducted with 10wt% Co_3O_4 added $\text{B}_2\text{O}_3+\text{C}$ mixtures for 1 hour, (b) after leaching product (a). (1) h-BN, (2) H_3BO_3 , (3) Co, (4) $\text{B}_2\text{CCo}_{11}$, (5) Co_2C .

4.4.2.4. Addition of Cu as Cupric Nitrate

Cu was added into the $\text{B}_2\text{O}_3+\text{C}$ mixture in the form of cupric nitrate ($\text{Cu}(\text{NO}_3)_2 \cdot 3\text{H}_2\text{O}$). The amount of cupric nitrate was calculated (0.2376g) so as to yield an amount of Cu corresponding to 2.5 wt% (0.0625g) of the initial $\text{B}_2\text{O}_3+\text{C}$ (2.5g) mixture. All of the reactants were ground and mixed in acetone in an agate mortar and pestle in acetone. The cupric nitrate dissolves in acetone therefore an intimate dispersion of Cu is expected to be obtained in the mixture.

XRD patterns of the product obtained with 2.5%Cu (in the form of cupric nitrate) addition and the leached product are given in Figure 4.48 (a) and (b), respectively. It can be seen that metallic Cu is present in the reaction products (Figure 4.48 (a)). $\text{Cu}(\text{NO}_3)_2 \cdot 3\text{H}_2\text{O}$ decomposes into copper(II) oxide, nitrogen dioxide and oxygen at 170°C. Formation of elemental Cu takes place by the reduction of copper(II) oxide with C. Melting point of Cu is 1084°C and boiling point is 2562°C. Therefore, Cu is expected to be in the liquid state during reaction at 1500°C. After leaching, Cu was completely removed as can be seen from the XRD pattern of the leached product (Figure 4.48 (b)).

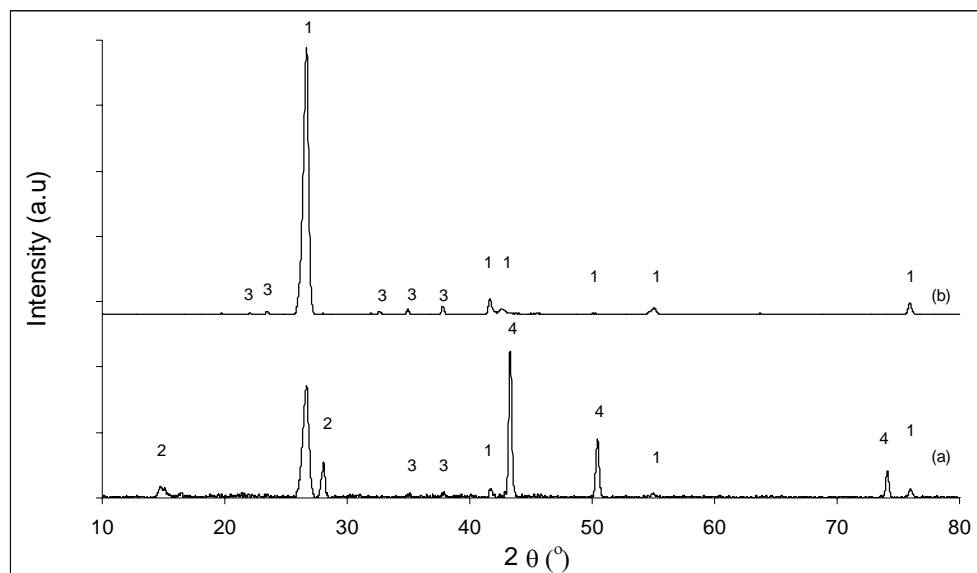


Figure 4.48. XRD patterns of (a) product of the experiment conducted with $\text{B}_2\text{O}_3+\text{C}$ mixtures with 2.5wt% Cu addition (in the form of cupric nitrate) for 1 hour. (b) after leaching product (a). (1) h-BN, (2) H_3BO_3 , (3) B_4C , (4) Cu.

It was determined by chemical analysis that 0.25g of h-BN and 0.06g B_4C had formed in 1 hour with the addition of Cu-nitrate. The value of h-BN is slightly higher and that of B_4C is slightly lower than the values obtained with plain

mixtures, indicating that Cu is not useful in increasing the amount of h-BN formed.

A SEM micrograph of an inner surface of a Cu added reaction product obtained in the experiment conducted for 30 minutes is presented in Figure 4.49. It is seen that small spherical formations have been developed on the inner surfaces of the reaction aggregate. This pattern is different from the ones observed in the products obtained from plain or CaCO₃ added mixtures. From the EDX analysis, these formations were found to contain Cu. The matrix phase was smooth. In the samples containing CaCO₃, the matrix phase seemed more perturbed and contained small grains of h-BN. This may be due to higher amount of h-BN formed with CaCO₃ addition.

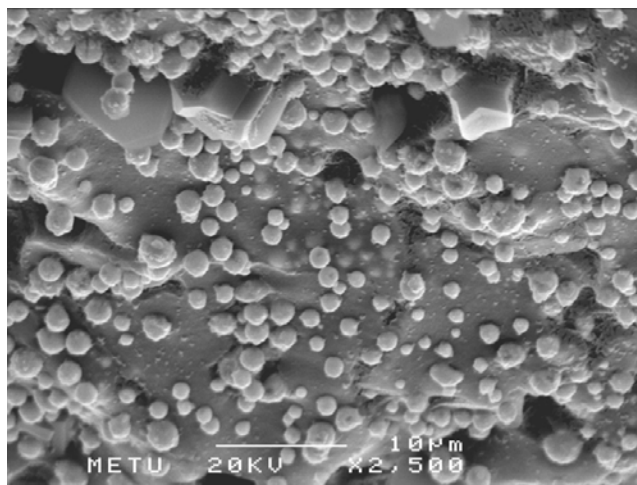


Figure 4.49. SEM micrograph of the product of the experiment conducted with Cu addition for 30 minutes.

A SEM micrograph of the h-BN powder obtained after leaching the product of the experiment conducted for 2 hours with Cu addition is presented in Figure 4.50. It was determined from SEM observations that the grains of the h-BN were $0.45\pm 0.12\mu\text{m}$. From the SEM investigations it can be inferred that the h-BN

obtained from Cu added samples had larger grains than the ones obtained from plain mixtures ($0.36\pm 0.08\mu\text{m}$), but the difference was not as much as the ones obtained with CaCO_3 addition ($0.70\pm 0.14\mu\text{m}$). It is believed that due to the interaction of the copper electronic orbitals with (002) planes of h-BN, h-BN crystallites align and adjoin and therefore grow. During this process the Cu atom is released [44,45].

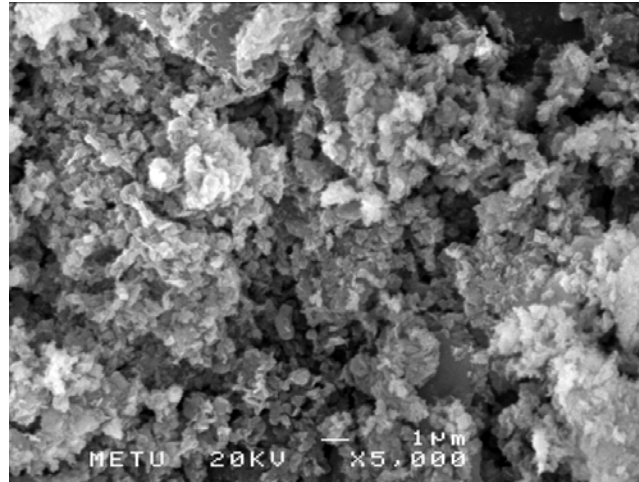


Figure 4.50. SEM micrograph of the h-BN powder obtained by leaching the product of the experiment conducted for 2 hours with Cu addition.

As stated before, Cu was found not to be as effective as CaCO_3 , MgO or BaCO_3 in increasing the yield of h-BN and it was found to increase the grain size of the formed h-BN. In addition, Cu was inert and did not form any secondary compound in the system such as its carbides or borides. Therefore, it was thought that addition of CaCO_3 and Cu together could provide better results in terms of increasing the yield and grain size of the formed h-BN. No study has been encountered in the literature for investigating the effect of Cu added together with a different additive. In the following section, results related to these experiments will be presented.

4.4.3. CaCO₃ + Cupric Nitrate Addition

In order to investigate the effect of CaCO₃ and Cu additions together, B₂O₃+C mixtures were mixed with 10 wt% CaCO₃ and 2.5 or 5 wt% Cu (in the form of cupric nitrate). XRD pattern of the product of the experiment conducted for 2 hours with 10wt% CaCO₃ and 2.5wt% Cu addition is presented in Figure 4.51 (a). The reaction product is seen to contain h-BN, B₂O₃ (H₃BO₃) and Cu; no peaks related to a calcium borate phase expected to be present in the system are observed as before, due to this phase being amorphous. Phases other than h-BN could be removed by leaching with dilute HCl as can be seen from Figure 4.51 (b). These results are similar to the ones obtained from addition of CaCO₃ and Cu individually.

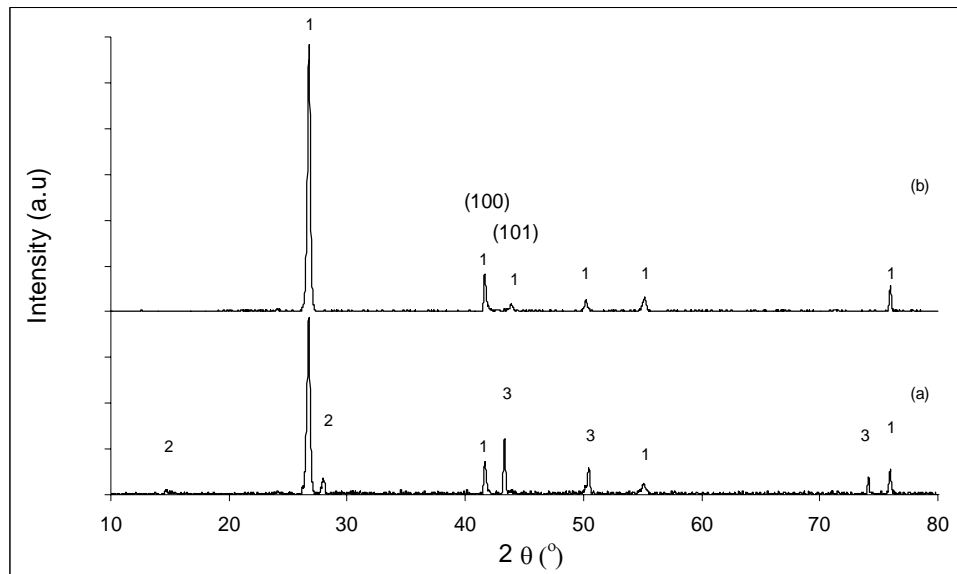


Figure 4.51. XRD patterns of (a) product of the experiment conducted for 2 hours with B₂O₃+C mixtures containing 10wt% CaCO₃ and 2.5wt% Cu addition (in the form of Cu-nitrate), (b) after leaching product (a). (1) h-BN, (2) H₃BO₃, (3) Cu.

A SEM micrograph of the product of the experiment conducted for 30 minutes with 10wt% CaCO_3 and 2.5wt% Cu addition is presented in Figure 4.52. Spherical droplets of Cu are seen on the matrix phase. The matrix phase is most probably a mixture of B_2O_3 and calcium borate. It can be seen that the matrix phase is not smooth, as opposed to the case of only Cu addition. There are formations of tiny h-BN grains. The surfaces of the Cu droplets are also rough. There are some tiny grains. It looks as if some h-BN formation is taking place on the surfaces of these Cu droplets. However, since it is a product obtained in 30 minutes, amount of h-BN is not high.

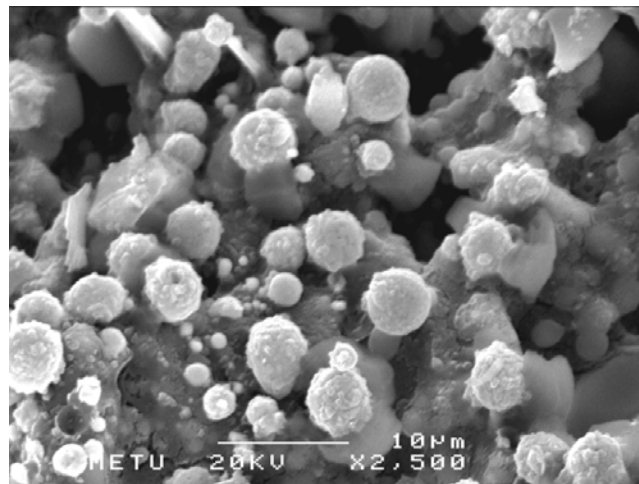


Figure 4.52. SEM micrograph of the product of the experiment conducted for 30 minutes with 10wt% CaCO_3 and 2.5wt% Cu addition.

The SEM micrograph of the product of the experiment conducted for 2 hours with 10 wt% CaCO_3 and 2.5 wt% Cu is presented in Figure 4.53. It can be seen in this figure that the formation of h-BN is taking place in two places. One of them is in the matrix. Matrix phase is composed almost entirely of h-BN grains at the end of 2 hours. This result is similar to the ones obtained with only CaCO_3 addition. The other place that h-BN formation is taking place is on the Cu droplets. It can be seen that the spherical shape of Cu droplets are distorted. In higher magnification

given in Figure 4.54, it can be seen more clearly that the second type of h-BN, formation of which is taking place on the Cu droplets, is in the form of thin platelets. The sizes of these second type h-BN grains are larger than the ones forming in the matrix phase.

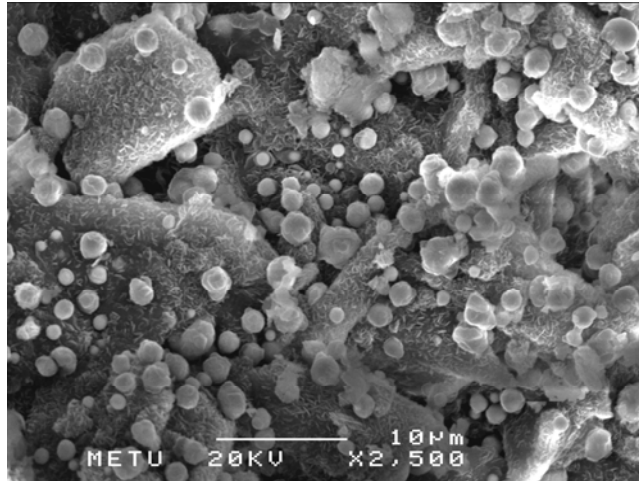


Figure 4.53. SEM micrograph of the product of the experiment conducted for 2 hours with 10wt% CaCO₃ and 2.5wt% Cu addition.

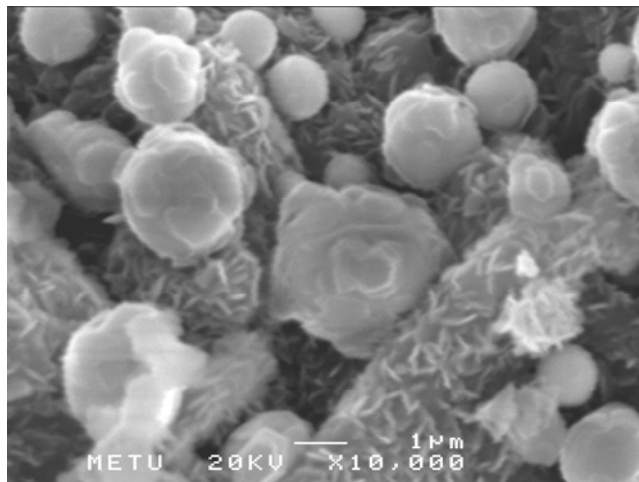


Figure 4.54. SEM micrograph of the product of the experiment conducted for 2 hours with 10wt% CaCO₃ and 2.5wt% Cu addition (higher magnification).

After leaching the product of the experiment conducted for 2 hours with 10wt%CaCO₃ and 2.5wt% Cu addition, pure h-BN powder was obtained as shown in Figure 4.55. The average grain diameter of the h-BN powder obtained after leaching was measured as 1.06±0.32μm. The specific surface area of this h-BN powder is 16m²/g.

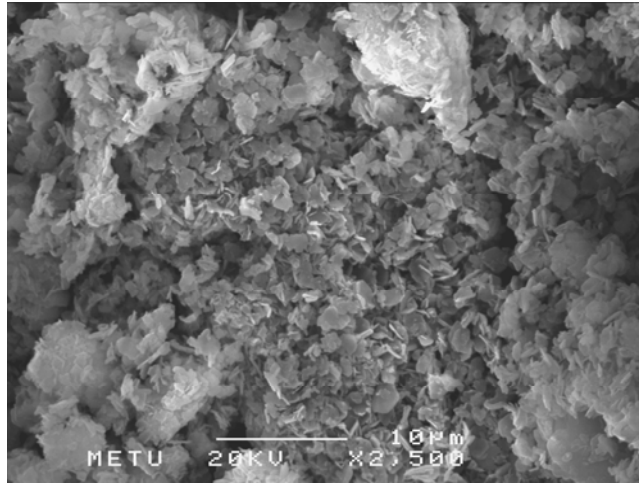


Figure 4.55. SEM micrograph of the product of the experiment conducted for 2 hours with 10wt% CaCO₃ and 2.5wt% Cu addition (after leaching with 1/1 (v/v) HCl/water solution).

The SEM micrograph of the outer surface of a product pellet obtained in 2 hours with 10wt%CaCO₃ and 2.5wt% Cu addition is presented in Figure 4.56. It was seen that h-BN grains were larger than the ones inside the pellet. This difference can be attributed to the higher duration of exposure of the outer surface of the aggregate to N₂ gas. With the intention of increasing the amount of the h-BN grains that have larger grain size, the amount of Cu addition was increased from 2.5wt% to 5wt%. However, it was inferred from the SEM observations that this increase did not cause a noticeable difference on the size of the formed h-BN. Furthermore, some spherical Cu droplets on which no h-BN had formed were observed to be present in the inner surfaces of the product pellet (Figure 4.57).

Therefore, it was inferred that additions of Cu higher than 2.5wt% do not have a contribution in this process under the given experimental conditions.

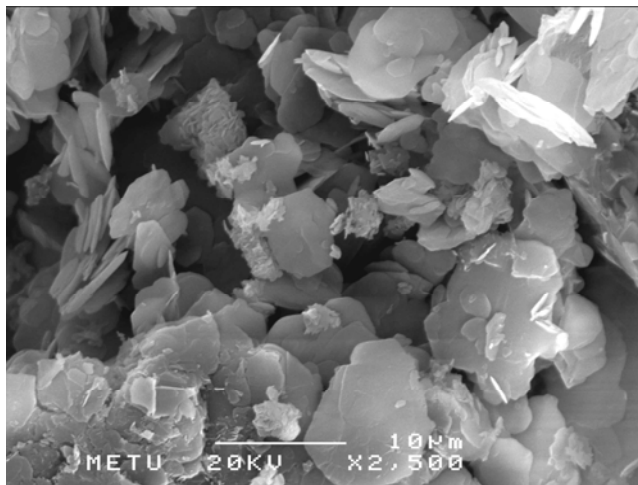


Figure 4.56. SEM micrograph of the product of the experiment conducted for 2 hours with 10wt% CaCO₃ and 2.5wt% Cu addition (outer surface of the pellet).

Peculiar formations composed of h-BN grains were observed on the SEM micrograph of the products of the experiments conducted with 10wt% CaCO₃ and 5wt% Cu added mixtures as seen in the upper right corner of Figure 4.57. The portion in white rectangle in Figure 4.57 is presented in higher magnification in Figure 4.58. These formations resemble flowers, petals of which are h-BN grains and there is a Cu droplet in the middle. These structures, which are believed to form by the effect of Cu addition, were observed also in other studies [44,45]. The Cu droplet in the middle of these structures seen in Figures 4.57 and 4.58 can be taken as an indication of the interaction between h-BN and Cu. In other studies [44,45], effect of Cu was investigated at very high temperatures such as 1950-2150°C. In the present study, experiments were performed at 1500°C and it was revealed that interaction between Cu and h-BN was operative and that Cu was effective in increasing the grain size of the formed h-BN by the carbothermic process at 1500°C.

The fact that Cu was more effective in increasing the crystal thickness and grain size of h-BN when it was used together with CaCO₃ is most probably due to the contribution of the catalytic effect of CaCO₃. Cu alone does have an effect in increasing the amount of h-BN formed, whereas CaCO₃ does. When Cu is used together with CaCO₃, it can be inferred that it is more effective in aligning and adjoining of the h-BN crystallites, the number of which is higher due to the catalytic effect of CaCO₃.

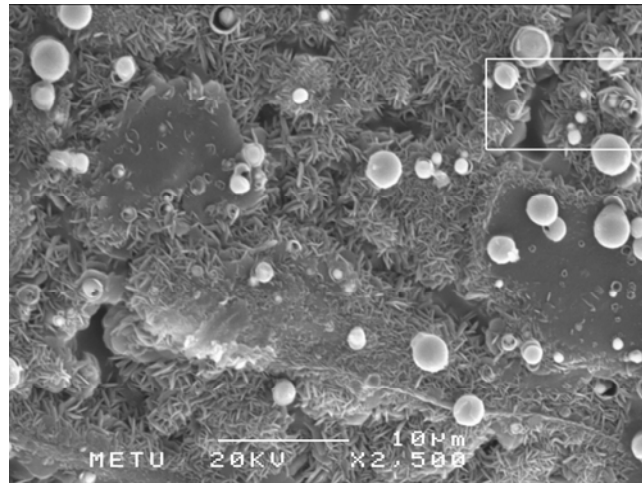


Figure 4.57. SEM micrograph of the product of the experiment conducted for 2 hours with 10wt% CaCO₃ and 5wt% Cu addition.

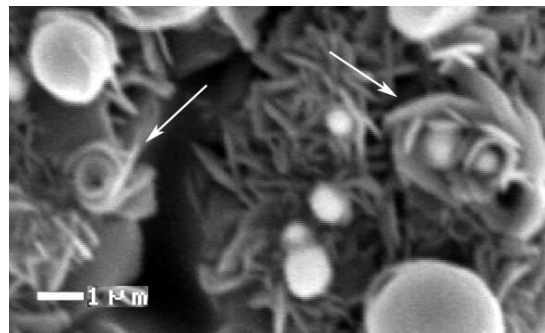


Figure 4.58. Magnified part of Figure 4.57.

In further efforts aiming to increase the grain size of the formed h-BN, the product obtained in 2 hours with 10wt% CaCO₃ and 2.5wt% Cu addition was crushed in an agate mortar and mixed with additional 2.5wt% Cu. Then, it was reacted for a second time under nitrogen atmosphere for 2 hours. A SEM micrograph of the produced h-BN powder obtained after leaching is presented in Figure 4.59. It was inferred from the SEM observations that the grains became larger and became angular. In the products obtained without additives the h-BN grains had round shapes and their size was much smaller. An important point noticed in this micrograph is the formation of perfect h-BN crystals which are marked with the white rectangle on the bottom right corner. The section in the white rectangle is presented in higher magnification in Figure 4.60. It can be seen that large and perfectly hexagonal shaped h-BN grains were formed in presence of Cu. The hexagonal shape is due to the intrinsic crystal structure of h-BN. Therefore, it can be concluded from the XRD analysis and SEM analysis that addition of CaCO₃ and Cu improves the crystal structure and grain size of the formed h-BN by the carbothermic method at 1500°C.

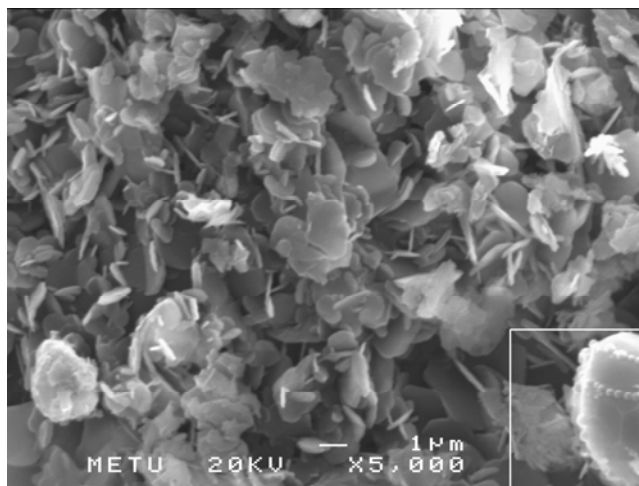


Figure 4.59. SEM micrograph of the product of the experiment conducted for 2 hours with 10wt% CaCO₃ and 2.5wt% Cu addition after further reaction for an additional 2 hours with 2.5wt% Cu addition, and leaching.

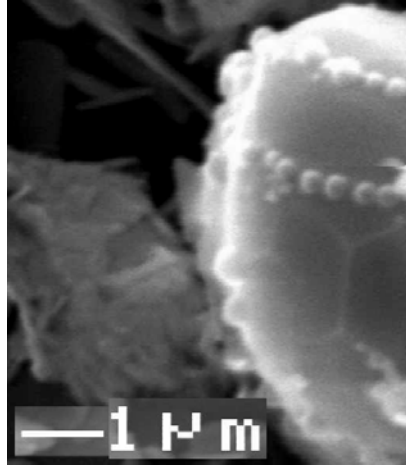


Figure 4.60. Magnified part of Figure 4.59

4.4.4 Comparison of the Effect of Additives

In order to increase the efficiency of the carbothermic reaction, addition of some catalysts has been investigated. Amounts of h-BN and B_4C formed in the experiments conducted with plain and catalyst added B_2O_3+C mixtures are presented in Table 4.9. As it can be seen from this table that 10 wt% $CaCO_3$ addition increased the amount of h-BN formed in 2 hours about 50% as compared to plain mixtures. From the SEM observations, BET specific surface area measurements and average crystal thickness calculations, it was inferred that addition of $CaCO_3$ provided an increase in the size and crystal thickness of the formed h-BN grains as presented in Table 4.10. The grain sizes reported in Table 4.10 are the diameters of the h-BN plates. They were estimated from the SEM observations by averaging at least 30 grains. Although these observations do not give accurate grain size distributions, approximate grain size values can be estimated.

It can be seen in Table 4.9 that MgO and $BaCO_3$ additions resulted in similar increase in the amount of h-BN as with $CaCO_3$ addition. They were effective in

reducing the amount of formed B_4C and the reaction products were porous, as well. These results and the fact that these additives are also basic oxides like CaO , indicate that similar mechanism to $CaCO_3$ addition may be taking place in the formation of h-BN with these additives.

Addition of transition metals and oxides, on the other hand, was found to be not useful in the carbothermic production of h-BN. Cu and MnO_2 did not change the amount of h-BN formed, as compared to the pure mixtures. Fe_3O_4 caused some increase. The transition metal oxides did not increase the h-BN amount as much as alkaline earth metal carbonates and also, formation of hard-to-leach borides or carbides was another drawback. However, it was deduced from the SEM observations that addition of Cu caused an increase in the size of the forming h-BN grains.

Cu was found to increase the grain size of the h-BN forming but it was not effective in increasing the amount of h-BN. In addition, Cu was inert and did not form any secondary compounds in the system such as its carbides or borides. Therefore, experiments were performed for investigating the positive effects of $CaCO_3$ and Cu together. It was found that addition of $CaCO_3$ and Cu together increased the grain size and crystal thickness of h-BN higher than when they were used individually as seen in Table 4.10. The grain size of the formed h-BN was above $1\mu m$. The specific surface area of this powder was measured to be $16m^2/g$.

Table 4.9. Amounts of h-BN and B₄C formed in the products of the experiments conducted with plain B₂O₃+C mixtures and compositions with various additives.

Additive	Duration	Amount of h-BN formed (g)	Amount of B₄C formed (g)
No additive	30 minutes	0.09	0.15
BaCO ₃	30 minutes	0.19	0.11
MgO	30 minutes	0.22	0.13
CaCO ₃	30 minutes	0.23	0.10
No additive	1 hour	0.23	0.10
BaCO ₃	1 hour	0.41	0.06
MgO	1 hour	0.46	0.06
CaCO ₃	1 hour	0.44	0.05
MnO ₂	1 hour	0.22	0.07
Cu(NO ₃) ₂	1 hour	0.25	0.06
Fe ₃ O ₄	1 hour	0.31	0.09
No additive	2 hours	0.40	0.03
BaCO ₃	2 hours	0.62	0.02
MgO	2 hours	0.63	0.02
CaCO ₃	2 hours	0.60	0.01

Table 4.10. Specific surface areas, observed grain sizes in SEM and average crystal thickness of h-BN powders obtained from plain, 2.5wt% Cu added, 10wt% CaCO₃ added, 10wt% CaCO₃ and 2.5wt% Cu added mixtures in 2 hours.

	No additive	Cupric nitrate added	CaCO₃ added	CaCO₃ + Cu added
Specific Surface Area (m²/g)	31.7	Not measured	21.0	16.0
Average Crystal Thickness (nm)	22	22	24	32
Grain Size from SEM (μm)	0.36±0.08	0.45±0.12	0.70±0.14	1.06±0.32

CHAPTER V

CONCLUSION

Carbothermic formation of h-BN was studied by holding B_2O_3+C mixtures under nitrogen atmosphere at $1500^\circ C$. B_4C was observed to be present in the reaction products in which formation of h-BN was not complete. It was found that all of the C was consumed and the formed B_4C was converted into h-BN, and the reaction was complete in 3 hours.

In order to understand whether B_4C was a necessary intermediate product in the carbothermic production of h-BN, B_4C was produced in the same experimental conditions as h-BN, but under argon atmosphere instead of nitrogen. The produced B_4C , morphology of which was observed to be similar to the one formed during h-BN formation, was mixed with B_2O_3 and reacted for 3 hours under nitrogen atmosphere in order to form h-BN. It was concluded from the unreacted B_4C remained in the system that the reaction of formation of h-BN from $B_4C+B_2O_3$ mixtures was slower than that from B_2O_3+C mixtures. Therefore, it was concluded that formation of h-BN did not necessarily proceed through the formation and utilization of B_4C , but directly by the reduction and nitridation of B_2O_3 and that B_4C formed as a side product in the reaction aggregate where N_2 pressure was too low for h-BN formation. B_4C forming is then converted into h-BN through its reaction with B_2O_3 and nitrogen. But this reaction retards the overall process.

It was inferred from the experiments performed with mixtures containing 50, 100 and 150% excess boric oxide that amount of B_4C decreased with increasing boric oxide in the starting mixture. It was found that the increase in the amount of B_2O_3 increased the conversion of B_4C into h-BN by Reaction (2.5). The amount of h-BN forming did not change much by use of excess amounts over 100%. However, it was less when 50% excess B_2O_3 was used. Formation of higher amount of B_4C and lower amount of h-BN when 50% excess B_2O_3 was used was attributed to the insufficient amount of B_2O_3 in the starting mixture.

Effects of addition of alkaline earth metal oxide and carbonates and transition metal oxides on the rate and amount of h-BN forming in the carbothermic process was investigated. It was found from the results of the experiments conducted with 5-50 wt% $CaCO_3$ addition for 30 minutes that the optimum amount in increasing the amount of h-BN and decreasing the amount of B_4C was 10 wt%. It was seen that 10 wt% $CaCO_3$ addition increased the amount of h-BN formed in 2 hours by about 50% as compared to plain mixtures. From the SEM observations, BET specific surface area measurements and average crystal thickness calculations, it was determined that addition of $CaCO_3$ provided an increase in the size and crystal thickness of the formed h-BN grains.

It is known [8] that carbothermic formation of h-BN in B_2O_3+C mixtures subjected to N_2 gas takes place by reaction of $B_2O_3(g)$ and $N_2(g)$ on solid C. h-BN formation is expected to be accelerated by easing the access of $N_2(g)$ into the pellet. Reaction products of the pellets into which $CaCO_3$ have been added and especially those containing lower than 20 wt% $CaCO_3$ were observed to be more porous than those of the plain pellets. Based on this observation, $CaCO_3$ was concluded to increase the porosity of the pellets. The effect of $CaCO_3$ in favoring the h-BN formation may therefore be due to increase in the porosity of the pellets.

It was seen from the XRD patterns of the reaction products at the end of 30 minutes that amount of B_2O_3 in the reaction products decreased with increasing

CaCO₃ content and diminished for CaCO₃ contents higher than 20%. CaO, which forms by decomposition of CaCO₃, was concluded to react with B₂O₃ and form calcium borate. The decrease in the amount of B₂O₃ may have caused the decrease in the amount of h-BN when more than 10% CaCO₃ was added into the B₂O₃+C mixtures.

Another reason for increase in rate of formation of h-BN when CaCO₃ is added into B₂O₃+C mixtures could be that a different additional mechanism becomes operative with addition of CaCO₃. It was deduced from SEM observations that when CaCO₃ was added, h-BN grains formed most probably in the melt, which is expected to be the liquid calcium borate phase. A possible mechanism may be suggested as follows:

Nitrogen is soluble in oxide melts (slags) and the nitrogen solubility depends on slag basicity for given O₂ and N₂ pressures and temperature. Slag basicity depends on the relative proportions of basic and acidic oxides in the slag. A basic oxide like CaO dissolves in oxide solution in accord with the reaction [59]:



When sufficient O²⁻ ions are present in the system, B₂O₃ is expected to form (BO₃)³⁻ according to:



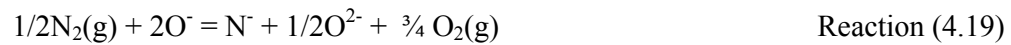
When the O²⁻ need of the acidic oxide for formation of simple anions like (BO₃)³⁻ in Reaction (4.15) exceeds the O²⁻ provided by the basic oxides, the slag will be acidic when the acidic oxides like B₂O₃ form more complicated anions like (B₂O₅)⁴⁻, (B₃O₇)⁵⁻, etc. by polymerization (chain formation, network formation) reactions like:



Nitrogen dissolution in basic slags is governed by Reaction (4.18) [59].



Nitrogen dissolution in acidic slags (Reaction (4.19)) is more complicated as nitrogen is considered to be combined to the acidic oxide anions [62].



h-BN solubility in the B_2O_3 -basic oxide systems was found to increase with the increase in the concentration of the basic oxide up to 0.1-0.2 mole fraction of the basic oxide and to decrease with further increase in the concentration of the basic oxide [63]. Nitrogen dissolved in B_2O_3 containing oxide melts may result in formation of h-BN if the solubility product of h-BN is exceeded. What the reactions for dissolution of h-BN in oxide melts or for formation of h-BN from oxide melts are not known. One possible reaction for formation of h-BN from nitrogen and B_2O_3 containing oxide melts may be:



If nitrogen is considered to be incorporated into the borate anions as suggested [59,62], reactions like Reaction (4.21) and (4.22) etc. may result in formation of h-BN.



In the experiments conducted with CaCO₃ additions, amount of h-BN forming was seen to increase up to 10 wt% CaCO₃ addition and then to decrease afterwards. The increase in the quantity of h-BN forming in the CaCO₃ added system was attributed to the increase in quantity of the calcium borate phase. That the increase in the quantity of BN with the increase in the quantity of CaCO₃ added continues up to 10% addition may be taken as an indication that crystallization of h-BN from the calcium borate phase is not the only mechanism of h-BN formation and that some h-BN forms by reaction of gaseous B₂O₃ with N₂(g) on carbon (Reaction (2.6)) [8], the rate of which was explained to decrease with increase in the quantity of CaCO₃ added.



Reaction (4.20), (4.21) and (4.22) do not use C for formation of h-BN. C is nevertheless probably necessary, however, as dissolution of nitrogen in the calcium borate melt in accord with Reactions (4.18) and (4.19) and also formation of BN with Reactions (4.20), (4.21) and (4.22) are favored by low O₂ pressures which is provided by C.

The quantity of h-BN forming in the mixtures containing CaCO₃ as additive were significantly larger than those containing no CaCO₃, although equal amounts of C was used in (B₂O₃+C) and (B₂O₃+C+CaCO₃) mixtures. This may be taken as an indication that some of the total h-BN forms according to Reaction (2.6) which uses C and some according to Reactions (4.20), (4.21) and (4.22) which do not consume C, on the conditions that C loss from the system does not change with addition of CaCO₃.

MgO and BaCO₃ additions resulted in a similar increase in the amount of h-BN as with CaCO₃ addition. They were effective in reducing the amount of formed B₄C and the reaction products were porous, as well. These results and the fact that these additives are also basic oxides like CaO, indicate that similar mechanisms to

CaCO₃ addition may be taking place in the formation of h-BN with these additives.

Addition of transition metal oxides in general provided only a slight increase in the amount of h-BN formed. Boride and carbide formations were observed as a result of addition of these oxides, which were difficult to remove from the h-BN. Therefore, they were not found to be suitable as additives in the carbothermic production of h-BN.

It was deduced from visual observations performed during the SEM analyses that Cu addition caused an increase in the grain size of the formed h-BN. In addition, Cu was inert and did not form any secondary compound in the system such as its carbides or borides. With the expectation of combining the positive effects of CaCO₃ and Cu, experiments were conducted with additions of both CaCO₃ and Cu into the B₂O₃+C mixtures. Two types of h-BN formation were observed in the SEM micrographs. One of them was forming in the matrix phase, which is expected to be a mixture of B₂O₃ and calcium borate. The other type was forming on the Cu droplets, which were on the inner surfaces of the reaction aggregate. The h-BN grains forming on Cu droplets were larger than those forming inside the reaction aggregate, indicating an interaction between Cu and h-BN. It is believed that due to the interaction of the copper electronic orbitals with (002) planes of h-BN, h-BN crystallites align and adjoin and therefore grow. During this process the Cu atom is released [44,45].

The average grain size of the formed h-BN when CaCO₃ and Cu were added together was observed to be above 1 μm from the SEM micrographs. The specific surface area of this powder was measured to be 16m²/g, whereas the specific surface area of the h-BN formed from plain mixtures was 31.7m²/g and it was 21m²/g when only CaCO₃ was added. It can be concluded that by addition of CaCO₃ in the carbothermic production of h-BN, amount and grain size of h-BN can be increased. Addition of Cu further increases the grain size.

It has been revealed in this study that interaction between Cu and h-BN was operative and Cu was effective in increasing the grain size and crystallinity of the formed h-BN by the carbothermic process at relatively low temperatures such as 1500°C. In other studies [44,45], effect of Cu was investigated at very high temperatures such as 1950-2150°C.

It can be concluded that alkaline earth metal carbonates can be recommended to be used as catalysts in the carbothermic production of h-BN and Cu can be used for increasing the grain size of the h-BN. The abundance and low cost of CaCO₃ makes it the most suitable material that has been investigated in the present study. Furthermore, the fact that it is found as a natural product in Turkey makes its utilization more feasible. In addition, there is extensive mining of boron minerals in Turkey, indicating the feasibility of the carbothermic production of h-BN with catalytic additions of CaCO₃ in Turkey.

As the future work it can be suggested that further investigation of the mechanism of h-BN formation by CaCO₃ (and Cu) addition will be beneficial for understanding the role of CaCO₃ (and Cu). Based on the encouraging results obtained in this work, studies aiming for the production of h-BN in larger quantities with the aid of catalysts can be performed.

REFERENCES

- [1] A. W. Weimer, "Carbide, Nitride and Boride Materials Synthesis and Processing", Chapman and Hall, London, 1997.
- [2] W. D. Callister, "Materials Science and Engineering", John Wiley and Sons, Toronto, 1995.
- [3] L. Kempfer, "The Many Faces of Boron Nitride", *Materials Engineering*; 107, 41-44, 1990.
- [4] R. Haubner, M. Wilhelm, R. Weissenbacher, B. Lux, "Boron Nitrides-Properties, Synthesis and Applications", Springer-Verlag, Berlin, 2002.
- [5] "The Economics of Boron", Roskill Information Services Ltd., London, 2002.
- [6] F. Altun, "Bor", Ulusal Bor Enstitüsü, Ankara, 2005.
- [7] S. N. Pikalov, "Mechanism of Formation of Graphitelike Boron Nitride in the Carbothermal Process", *Soviet Powder Metallurgy and Metal Ceramics* 27, 1988; 404-406.
- [8] A. Aydoğdu, and N. Sevinç, "Carbothermic Formation of Boron Nitride", *Journal of the European Ceramic Society*, 23, 2003; 3153-3161.
- [9] A. A. R. Wood and E. C. Shears, "Method of Manufacturing Boron Nitride", US Patent 3189412, 1965.
- [10] T. S. Bartnitskaya, M. V. Vlasova, T. Y. Kosolapova, N. V. Kostyuk and I. I. Timofeeva, "Formation of Boron Nitride During Carbothermal Reduction", *Soviet Powder Metallurgy and Metal Ceramics*, 29, 1990; 990-994.
- [11] R. T. Paine, C. K. Narula, "Synthetic Routes to Boron Nitride", *Chem. Rev.*, 90, 1990, 73-91.
- [12] S. Rudolph, "Boron Nitride", *Minerals Review*, 73, 1994, 89-90.
- [13] H. O. Pierson, "Handbook of Refractory Carbides and Nitrides", Noyes Publications, Westwood, New Jersey, 1996.

- [14] J. E. Havek, "BN: High Cost Material with a Promising Future", *Materials Design and Engineering*, 65,1967, 70.
- [15] D. A. Lelonis, "Boron Nitride Powder-A Review", General Electric Company, Publication Number: 81505, 2003.
- [16] Wikipedia, "Boron Nitride", http://en.wikipedia.org/wiki/Boron_nitride, 2006.
- [17] Accuratus, "Boron Nitride-BN", www.accuratus.com/boron.html, 2002.
- [18] A. Aydođdu, "Production of Boron Nitride", Ph.D Thesis, METU, Ankara, 1993.
- [19] D. A. Lelonis, "New Applications in Boron Nitride Coatings", General Electric Company, Publication Number: 81504, 2003.
- [20] T. Saito, F. Honda, "Low Friction Behavior of Sintered hBN Sliding in Sodium Chloride Solution", *Wear*, 244, 2000, 132.
- [21] Y. Kimura, T. Wakabayashi, K. Okada, T. Wada, H. Nishikawa "Boron Nitride as a Lubricant Additive", *Wear* 232, 1999, 199-206.
- [22] D. A. Lelonis, J. W. Tereshko, C. M. Andersen, "New Applications in Boron Nitride Coatings", General Electric Company, Publication Number: 81506, 2003.
- [23] D. A. Lelonis, "Hot Pressed Boron Nitride Shapes", General Electric Company, Publication Number: 81507, 2003.
- [24] M. Hubacek, M. Ueki, "Pressureless-sintered Boron Nitride with Limited Content of Boric Oxide", *Materials Science Research International*, 1, 1995, 209-212.
- [25] P. Popper, "Special Ceramics", Heywood and Company Ltd., London, 1960.
- [26] T. E. O'Connor, "Synthesis of Boron Nitride", *Journal of the American Chemical Society*, 84, 1962, 1753-1754.
- [27] F. Fauzi, M. Tani, M. Suzue, "Boron Nitride and Process for Producing the Same" US Patent 6319602, 2001.
- [28] O. Yamamoto, "Crystalline Turbostratic Boron Nitride Powder and Method for Producing the Same", US Patent 6306358, 2001.
- [29] M. Hubacek, M. Ueki, "Chemical Reactions in Hexagonal Boron Nitride System", *Journal of Solid State Chemistry*, 123, 1996, 215-222.

- [30] R. J. Brotherson and H. Steinbert, "Progress in Boron Chemistry", Vol. 2, Pergamon Press, 1970.
- [31] K. A. Schwetz, G. Vogt, A. Lipp, "Manufacture of Hexagonal Boron Nitride", US Patent 4107276, 1978.
- [32] T. E. Warner, D. J. Fray, "Nitriding of Iron Boride to Hexagonal Boron Nitride", *Journal of Materials Science*, 35, 2000, 5341-5345.
- [33] A. C. Adams, C. D. Capio, "The Chemical Deposition of Boron-Nitrogen Films", *Journal of Electrochemical Society*, 127, 1980, 399-405.
- [34] O. Gafri, A. Grill, D. Itzhak, R. Avni, "Boron Nitride Coatings of Steel and Graphite Produced with a Low Pressure R.F. Plasma", *Thin Solid Films*, 72, 1980, 523-527.
- [35] T. S. Bartnitskaya, N. F. Ostrovskaya, V. M. Vereshcaka and A. V. Kurdyumov, "Preparation of Boron Nitride Fibers using Hydrated Cellulose. III. Nitriding Hydrated Cellulose Fibers Impregnated with Boric Acid", *Powder Metallurgy and Metal Ceramics*, 40, 2001, 537-543.
- [36] R. Heyder, "Manufacture of Boron Nitride", US Patent 1077712, 1913.
- [37] S. Peacock, "Process of Producing Boron Nitride", US Patent 1465292, 1923.
- [38] F. M. May, C. C. Cook, "Process for Production of Boron Nitride", US Patent 2959469, 1960.
- [39] T. Hagio, K. Nonaka, T. Sato, "Microstructural Development with Crystallization of Hexagonal Boron Nitride", *Journal of Materials Science*, 16, 1997, 795-798.
- [40] L. N. Parrish, C. C. Chase, "Process for Producing Boron Nitride", US Patent 4749556, 1988.
- [41] S. Alkoy, C. Toy, T. Gönül, A. Tekin, "Crystallization Behavior and Characterization of Turbostratic Boron Nitride", *Journal of the European Ceramic Society*, 17, 1997, 1415-1422.
- [42] J. Ichihara, A. Kawasaki, S. Nakagawa, Y. Kuroda, "Hexagonal Boron Nitride Coarse Particles", Japan Patent 11029307, 1999.
- [43] K. Hisamitsu, "Manufacture of Hexagonal Boron Nitride Powders", Japan Patent 07041311, 1995.
- [44] M. Hubacek, T. Sato, "The Effect of Copper on the Crystallization of Hexagonal Boron Nitride", *Journal of Materials Science*, 32, 1997, 3293-3297.

- [45] M. Hubacek, T. Sato, M. Ueki, "Copper-Boron Nitride Interaction in Hot-Pressed Ceramics", *Journal of Materials Research*, 12, 1997, 113-118.
- [46] S. J. Yoon, and A. Jha, "A. Vapour-Phase Reduction and the Synthesis of Boron-Based Ceramic Phases" *Journal of Materials Science*, 30, 1995, 607-614.
- [47] E. T. Turkdogan, "Physical Chemistry of High Temperature Technology" Academic Press, London, 1980.
- [48] R. H. Lamoreaux, D. L. Hildenbrand and L. Brewer, "High Temperature Vaporization Behavior of Oxides II: Oxides of Be, Mg, Ca, Sr, Ba, B, Al, Ga, In, Ti, Si, Ge, Sn, Pb, Zr, Cd and Hg" *Journal of Physical and Chemical Reference Data*, 16, 1987, 419-443.
- [49] T. S. Bartnitskaya, A. V. Kurdyumov, V. I. Lyashenko, N. F. Ostrovskaya and I. G. Rogovaya, "Catalytic Synthesis of Graphite-Like Boron Nitride", *Powder Metallurgy and Metal Ceramics*, 35, 1996, 296-300.
- [50] N. F. Ostrovskaya, T. S. Bartnitskaya, V. I. Lyashenko, V. B. Zelyavskii and A. V. Kurdyumov, "Crystallization of Boron Nitride from Solution in a Lithium Borate Melt", *Powder Metallurgy and Metal Ceramics*, 35, 1996, 636-639.
- [51] T. S. Bartnitskaya, A. V. Kurdyumov, V. I. Lyashenko, and N. F. Ostrovskaya, "Structural-Chemical Aspects of the Catalytic Synthesis of Graphite-Like Boron Nitride", *Powder Metallurgy and Metal Ceramics*, 37, 1998, 26-32.
- [52] T. S. Bartnitskaya, T. Ya. Kosolapova, A. V. Kurdyumov, G. S. Oleinik and A. N. Bilyankevich, "Structure and Some Properties of Fine-Grained Graphite-Like Boron Nitride", *Journal of Less-Common Metals*, 117, 1986, 253-257.
- [53] N. H. Furman, "Scott's Standard Methods of Chemical Analysis", 5th edition, Vol.2, 1962.
- [54] R. A. Nyquist, R. O. Kagel, "Infrared Spectra Atlas of Inorganic Compounds", Academic Press, New York, 1971.
- [55] B. D. Cullity, S. R. Stock, "Elements of X-Ray Diffraction", Prentice Hall, New Jersey, 2001.
- [56] S. V. Gurov, T. V. Rezchikova, V. I. Chukalim, V. I. Torbov and V. N. Troitskii, "X-Ray Diffraction Investigation of Ultrafine Boron Nitride Powders", *Powder Metallurgy and Metal Ceramics*, 24, 1985, 607-609.

- [57] A. Sinha, T. Mahata and B. P. Sharma, "Carbothermal Route For Preparation of Boron Carbide Powder from Boric Acid–Citric Acid Gel Precursor", *Journal of Nuclear Materials*, 301, 2002, 165-168.
- [58] E. M. Levin, C. R. Robbins and H. F. McMurdie, "Phase Diagrams for Ceramists", The American Ceramic Society, Ohio, 1964.
- [59] E. Martinez, N. Sano, "Nitrogen Solubility in CaO-SiO₂, CaO-MgO-SiO₂, and BaO-MgO-SiO₂ Melts", *Metallurgical Transactions B*, 21B, 1990, 97-104.
- [60] H. O. Mulfinger, "Gases in Glass", *Journal of the American Ceramic Society*, 49, 1966, 462-467.
- [61] Y. Iguchi, S. Kashio, T. Goto, Y. Nishina and T. Fuwa, "Raman Spectroscopic Study on the Structure of Silicate Slags", *Canadian Metallurgical Quarterly*, 20, 1981, 51-56.
- [62] D. J. Min, R. J. Fruehan, "Nitrogen Solution in BaO-B₂O₃ and CaO-B₂O₃ Slags", *Metallurgical Transactions B*, 21B, 1990, 1025-1032.
- [63] T. Wakasugi, F. Tsukihashi and N. Sano, "The Solubility of BN in B₂O₃ Bearing Melts", *Journal of Non-Crystalline Solids*, 135, 1991, 139-145.

VITA

Hasan Erdem amurlu was born in Ankara on 21st October 1975. He graduated from Eskişehir Anatolian High School in 1993. He received his B.S. degree at the Metallurgical and Materials Engineering Department, in Middle East Technical University (METU) in 1998 and joined the Department as a research assistant in the same year. He completed his M.S. degree in August 2001 under the supervision of Prof. Dr. Muharrem Timuçin in the field of “Production and Characterization of PMN-PT Piezoelectric Ceramics”. He began his PhD. study in 2001 under the supervision of Prof. Dr. Naci Sevinç and Prof. Dr. Yavuz A. Topkaya in the field of hexagonal boron nitride production. In 2003 he was accepted for the Academic Human Resources Program (ÖYP) supported by the State Planning Organization, and he continued his studies in METU on behalf of Akdeniz University. He worked as a visiting scientist at the Department of Physical Chemistry of University of Pavia, Italy from June 2005 to March 2006.